Public

Report

Document ID	Version	Status	Reg no	Page
1399768	2.0	Approved		1 (114)
Author Jan Hernelind 5T Engineering AB			Date 2015-02-27	
Reviewed by Lisette Åkerman (QA)			Reviewed date 2015-03-05	
Approved by Jan Sarnet			Approved date 2015-03-05	

Analysis of creep in the KBS-3 copper canister due to internal and external loads

Abstract

Earlier simplified analyses indicate that internal pressure and different thermal expansion in copper shell and insert in combination with certain load cases could give rise to tensile stresses in the canister copper shell. This report is aimed to further investigate this effect. The presented analysis covers loads due to internal processes and external loads. Internal loads are due to thermal evolution and gas production whilst external loads are external pressure from swelling buffer and water pressure also including glaciations effects. The analyses are based on different assumptions for these factors.

All simulations are based on the BWR-design of the insert. The geometry of the FSW (Friction Stir Welding) weld is modelled by an axial slit and a root defect in radial direction. Four axial-symmetric analyses have been performed using different histories for temperature and external pressure. In addition, a 3D model has been produced in order to verify that an axial symmetric approximation is sufficiently accurate. The 3D model also gives information about the stresses in the BWR insert.

In order to study the strains in the bottom region of the copper shell an additional analysis has been performed.

The results from the analysis shows that the thermal expansion of- and internal over pressure in the canister gives negligible strain effects in the copper shell. The dominant factor that couses strains in the copper shell is the applied external pressure.

Sammanfattning

Tidigare förenklade analyser indikerar att inre tryck och olika termisk expansion i kopparhölje och insats kombinerat med vissa lastfall orsakar dragspänningar i kapselns kopparhölje. Denna analys syftar till att undersöka denna effekt vidare. Analysen omfattar både laster orsakade av inre processer hos kapseln och yttre laster. Inre laster orsakas av termisk utveckling och gasbildning medan yttre laster utgörs av trycket från svällande buffert och vatten samt glaciationseffekter. Analyserna baseras på olika antaganden för dessa faktorer.
Alla simuleringar är baserade på BWR-design av insatsen. Geometrin av FSW-svetsen (Friction Stir Welding) modelleras som en axiell slits och en rotdefekt i radiell riktning.
Fyra axial-symmetriska analyser har utförts med olika tidsförlopp av temperatur och extern tryckutveckling. Dessutom har en 3D-modell gjorts för att verifiera att en axial-symmetrisk approximation är tillräckligt noggrann för en studie av påverkan på kopparhöljet. 3D-modellen ger också en uppfattning om spänningarna i en BWR insats.

För att studera töjningarna i kopparhöljets bottenområdet har ytterligare en analys genomförts.

Svensk Kärnbränslehantering AB
Swedish Nuclear Fuel and Waste Management Co
PO Box 925, SE-572 29 Oskarshamn
Visiting address Gröndalsgatan 15
Phone +46-491-76 79 00 Fax +46-491-76 79 30
www.skb.se
556175-2014 Seat Stockholm

Resultatet från analysen visar att termiska utvidgningseffekter och inre övertryck ger försumbara töjningseffekter i kopparhöljet. Den dominerande faktorn som ger upphov till töjningar i kopparhöljet är det pålagda yttre trycket.

Contents

1 Introduction

To investigate how the thermal and gas expansion effects give loads on the copper numerical calculations have been carried out as reported in”Inre övertyck i kapseln” (SKBdoc 1333208) and ”Svar på begäran om kompletteringar angående kapselfrågor” (SKBdoc 1333256). The conclusion was that the combined effect of creep deformation when the axial gap between the copper lid and the insert closes due to buffer swelling and contraction effects during the subsequent cooling process must be analyzed with FEM-based creep calculations.

Since there are some uncertainties regarding the assumptions, two temperature histories and two swelling pressure histories were studied (four cases) in this analysis.

Since the surrounding buffer (bentonite) isn’t included in this study the copper shell needs boundary conditions to prevent rigid body motion. For the axi-symmetric model, two sets of boundary conditions have been used to simulate the worst case for the upper and the lower part of the copper shell, respectively, see also chapter 8.

1.1 Context for this report

The insert (nodular cast iron) material properties are based on experimental results. The steel lid and the steel cassette material properties are based on supplier’s available information. The copper shell material model includes creep and is developed by Rolf Sandström (Sandström and Andersson 2008, Jin and Sandström 2008, Sandström et al. 2009).

This report summarizes the results for analyses performed by using an axi-symmetric approach based on:

- Temperature history
- Buffer condition (wet or dry)
- Pressure history (inside and outside)
- Creep material model for the copper shell

1.2 Background

The canister reference design takes into account the difference in the temperature and the associated thermal expansion between the cast iron insert and the copper shell. This is done by providing an axial gap between the insert and copper shell. The gap is sufficient to prevent any contact between the insert lid and the copper lid under unloaded conditions according to ”Svar på begäran om kompletteringar angående kapselfrågor” (SKBdoc 1333256). In order to examine if external loads in combination with thermal expansion effects could create harmful effects it is necessary to take into account both the thermal and the swelling load evolution and their interaction.

2 Simulation considerations

2.1 Factors considered in the simulation

The following factors are taken into account in the simulations.

Canister geometry

- Tolerances in the nominal gap between the insert and the copper lid.
- The weld is modelled by the nominal axial slit but also with a circumferential root defect with a radial extension of 3 mm.

Thermal evolution

Differences in wet, and dry holes under mean and dimensioning temperature evolution. *"Mean"* is based on mean value of the thermal conductivity of the bedrock whilst *"dim"* the highest expected temperature (upper limit) used as a dimensioning case.

Thermal expansion effects

- Thermal expansion coefficients for nodular cast iron and copper.

Load evolution

- Hypothetic local swelling effects due to uneven water saturation.
- Isostatic pressure from buffer swelling, water and glaciations.

Internal gas pressure effects

- The expected pressure evolution due to gas production and thermal expansion of the gas in the canister have been calculated in "Inre övertyck i kapseln" (SKBdoc 1333208). This pressure is included in the simulations.

2.2 Parameters used in the simulations

2.2.1 Canister geometry

The dimensions of the reference design are specified in TR-10-14 (SKB 2010).

- nominal length of the insert is 4573 (+0/-0.5) mm (at 20° C).
- nominal internal length of the copper shell is 4575 (+0.6/-0.1) mm (at 20° C).
- nominal axial gap can be calculated to 2 (+1.1/-0.3) mm, on account of steel lid tolerances.

The maximum strain increases with the size of the initial gap between the copper lid and the steel lid which is set to 3.1 mm according to the tolerances above.

All other dimensions are nominal.

2.2.2 Thermal evolution

The temperature evolution in different bedrock domains in the planned repository in Forsmark have been modelled by Hökmark et al. (2010).

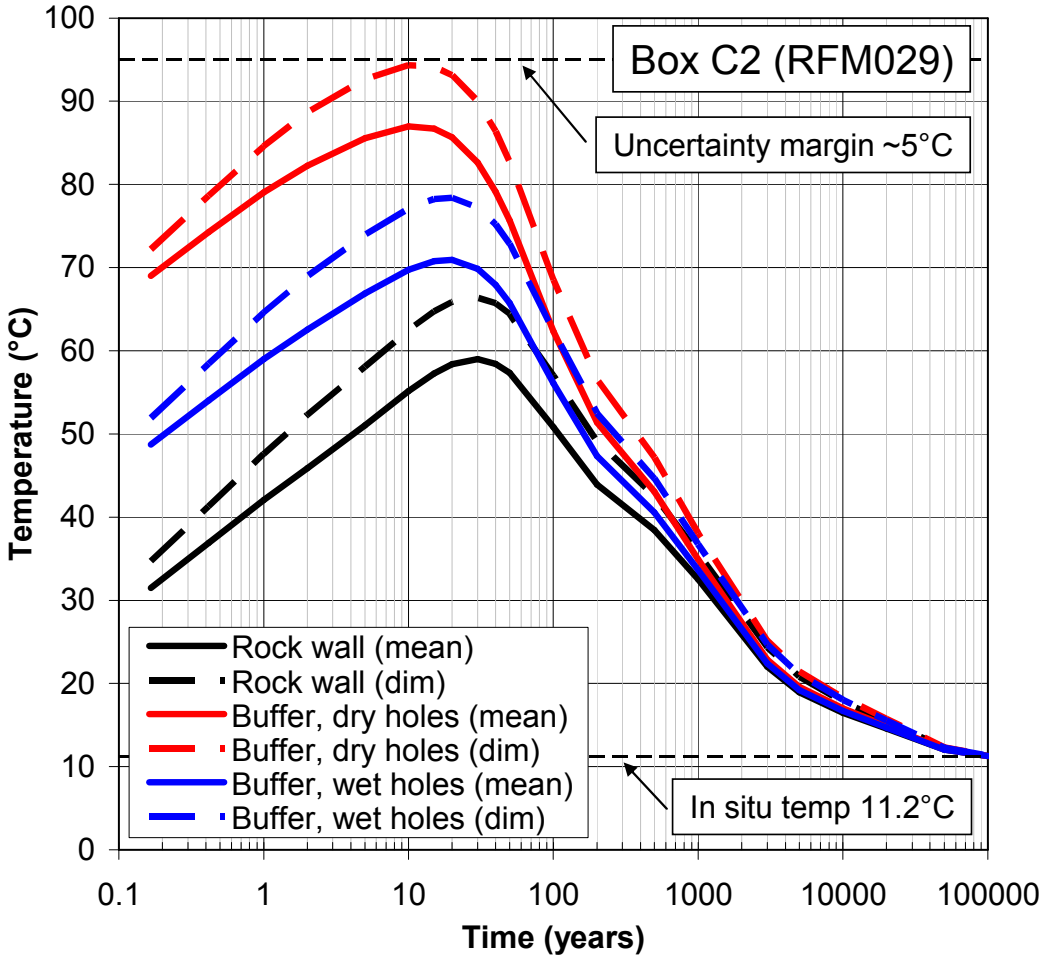

Figure 2-1.*Comparison between rock wall and buffer temperature at the the axial position corresponding to canister mid height for dry - and wet deposition holes (Hökmark et al. 2011, Figure 5-15).*

The blue curves correspond to wet holes. A wet hole is an idealization assuming that the wetting and the corresponding swelling of the buffer starts directly. In a wet hole contact is established between the copper shell and the buffer due to the swelling forces, and the buffer temperature presented is given at the axial midpoint of the canister. It is assumed that the copper shell and the bentonite have the same temperature.

The red curves correspond to dry holes meaning that no wetting will take place. Consequently no overall contact is assumed to exist between the insert, the copper shell and the dry buffer, except in the contact point at the base and top. The presented temperature is the peak temperature in the bentonite at the contact point in the top. The thermal conductivity of a wet buffer is higher compared to a dry buffer which also is reflected in Figure 2-1.

In the analysis, the following assumptions are made:

- No temperature gradients exist in the canister. It is however likely that the temperature in reality is somewhat higher in the insert than in the copper. The coefficient of thermal expansion is higher for copper than for nodular iron which implies that the maximum gap of interest is overestimated. The external pressure will close the gap followed by a temperature decrease. The resulting creep strain will thus be overestimated with the assumption made.

- The outside pressure, corresponding to buffer swelling, is treated as a parameter, independent of the temperature. This is further commented in section 2.2.4 Load evolution.

2.2.3 Thermal expansion effects

The thermal expansion effect is included using the following expansion coefficients (oxygen free) copper and ductile iron, see ”Inre övertyck i kapseln” (SKBdoc 1333208).

$$\alpha_{Cu} = 1.77 \cdot 10^{-5}\ m/m,K$$
$$\alpha_{Fe} = 1.18 \cdot 10^{-5}\ m/m,K$$

2.2.4 Load evolution

The loads are chosen in a conservative way in order to provide limit-setting load cases. Hence the glacial load of 60 MPa assumed in the analyses is higher than the design pressure of 45 MPa for the canister.
The definition of the simulation cases for wet and dry holes, respectively, is provided below and Figures 2-2 and 2-3 show the evolution of temperature and pressure.

Wet holes

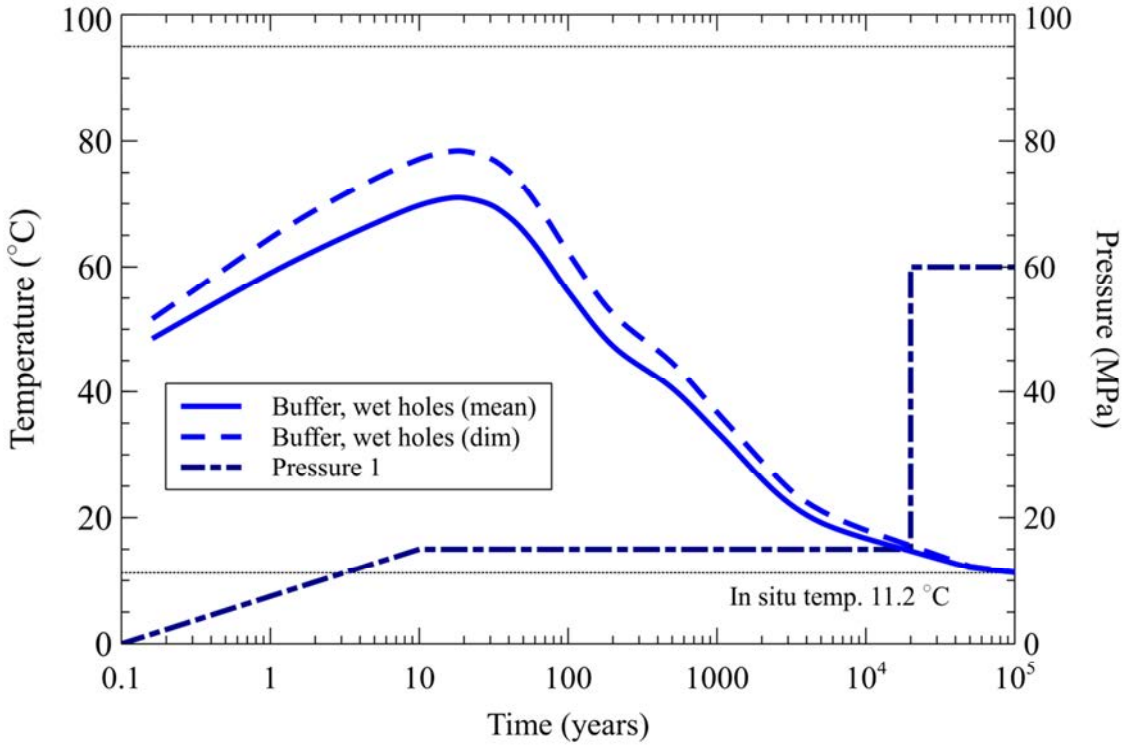

Figure 2-2. *Pressure and temperature development in wet holes, case a) and b)*

Case a). The water saturation process is assumed to start immediately and full swelling- and water pressure are reached after 10 years (blue dotted line, Pressure 1). The canister temperature is following the blue solid line (mean case).The case is chosen to examine a normal evolution in a wet area. A hypothetic glacial load is applied after 20,000 years (Pressure 1).

Case b). Same as case a) except that the canister temperature is following the blue dashed line (dim case). This case is chosen to examine the influence of elevated temperature in a wet hole.

Dry holes

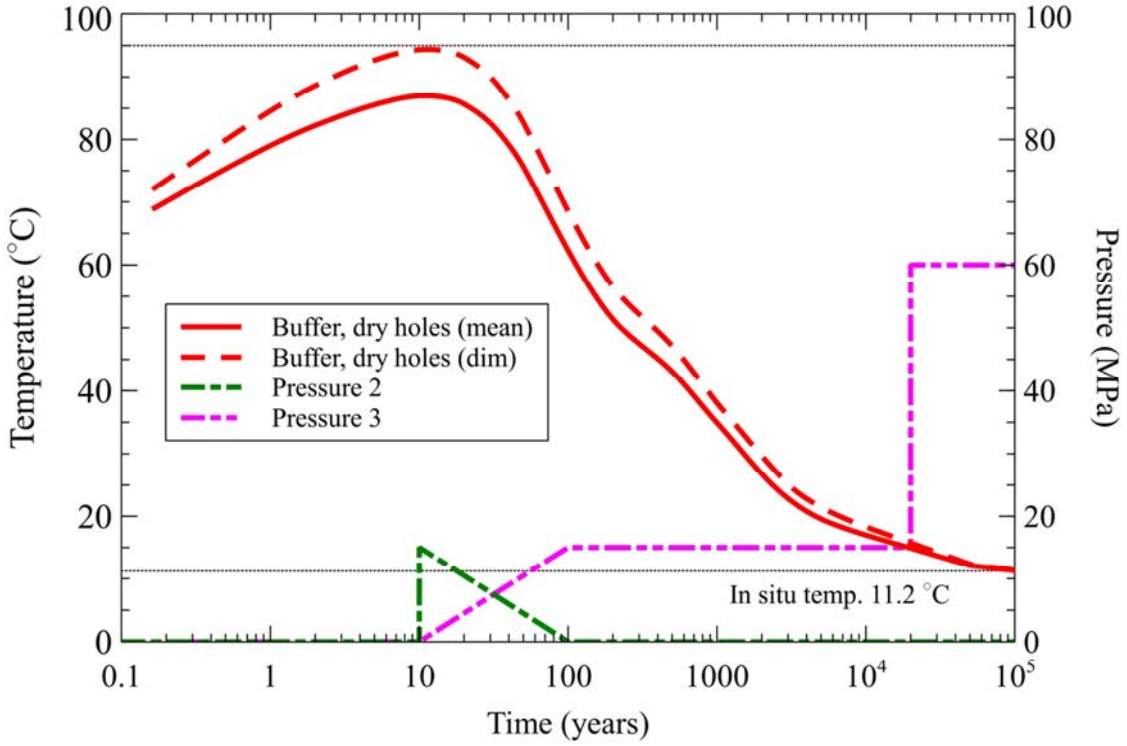

Figure 2-3. *Pressure and temperature development in dry holes, case c) and d)*

Case c). The water saturation process is assumed to start after ten years and full pressure is reached after 100 years (magenta dotted line, Pressure 3). The load component in axial direction (green dotted line, Pressure 2) is assumed to develop quickly at the canister top and will gradually be replaced by the isostatic pressure (magenta dotted line) assumed to gradually develop under 100 years and a hypothetic glacial load is applied after 20,000 years (Pressure 3).
The canister temperature is following the red solid line (mean case).

It should be emphasised for this case that the temperature in reality will drop when the swelling takes place and merge to wet-hole conditions. For the analysis, maintaining the temperature evolution is a pessimistic assumption as both the creep rate and the temperature dependent gap is overestimated.

Case d). Same as case c) except that the canister temperature is following the red dashed line (dim case).

2.2.5 Internal gas pressure effects

SKB has presented the expected pressure evolution due to gas production and thermal expansion of the gas in the canister in ”Inre övertyck i kapseln”(SKBdoc 1333208), see Figure 2-4. Taken into account that the steel lid initially is tested to be leak tight it is assumed in this analysis that the pressure acting on the copper shell will gradually build up during the first ten years to mimic a minor leakage (under the detection limit in the leak test). The time variation used in the analyses is shown in Figure 2-5.

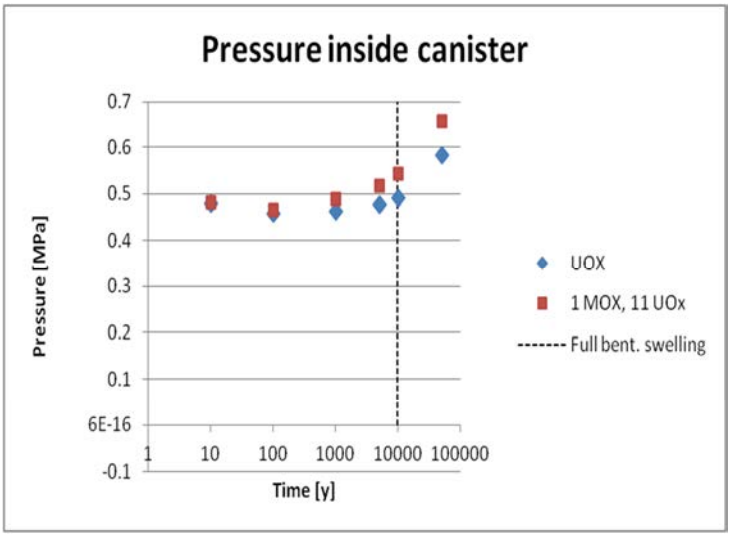

Figure 2-4. *Evolution of the internal pressure in the canister. Argon, water/hydrogen and helium from pre-pressure treatment of the fuel rods are included, see "Inre övertyck i kapseln"(SKBdoc 1333208). Full bentonite swelling is there assumed at 10,000 years as a pessimistic assumption.*

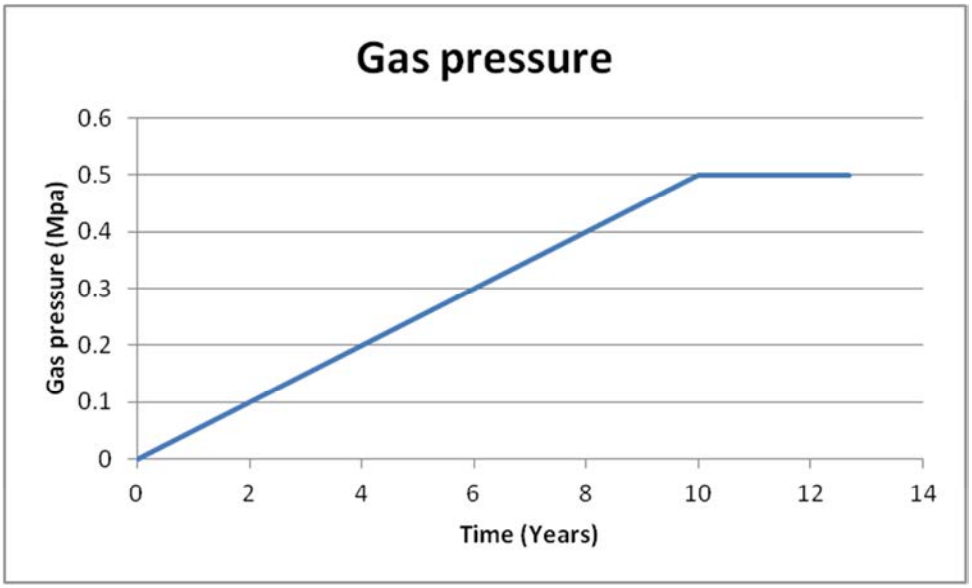

Figure 2-5. *Gas overpressure variation used in the analyses. This initial phase is not included in Figure 2-4.*

3 Simulation strategy

The performed simulations are all based on the same geometry defined in a 3-dimensionell model which will be used for verification of a simplified axi-symmetric model. It consists of a copper shell, insert (iron), steel tubes and insert lid (steel).The insert is assumed to completely consist of cast iron when defined by the axi-symmetric model.
All analyses are performed using the '*visco'-procedure in ABAQUS which will consider creep effects. The procedure works as a static analysis with special attention to the creep material definition.

4 Geometry definitions and meshes

4.1 General

The geometry is based on CAD-geometries received from SKB "Ritningförteckning för kapselkomponenter" (SKBdoc 1203875) and should therefore correspond to the current design.

Due to symmetry only one half of the system has been modelled. The mesh is generated by 3-dimensional solid elements, mainly 8-noded hexahedral (most of them using full integration technique) and a few 6-noded wedge elements, see Figure 4-1. The model size is defined by about 140,000 elements and 170,000 nodes (total number of variables about 800,000).

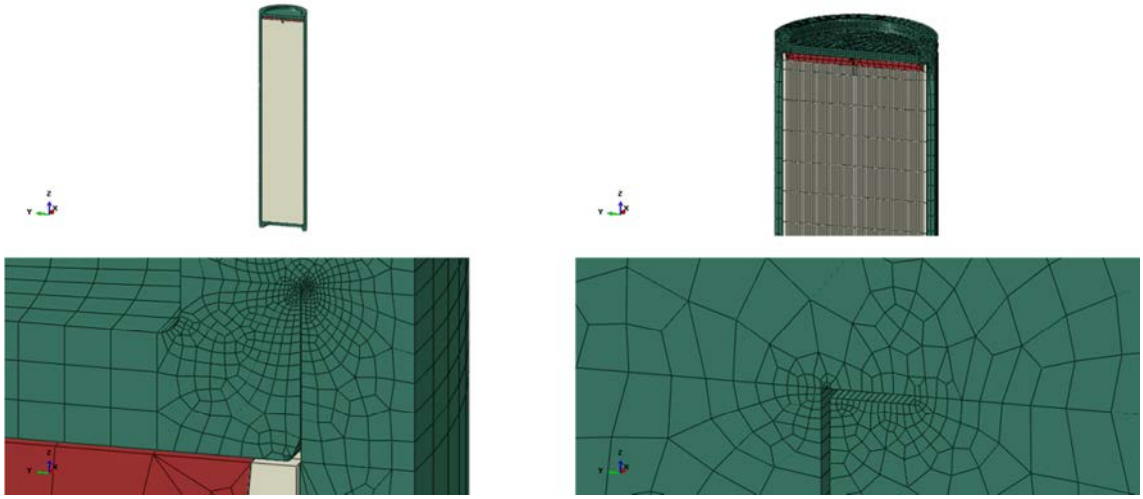

Figure 4-1. *Top left figure shows the 3D- model with mesh. Top right shows detail of the mesh, bottom left figure show details of the mesh (green – copper shell, red – steel lid, grey – insert) and bottom right details of the weld and the circumferential 3 mm root defect.*

The 3-dimensional model consists of the insert (made of nodular cast iron), the steel tubes (made of steel and tied to the insert), the insert lid (made of steel) and the surrounding copper shell. The model is only used to verify the simplified axi-symmetric model which is used for detailed analysis of how the copper shell is affected by creep caused by the temperature and pressure history until glaciations occurs.

An axi-symmetric approach is used since the main focus in this study is on the copper shell and the insert stiffness could be approximated by an axi-symmetric geometry based on previous analyses.

The axi-symmetric model neglects the steel tubes and thus only consists of the insert, the insert lid and the surrounding copper shell; see Figures 4-2 – 4-3. The mesh is then generated by 2-dimensional solid elements, mainly 4-noded quads and a few 3-noded elements. The axi-symmetric model size is defined by about 13,000 elements and 14,000 nodes (total number of variables about 36,000).

Figure 4-2. *Axi-symmetric mesh (green – copper shell, red – steel lid, grey – insert).*

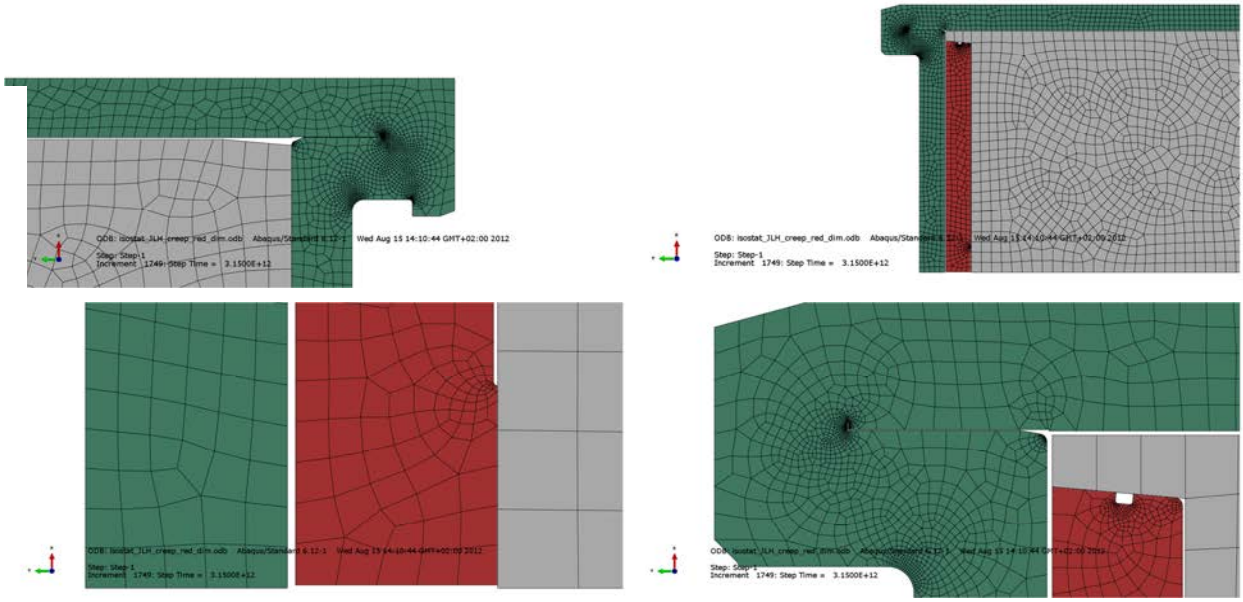

Figure 4-3. *Plot of details in the axi-symmetric model (green – copper shell, red – steel lid, grey – insert).*

4.2 Geometry of parts (3D-model)

4.2.1 Insert

The insert has been simplified regarding the square steel tubes which are assumed to be tied to the nodular cast iron insert and thus these contribute as added material to the insert. This simplification will probably overestimate stresses and strains in this region.

The insert is modelled as a homogeneous part with 3D solids, see Figure 4-4.

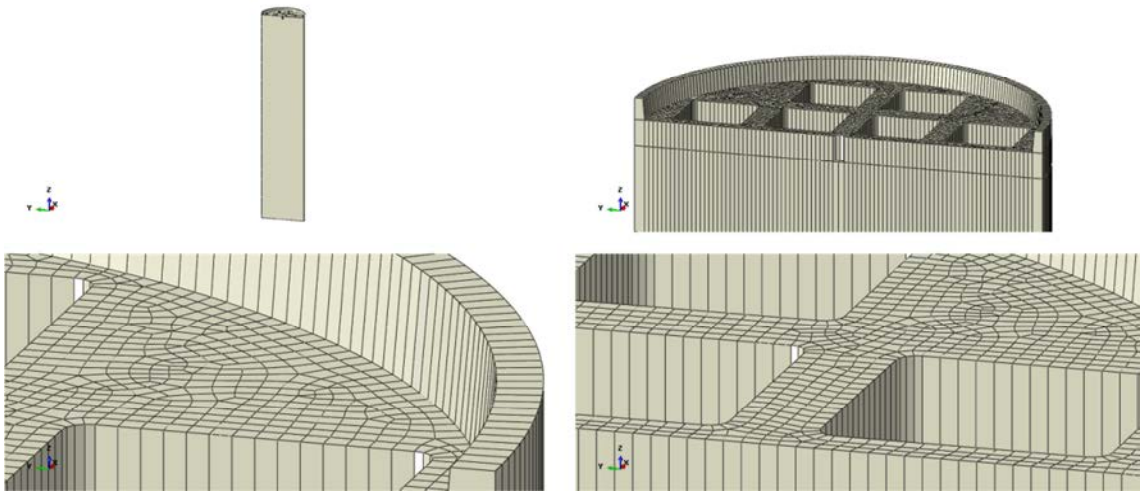

Figure 4-4. *Insert BWR geometry (top left), mesh details (top right, bottom left and bottom right).*

4.2.2 Insert lid

The insert lid is modelled with 3D solids, see Figure 4-5.

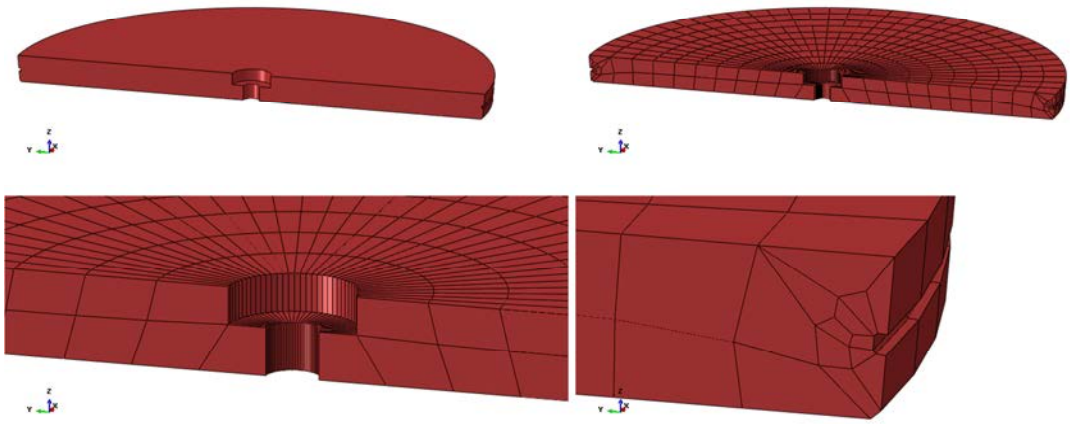

Figure 4-5. *Insert lid geometry and mesh.*

4.2.3 Copper shell

The copper shell surrounds the insert. The canister has been modelled rather accurately in order to catch “hot spots” where large strains are expected, e.g. the fillets at the bottom and top (the lid). The lid is welded to the flange (modelled by an axial slit and a root defect in radial direction with 3 mm in size) - the canister will thus act as one part, see Figure 4-6.

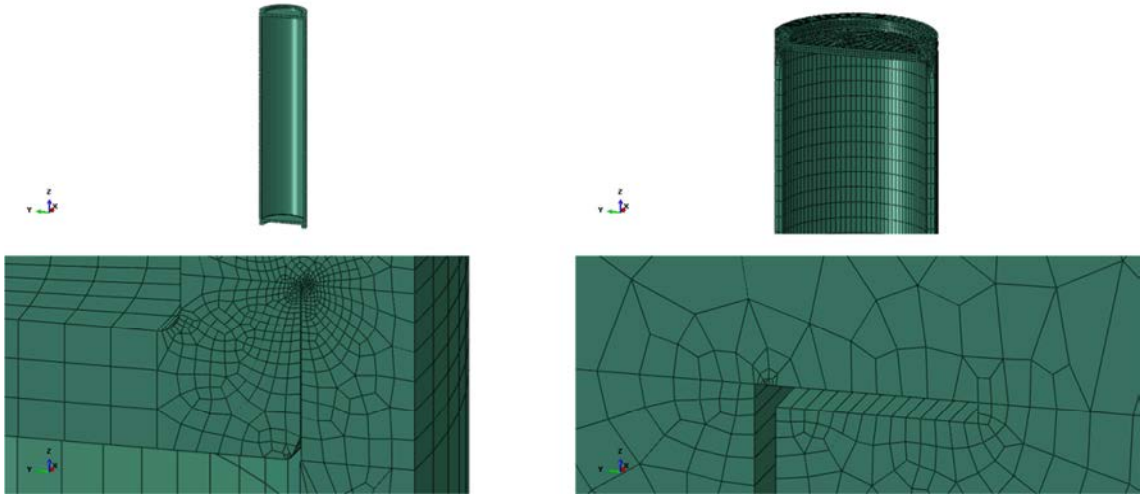

Figure 4-6*. Copper shell geometry (top left), mesh (top right), weld mesh (bottom left) and weld root (bottom right).*

5 Material models

The finite element code ABAQUS version 6.12 (ABAQUS 2012) was used for the calculations. The materials have been modelled as elastic-plastic with stress-strain properties that correspond to each material and the applied shear load induced strain rate, when applicable.

5.1 Nodular cast iron (insert)

The material model for the insert"Dragprovning av gjutjärn" (SKBdoc 1201865), is based on a von Mises' yield surface with elastic behaviour defined by Young's modulus and the Poisson's ratio and the plastic behaviour defined through yield surface (true stress) versus plastic strain (defined as logarithmic strain), see Table 5-1 and Figure 5-1.

The experiments were performed at 0^{o} C.

Table 5-1. *Stress-strain definition for the insert.*

Plastic Strain (%)	Stress (MPa)			
	Strain rate=0	Strain rate=$2x10^{-4}$	Strain rate=0.5	Strain rate factor at strain rate=0.5
0	293	293	348	1.19
1	324	324	367	1.13
2	349	349	385	1.10
3	370	370	406	1.10
4	389	389	423	1.09
5	404	404	438	1.09
6	418	418	451	1.08
7	428	428	464	1.08
8	438	438	474	1.08
9	447	447	483	1.08
10	456	456	490	1.07
11	465	465	498	1.07
12	472	472	504	1.07
13	478	478	510	1.07
14	484	484	516	1.07
15	488	488	520	1.07
16	491	491	521	1.06

The strain rate dependency is defined by assuming that the yield surface is proportional to the strain rate factor (at the strain rate 0.5 1/s the factor 1.08 has been chosen and at strain rate 0 1/s the factor is 1.0).The instantaneous strain rate factor is then linearly interpolated between 1 and 1.08 using the instantaneous strain rate.

Furthermore, Young's modulus E = 166 GPa and Poisson's ratio ν = 0.32 (Raiko et al. 2010).

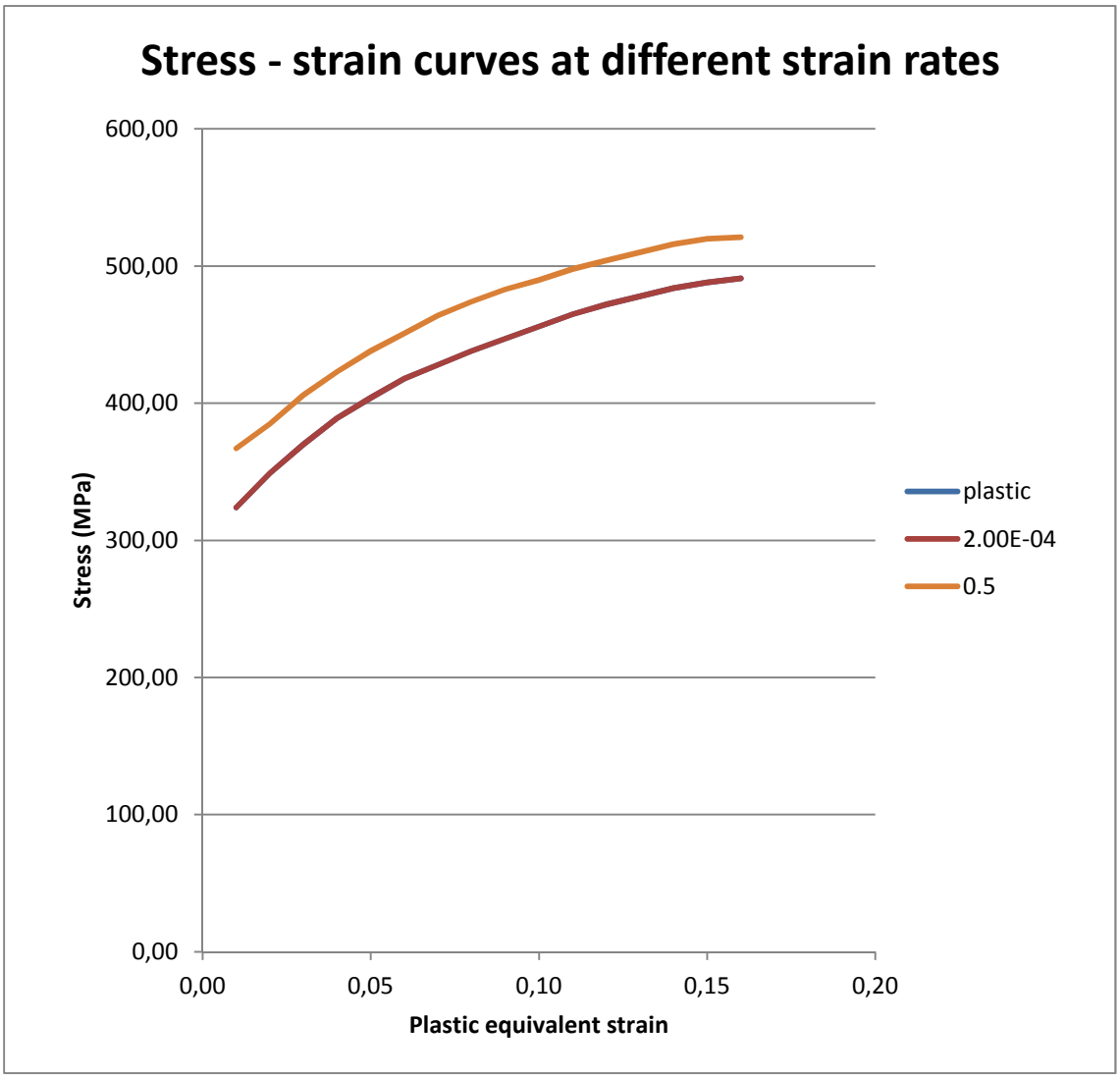

Figure 5-1. *Stress [MPa] versus plastic strain at different plastic strain rates[1/s] for cast iron. Note that the base (plastic) is defined to coincide with strain rate = $2x10^{-4}$ [s^{-1}].*

5.2 Steel (channel tubes in the insert)

The material model for the channel tubes in the insert is based on a von Mises' material model with elastic behaviour defined by Young's modulus and the Poisson's ratio. The plastic behaviour is defined through yield surface (true stress) versus plastic strain (using logarithmic strain).

The steel channel tubes are manufactured by steel S355J2H, for example Domex 355 MC B. SKB has earlier supplied test data for the yield point of their material, however no stress-strain data to be used in a plastic analysis. The stress-strain curve for Domex 355 MC B (SSABDirect 2008) can be scaled using the yield stress and tensile ultimate strength measured by SKB, Re = 412 MPa (yield stress) and Rm = 511 MPa (ultimate stress). With this procedure a simplified stress-strain curve is obtained as shown in Table 5-2 and Figure 5-2.

Table 5-2. Stress-strain definition for channel tubes used in the insert.

Strain (%)	Stress (MPa)	Log Strain (%)	True Stress (MPa)
0	0	0	0
0.196	412	0.196	412
15	511	14.3	587
20	511	18.5	613

Furthermore, Young's modulus E = 210 GPa and Poisson's ratio ν = 0.3 according to Raiko et al. (2010, Table 4-3).

The data with the lowest value from the experiment has been chosen for the yield surface. However, the plasticity definition for the steel channel tubes has minor influence on the overall results due to almost elastic behaviour.

5.3 Steel (insert lid)

The material model for the insert lid is based on a von Mises yield surface with elastic behaviour defined by Young's modulus and the Poisson's ratio. The plastic behaviour is defined through yield surface (true stress) versus plastic strain (calculated as logarithmic strain).

Manufacturing drawings for the lid specify steel S355J2G3. Strain versus stress for steel Domex 355 MC with Re = 389 MPa (yield stress) and Rm = 484 MPa (ultimate stress) can be found from (SSAB (2008). According to SS-EN 10025-2:2004, the material S355 with nominal thickness 40-63 mm has Re = 335 MPa (yield stress) and Rm = 470-630 MPa (ultimate stress). Scaling stress-strain curves for Domex 355 by the minimum values given in SS-EN 10025-2:2004 implies the simplified material definition (engineering data) shown in Table 5-3.

Table 5-3. Nominal stress-nominal strain definition for the insert lid.

Strain (%)	Stress (MPa)	Log Strain (%)	True Stress (MPa)
0	0	0	0
0.1595	335	0.1593	335
15	470	13.98	540
20	470	18.2	564

Furthermore, Young's modulus E = 210 GPa and Poisson's ratio ν = 0.3 according to Raiko et al. (2010, Table 4-2).

5.4 Copper model

The stress-strain properties of the copper in the copper shell were investigated by Swerea KIMAB, and the results are then represented by a creep material model developed by Rolf Sandström, see Sandström and Andersson (2008), Jin and Sandström (2008) and Sandström et al. (2009).

The short and long term duration has been simulated using the creep model implemented in ABAQUS as a user supplied subroutine (CREEP) which is essentially based on eqn. 50 in Andersson-Östling and Sandström (2009).

6 Contact definitions

All the boundaries of the buffer, the copper shell, the insert and the insert lid interact through contact surfaces allowing finite sliding. All contact surfaces have friction at sliding with no cohesion and the friction coefficient 0.1, i.e. the friction angle (ϕ) is 5.7˚ and the cohesion (c) is 0 kPa.

The contact is released when the contact pressure is lost.

The 3D model has a few contact pairs which are tied together (tied means that the surfaces are constrained together and will not allow for opening/closing or sliding). This is done in order to improve the numerical convergence rate. This applies at the contact pairs between the insert and insert lid and also at the bottom of insert and copper shell bottom.

The axi-symmetric model has no tied contacts and has contact definitions between all parts.

7 Initial conditions

Initial conditions are defined as:

Temperature for all nodes in the model as 293 K. The temperature change during the analysis is specified through an amplitude definition (magnitude versus time).

8 Boundary conditions

For the 3D model symmetry conditions have been specified for the symmetry plane (displacements in the normal direction to the symmetry plane are prescribed to zero). The buffer and the rock is not included and thus rigid body motion in the vertical direction (z-direction) and in the y-direction must be prevented. For the 3D model the copper shell has prescribed zero displacements in the vertical direction at the base, see Figure 8-1, which means that most of vertical displacements occurs at the top and imply a pessimistic estimate of strains at the top.

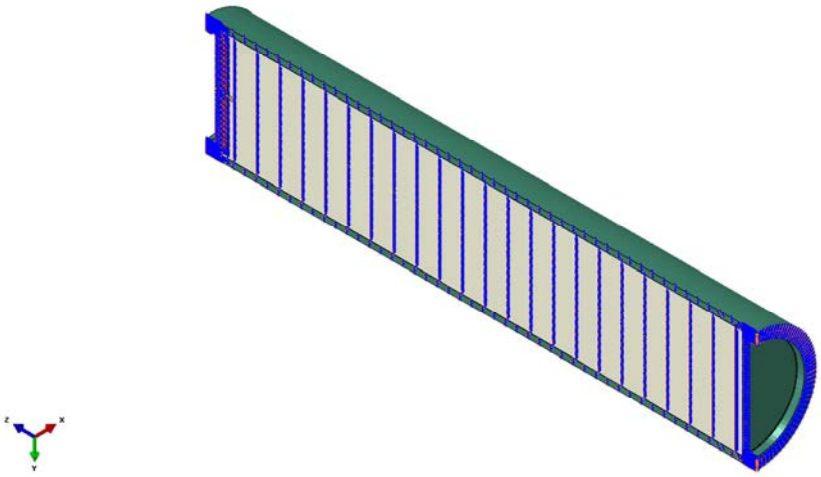

Figure 8-1. *Prescribed boundary conditions, 3D model. Symmetry conditions for the yz-plane and zero vertical displacements (z-direction) at the copper base flange. Furthermore is one node in the copper shell constrained in y-direction to prevent rigid body motion. Boundary conditions are illustrated with blue and orange colours.*

For the axi-symmetric model two cases have been analyzed (Figure 8-2):

- one where the bottom flange is prescribed zero displacements in the vertical direction (y-direction) implying a worst case for the upper weld, since most of the vertical displacements occurs at the top
- one where the base plate have a circle at the center which is prescribed zero displacements in the vertical direction implying a worst case for the lower weld, since with this boundary condition the cylindrical shell can move downwards caused by gravity and axial load at the copper lid.

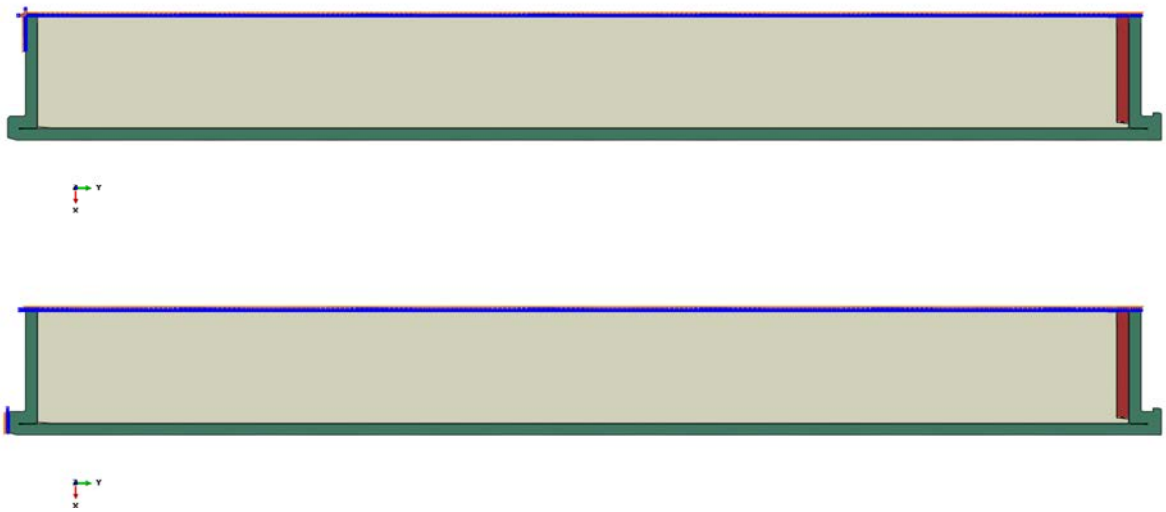

Figure 8-2. *Prescribed boundary conditions, axi-symmetric model. Upper plot used for worst case for the lower weld and the bottom plot used for worst case for the upper weld. The boundary conditions are illustrated by blue (rotational components) and orange (normal displacements) colours.*

9 Calculations

9.1 General

9.1.1 Creep analysis until glaciations

The reference case for BWR is based on buffer material consisting of Na-bentonite converted to Ca-bentonite with density 2050 kg/m^3. The four cases a-d, according to section 2.2.1, have been analyzed and are denoted as follows:

Dimensioning temperature history when buffer is placed in a dry hole (red_dim).
Jobnames are isostat_JLH_creep_red_dim and half_3d_JLH_red_dim (3D-analysis)

Mean temperature history when buffer is placed in a dry hole (red_mean).
Jobname is isostat_JLH_creep_red_mean

Dimensioning temperature history when buffer is placed in a wet hole (blue_dim).
Jobname is isostat_JLH_creep_blue_dim

Mean temperature history when buffer is placed in a wet hole (blue_mean).
Jobname is isostat_JLH_creep_blue_mean

9.1.2 Analysis approach

The numerical calculations are performed using the FE-code ABAQUS version 6.12 (ABAQUS 2012) assuming non-linear geometry and material definitions. This means that all non-linearities defined by the input will be considered such as large displacements, large deformations, non-linear interactions (contact) and non-linear materials. All non-linear contributions will be used when forming the equations to be solved for each equilibrium iteration. The long term analyses are based on static response but the results will depend on the time used for the simulation since rate-dependent material data is used. The code will choose suitable time-increments for the loading based on (in most cases) default convergence tolerances.

9.2 Long term analyses

The long term analyses (100 000 years) consist of one step where the loading (temperature and pressure) is specified by amplitude definitions (magnitude versus time).

The results are shown in Appendix 1-4.

10 Results

For each analysis a large amount of results are available. However, only a few values are reported for the most extreme case, isostat_JLH_creep_red_dim, since it is enough for the evaluation of the analyses.

When creep is defined by a user defined subroutine all inelastic strains are calculated as equivalent creep strain and thus the traditional plastic strain is included in the creep strain. The subroutine has as input Mises stress and returns creep increment and the derivative $\frac{\partial \varepsilon_{cr}}{\partial \sigma_{Mises}}$. Based on this ABAQUS calculates strain components and also the equivalent creep strain (see below). The definitions of equivalent creep strain, equivalent plastic strain and equivalent stress (Mises) are (ABAQUS 2012):

MISES

Mises equivalent stress, defined as

$$q = \sqrt{\tfrac{3}{2}\mathbf{S} : \mathbf{S}},$$

where $\mathbf{S}$ is the deviatoric stress tensor, defined as $\mathbf{S} = \boldsymbol{\sigma} + p\,\mathbf{I}$, where $\boldsymbol{\sigma}$ is the stress, p is the equivalent pressure stress (defined below), and $\mathbf{I}$ is a unit matrix. In index notation

$$q = \sqrt{\tfrac{3}{2} S_{ij} S_{ij}},$$

where $S_{ij} = \sigma_{ij} + p\,\delta_{ij}$, $p = -\frac{1}{3}\sigma_{ii}$, and δ_{ij} is the Kronecker delta.

PEEQ

Equivalent plastic strain. This identifier also provides a yes/no flag (1/0 on the output database) telling if the material is currently yielding or not (AC YIELD: "actively yielding"; that is, the plastic strain changed during the increment).

The equivalent plastic strain is defined as $\bar{\varepsilon}^{pl}|_0 + \int_0^t \dot{\bar{\varepsilon}}^{pl} dt$, where $\bar{\varepsilon}^{pl}|_0$ is the initial equivalent plastic strain.

The definition of $\dot{\bar{\varepsilon}}^{pl}$ depends on the material model. For classical metal (Mises) plasticity $\dot{\bar{\varepsilon}}^{pl} = \sqrt{\frac{2}{3}\dot{\boldsymbol{\varepsilon}}^{pl} : \dot{\boldsymbol{\varepsilon}}^{pl}}$.

CEEQ

Equivalent creep strain, defined as $\int_0^t \dot{\bar{\varepsilon}}^{cr} dt$.

The definition of $\dot{\bar{\varepsilon}}^{cr}$ depends on the material model. For classical metal (Mises) creep $\dot{\bar{\varepsilon}}^{cr} = \sqrt{\frac{2}{3}\dot{\boldsymbol{\varepsilon}}^{cr} : \dot{\boldsymbol{\varepsilon}}^{cr}}$.

Additional results can be found in the appendices for the time 10 years (helium gas pressure applied) and the time 100,000 years (glaciation load applied):

Appendix 1 shows results for isostat_JLH_creep_red_dim

Appendix 2 shows results for isostat_JLH_creep_red_mean

Appendix 3 shows results for isostat_JLH_creep_blue_dim

Appendix 4 shows results for isostat_JLH_creep_blue_mean

10.1 Axi-symmetric analysis, worst case boundary condition for the lid area

The worst case for the upper weld in the copper shell arises when the bottom flange is prescribed to zero displacements, see Figure 8-2 where the bending effect from the applied axial pressure on the copper lid implies the largest possible strains in the upper weld.

The creep strain in the copper shell after 100 000 years based on the axi-symmetric analysis is presented in Figure 10-1. The results are very similar to the results from the 3D analysis (Figure 10-33) but gives somewhat higher strain levels and also larger affected areas except for a local area in the root of the lid weld. Hence the use of the axi-symmetric model is pessimistic.

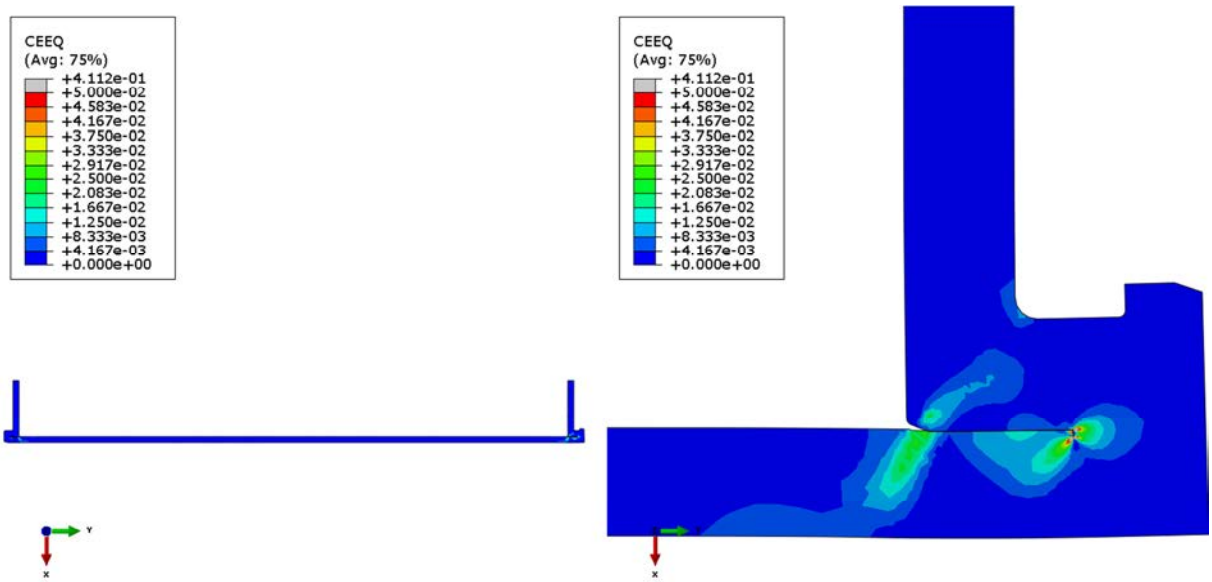

Figure 10-1. *Equivalent creep strain (CEEQ) in the (top of) copper shell after 100 000 years, axi-symmetric analysis. This represents the situation after glaciations. Distorted element 946 removed before generating the contour plots, see also Figures 10-8 and 10-9.*

Mises and CEEQ (equivalent creep strain) doesn't contain any information about directions and thus also principal values are of interest. Figures 10-2 to 10-5 show maximum and minimum principal values for stress and logarithmic strain (the logarithmic total strain components, LE, also include the inelastic strain components, CE – creep strain, and LE and CE almost coincide since the elastic part is much smaller).

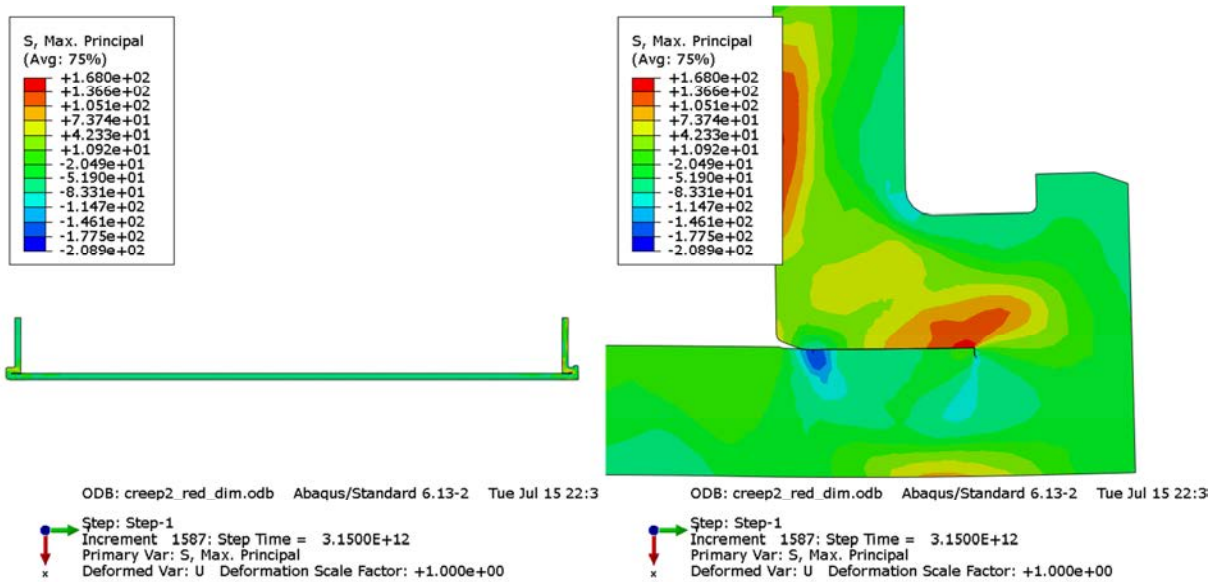

Figure 10-2. *Maximum principal stress [MPa] in the copper shell after 100 000 years, axi-symmetric analysis. This represents the situation after glaciations. No elements removed.*

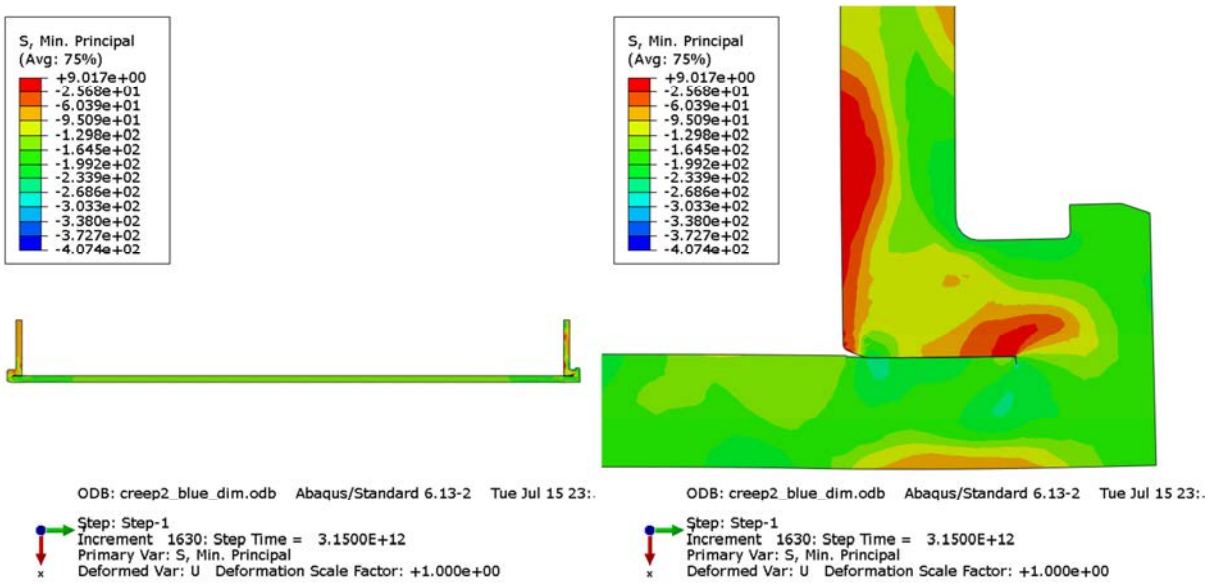

Figure 10-3. *Minimum principal stress [MPa] in the copper shell after 100 000 years, axi-symmetric analysis. This represents the situation after glaciations. Peak value at the crack tip. No elements removed.*

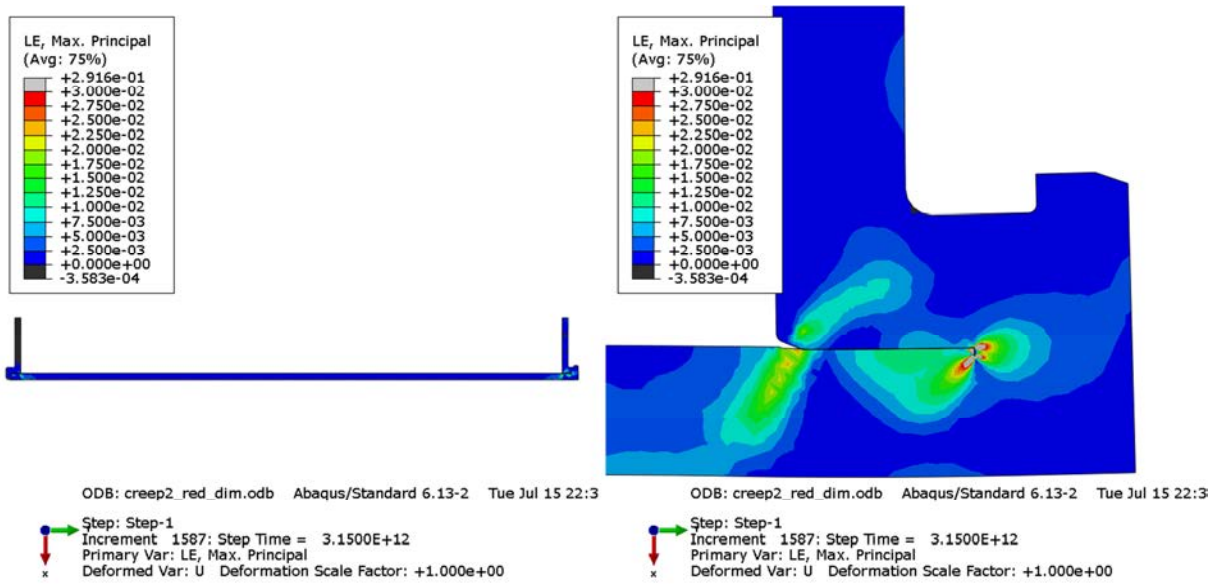

Figure 10-4. *Maximum principal strain in the copper shell after 100 000 years, axi-symmetric analysis. This represents the situation after glaciations. Peak value at the crack tip. No elements removed.*

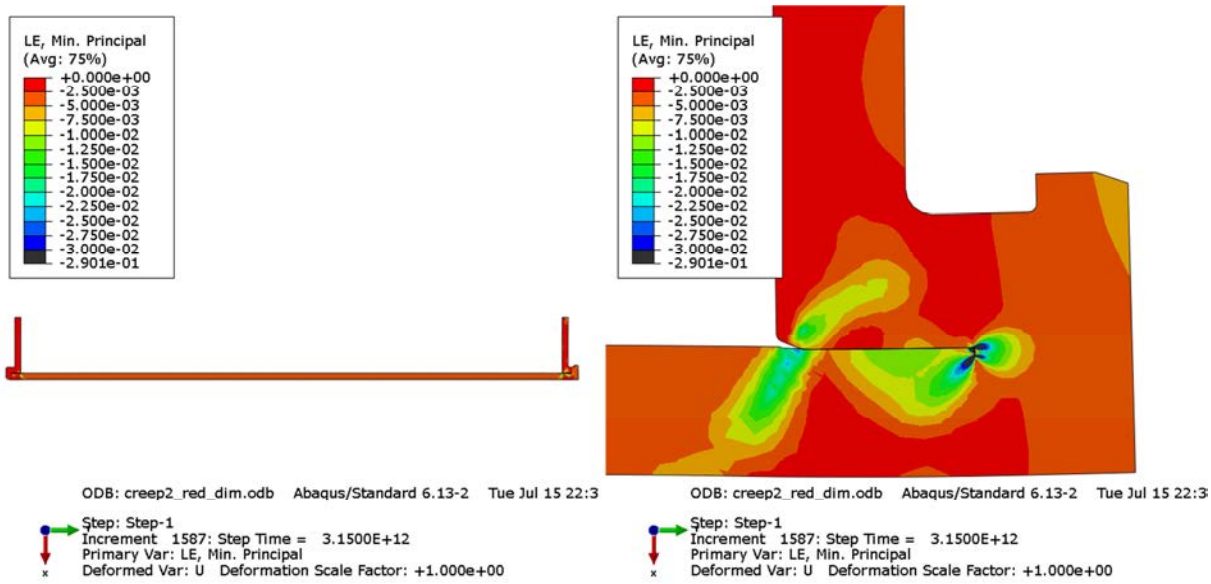

Figure 10-5. *Minimum principal strain in the copper shell after 100 000 years, axi-symmetric analysis. Peak value at the crack tip. No elements removed.*

Comparing Figures 10-4 and 10-5 shows that maximum tension and compression strains are almost identical (is expected since the out of plane strain is much smaller and that the inelastic strains are based on no volume change). Comparing Figures 10-2 and 10-3 shows a different behaviour for the principal stresses with much higher values for compressive stresses.

Figures 10-6 to 10-19 show the mesh and detailed results at the top and bottom of the copper shell without removing any elements in the plotted regions.

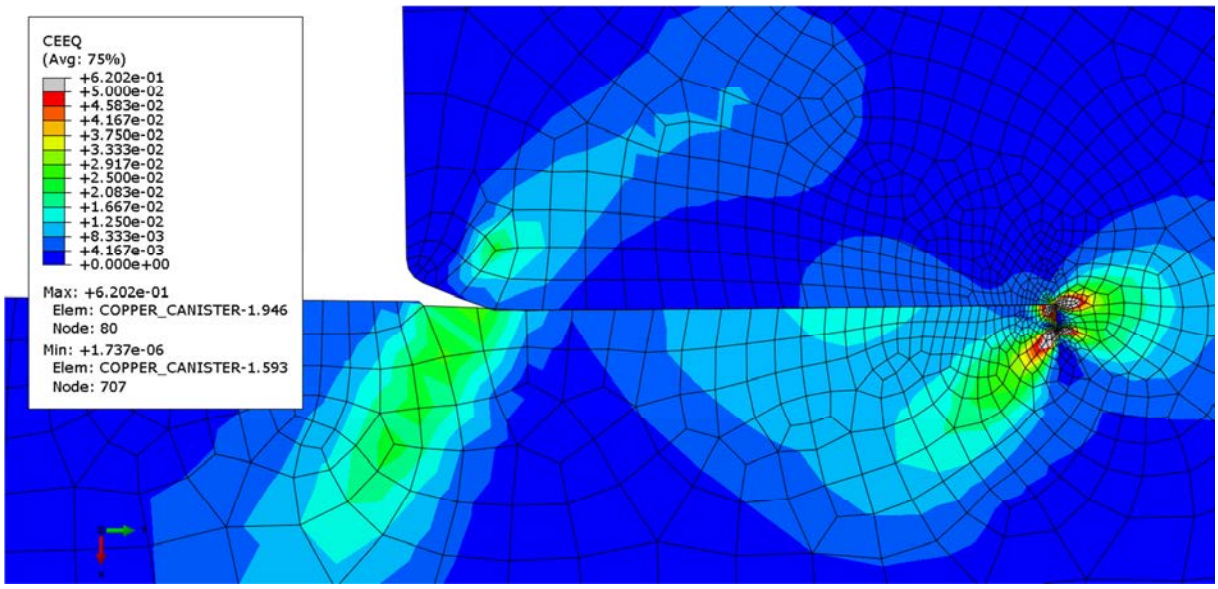

Figure 10-6. *Equivalent creep strain (CEEQ) at the top of the copper shell after 100 000 years, axi-symmetric analysis. This represents the situation after glaciations. No elements removed.*

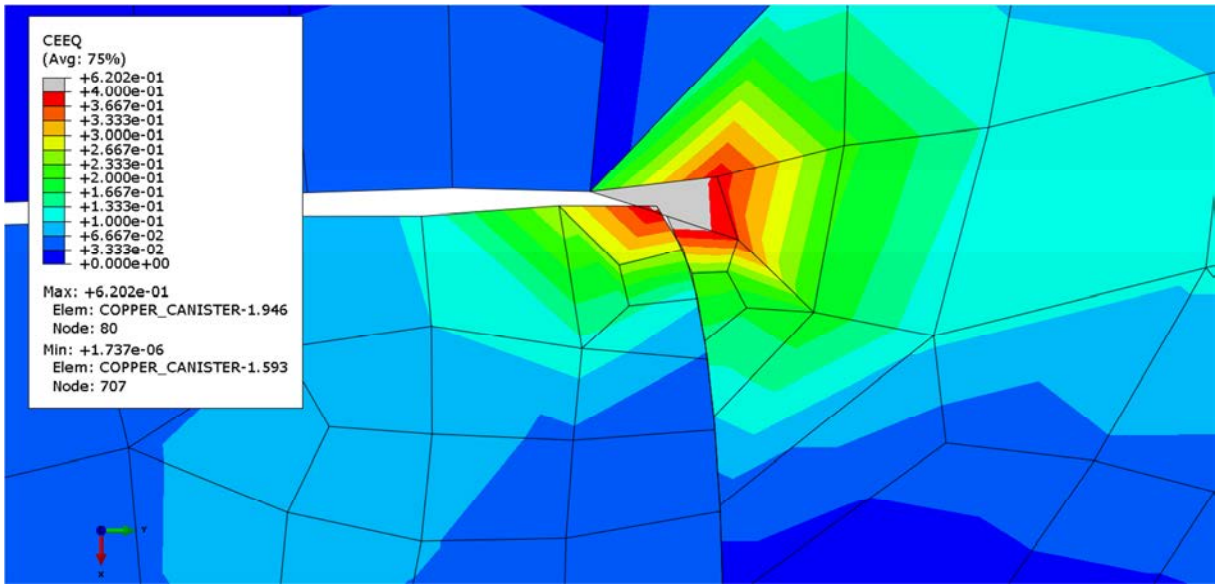

Figure 10-7. *Equivalent creep strain (CEEQ) at the top of the copper shell after 100 000 years, axi-symmetric analysis. This represents the situation after glaciations. The peak value is very local and occurs in a highly distorted element. No elements removed.*

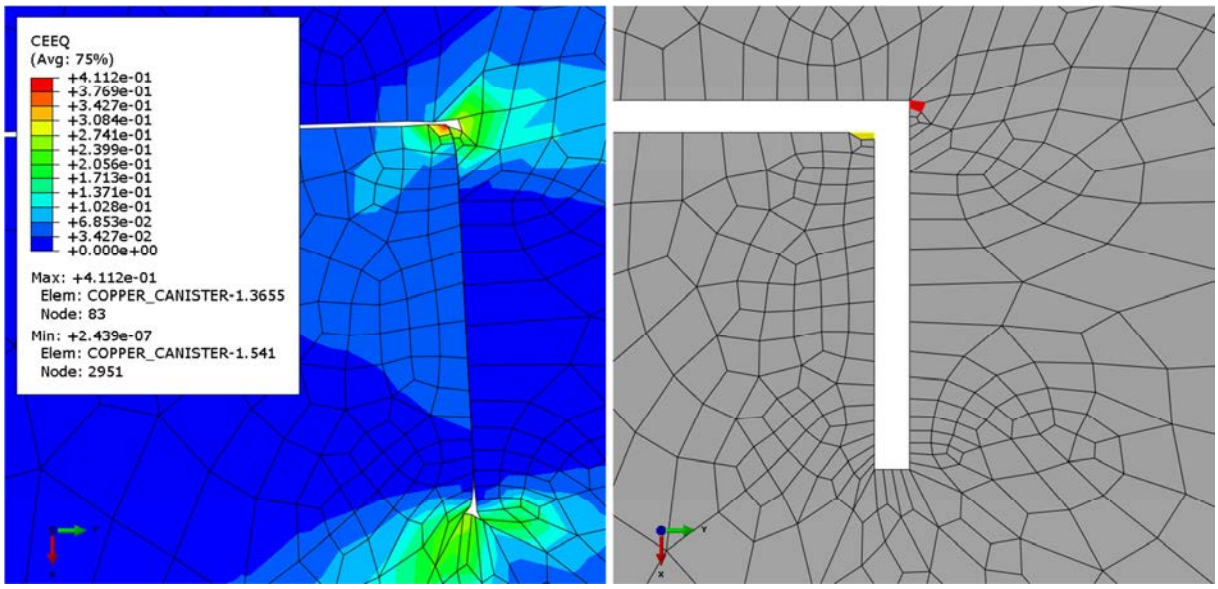

Figure 10-8. *Equivalent creep strain (CEEQ) at the top of the copper shell after 100 000 years, axi-symmetric analysis. This represents the situation after glaciations. Element 946 (red in the right plot showing un-deformed geometry) is removed before generating the contour plot. Element 3655 (yellow in the right plot) is used for history plot of creep strain components (Figure 10-12).*

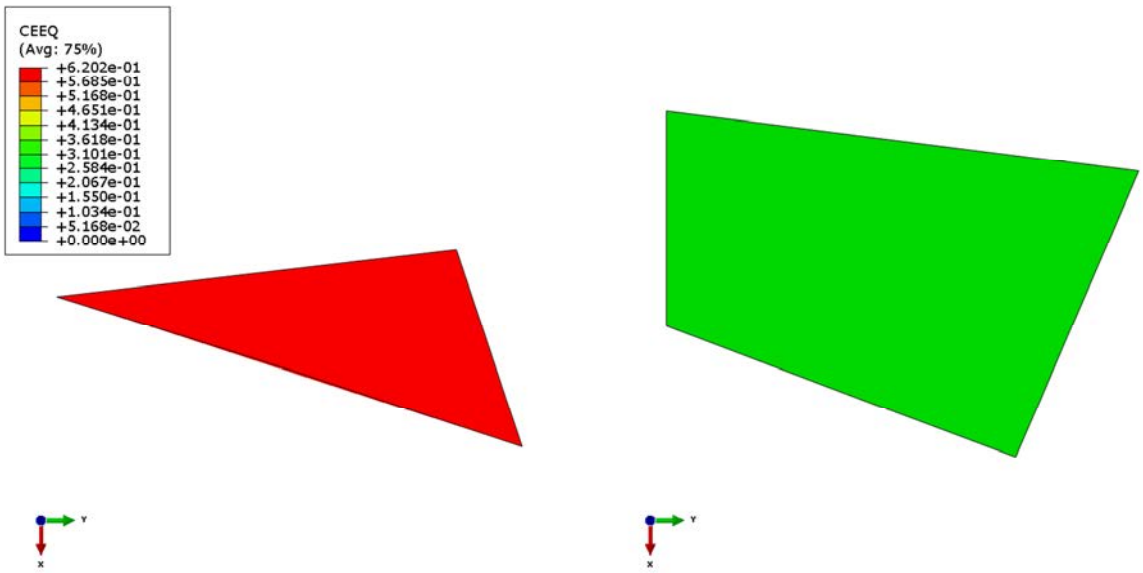

Figure 10-9. *Equivalent creep strain (CEEQ) for the distorted element (946) in the copper shell after 100 000 years, axi-symmetric analysis. This represents the situation after glaciations. Note that the element has been distorted to a triangular shape and has not any representative results. The original shape (green colour) is shown in the right plot.*

As can be seen in Figure 10-9 element distorsion occurs at the geometric discontinuity at the end of the slit. This results in a very local strain peek which is judged as a non-relevant result.

The principal strains in the top weld area are illustrated in Figures 10-10 and 10-11.
The in plane strains are represented by arrows,
Arrows denoted "< >" indicate tension and arrows denoted " > < " indicate compression.
The magnitude for the strains are given according to the colour palette but also indicated by the length of the arrows.

The out of plane principal strains are indicated by the symbol "+" but too small to be noticed. The magnitude for the strains are given according to the colour palette but are also indicated by the size of the symbols.

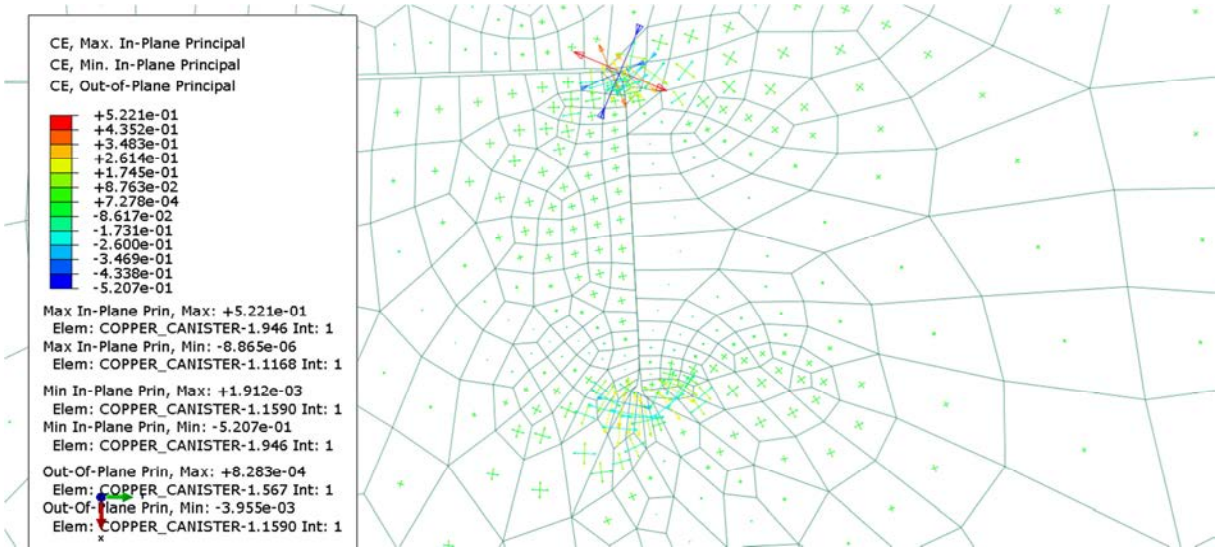

Figure 10-10. *Principal creep strains at the top of the copper shell after 100 000 years, axi-symmetric analysis. This represents the situation after glaciations.*

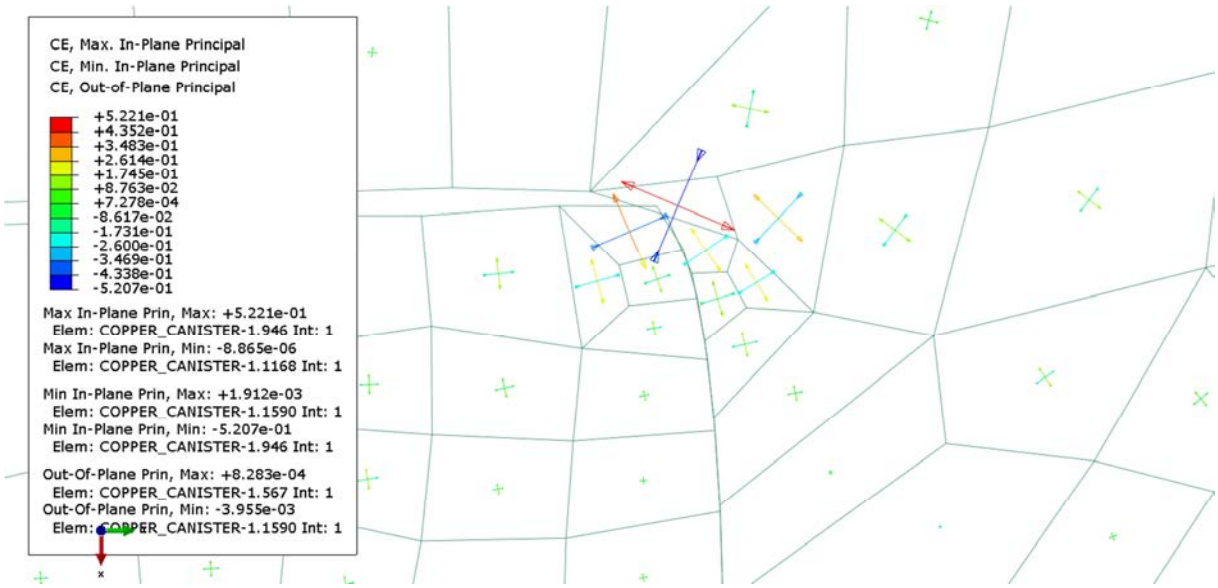

Figure 10-11. *Principal creep strains at the root area of the weld in the copper lid after 100 000 years, axi-symmetric analysis. This represents the situation after glaciations.*

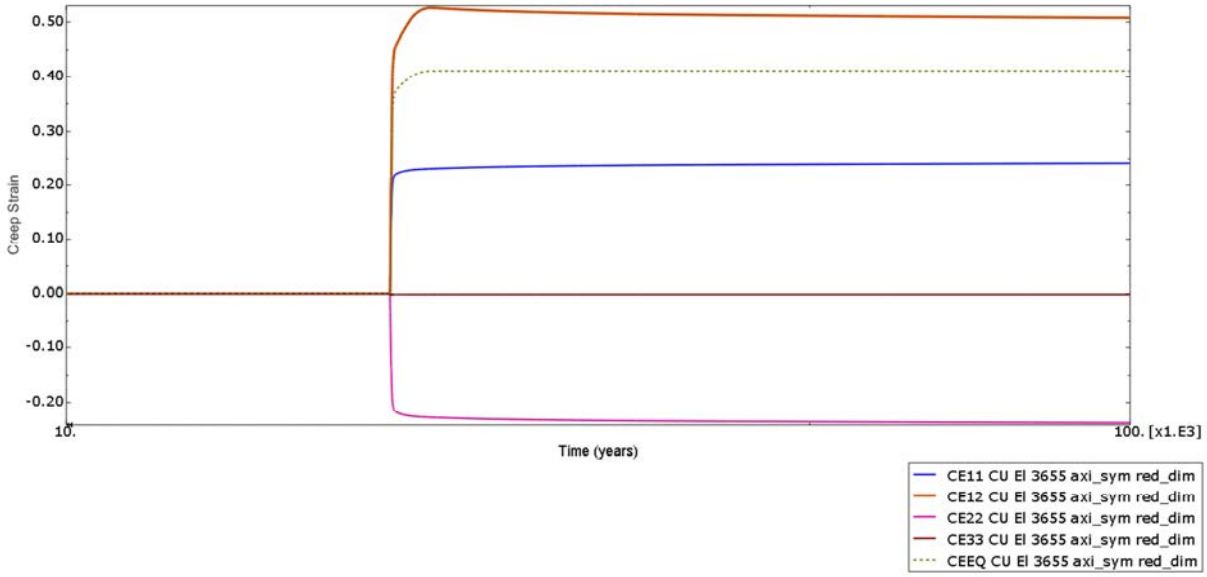

Figure 10-12. *Creep strain direct components and creep equivalent strain versus time for element 3645 (see Figure 10-8), axi-symmetric analysis. CE12 (shearing in xy-plane) shows largest magnitude.*

Analysis of the copper shell area close to the start of the slit.

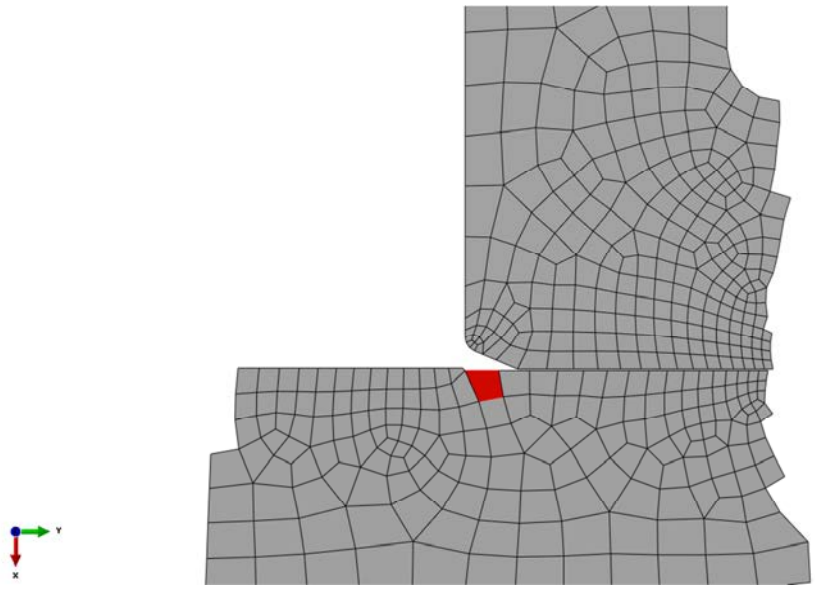

Figure 10-13. *Undeformed mesh at the top of the copper shell where large magnitude of the equivalent creep strain occurs close to the start of the slit. The red element (element number 1155) is used for history plot (Figure 10-16) of creep strain components.*

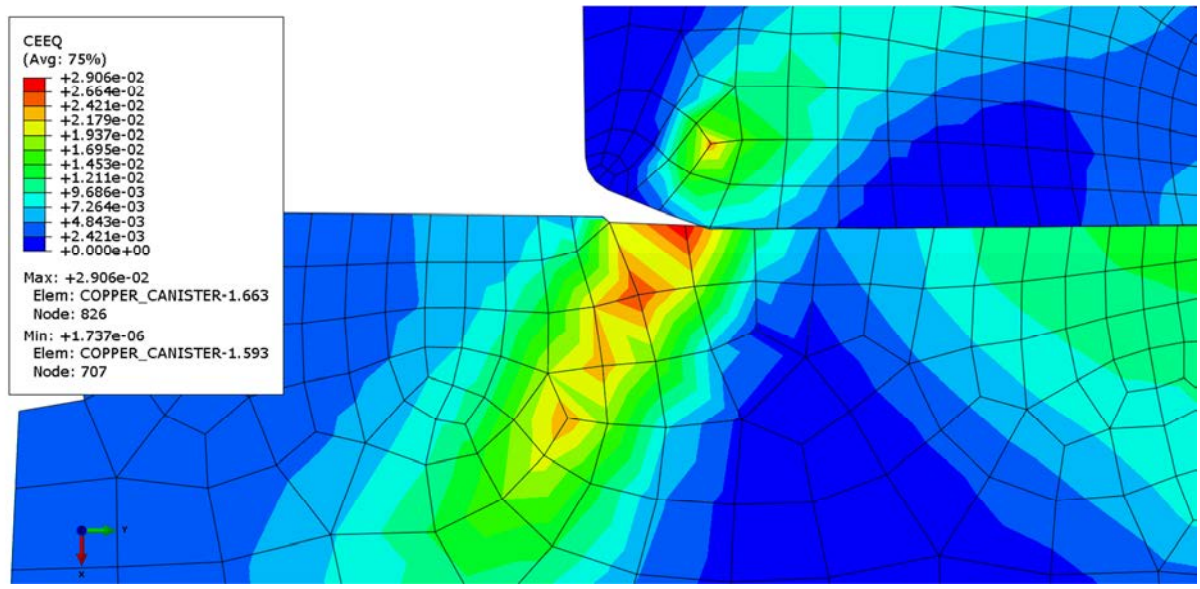

Figure 10-14. *Equivalent creep strain (CEEQ) at the top of the copper shell after 100 000 years, axi-symmetric analysis. This represents the situation after glaciations.*

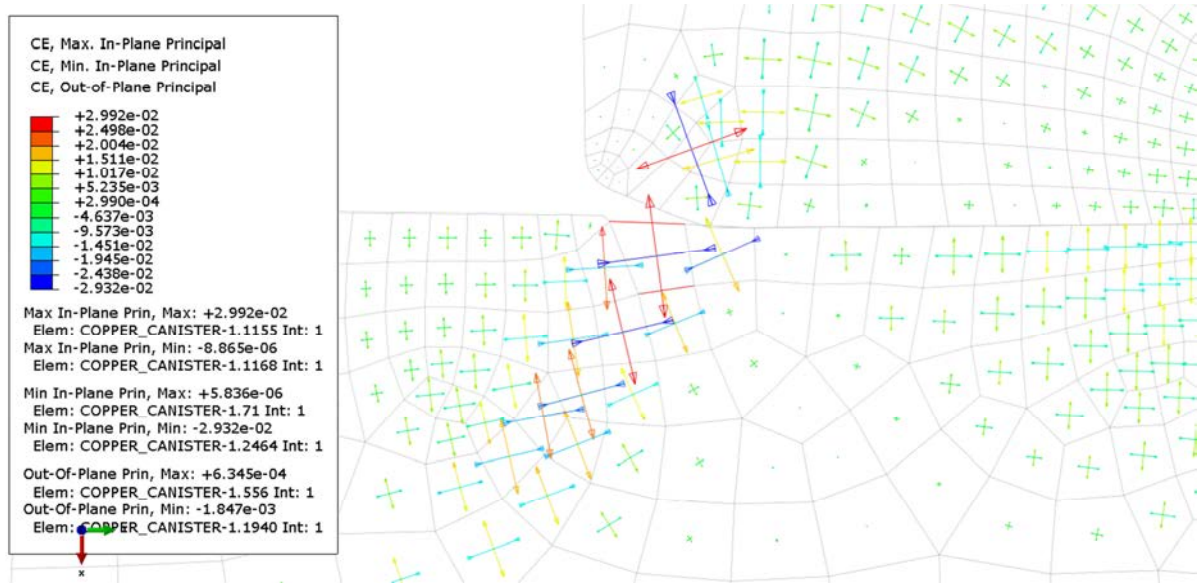

Figure 10-15. *Principal creep strain at the top of the copper shell after 100 000 years, axi-symmetric analysis. This represents the situation after glaciations.*

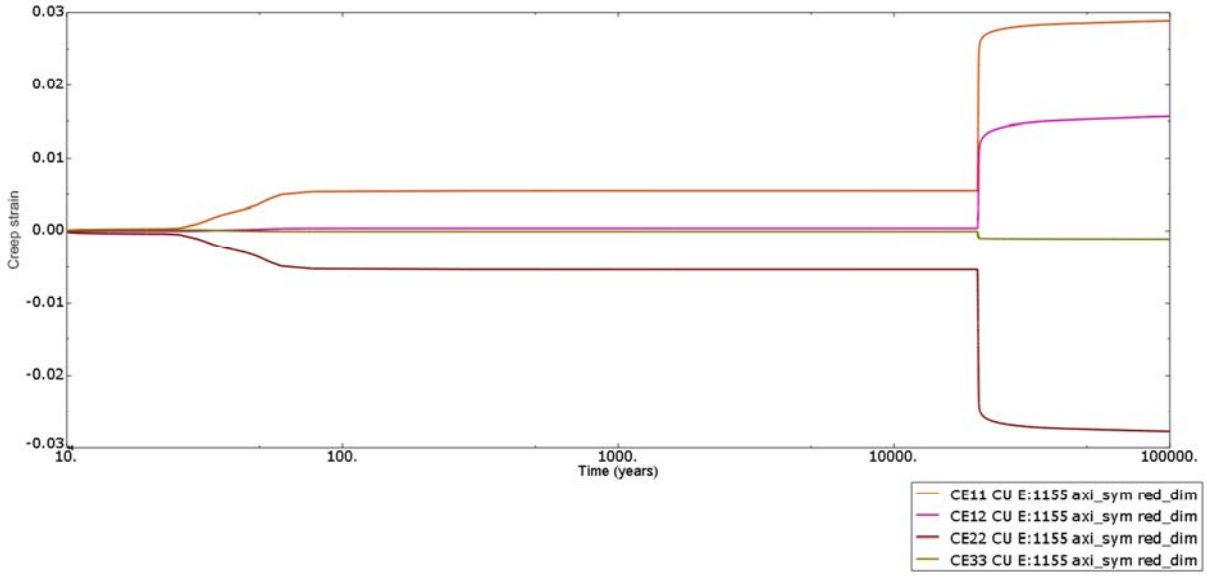

Figure 10-16. *Creep strain direct components versus time for element 1155 (see Figure 10-13), axi-symmetric analysis. CE11 (direct component in radial direction) shows largest magnitude.*

The copper shell and the cast iron insert have different coefficient of thermal expansion which means that the copper shell will expand more when the temperature is increasing. The external pressure will compress the copper shell until it gets in contact with the insert. A following temperature decrease will then eventually increase the creep strain in the copper shell.

However, the difference in the coefficient of thermal expansion for copper and iron ($1.7*10^{-5}$ respectively $1.18*10^{-5}$) is rather small which will only contribute with additional thermal strains of about $50*(1.7-1.18)*10^{-5}=2.6*10^{-4}$ for 50 ^{o}C temperature increase.

Figure 10-17 shows how all creep strain components change when the external pressure is increased to 60 MPa and from the figure it is obvious that the shear strain (CE12) is the component most affected. The component CE11 is in the radial direction, CE22 is in the axial direction, CE33 is in the hoop direction and CE12 is shearing in the radial/axial plane.

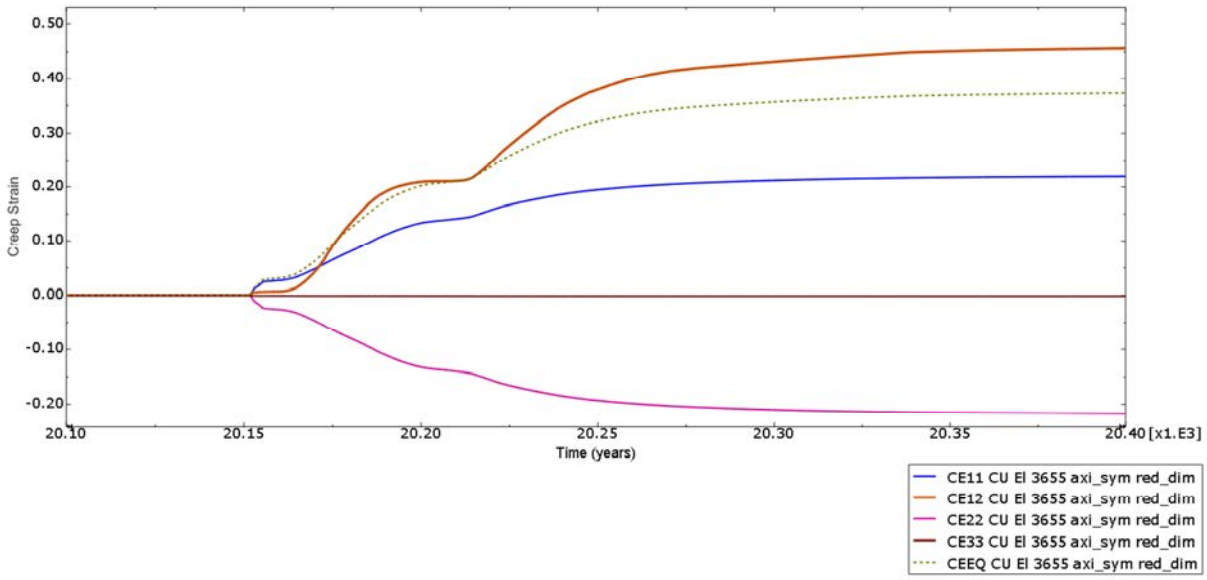

Figure 10-17. *Creep strain components and creep equivalent strain in the time window close to when the external pressure is increased to 60 MPa. Maximum creep strain is about 45% and occurs for CE12 for the axi-symmetric case.*

Figure 10-18 shows displacements at the outer corner for the insert and the copper shell. Also the gap between these nodes is plotted. The temperature is increased for 10 years implying a gap increase. After 10 years the axial pressure is applied implying a gap decrease. Increasing the outer pressure (15 MPa is reached after 100 years) results in a gap increase because only the radial component is increasing which forces the copper shell to move upward. The temperature is then slowly decreased to about 10^{o} C which causes the gap to slightly decrease. Increasing the external pressure (axial and radial) to 60 MPa implies further decrease of the gap and at the end of the process the gap is almost closed.

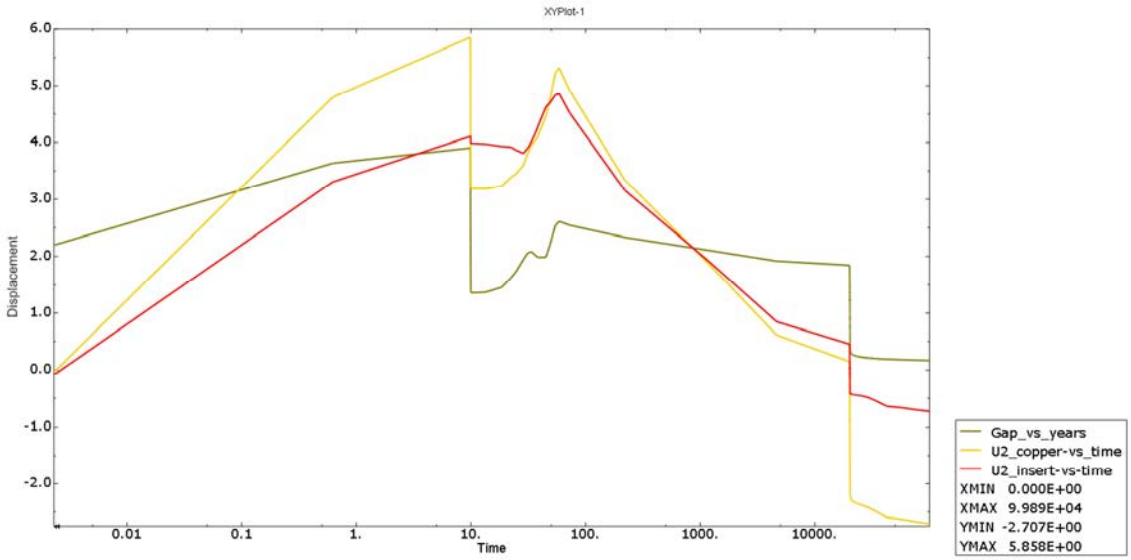

Figure 10-18. *Axial displacement for the outer corner of the insert and corresponding coordinate for the copper shell. The gap is represented by the green line. Time is in years and displacement is in mm.*

Figure 10-19 shows the hydrostatic pressure in the copper shell close to where the maximum equivalent creep strain occurs at 60 MPa. The figure shows that in this region the stresses are compressive in this region.

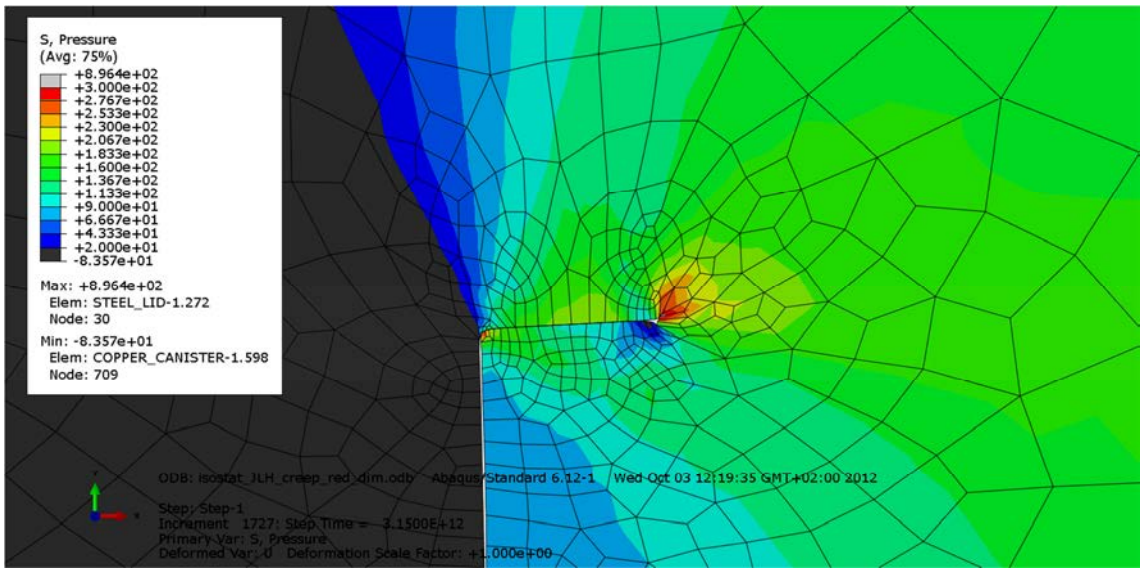

Figure 10-19. *Plot of hydrostatic pressure [MPa] close to the upper weld in the copper shell at the end of the process.*

Figures 10-20 to 10-34 show the mesh and detailed results for the top and bottom of the copper shell without removing any elements in the plotted regions.

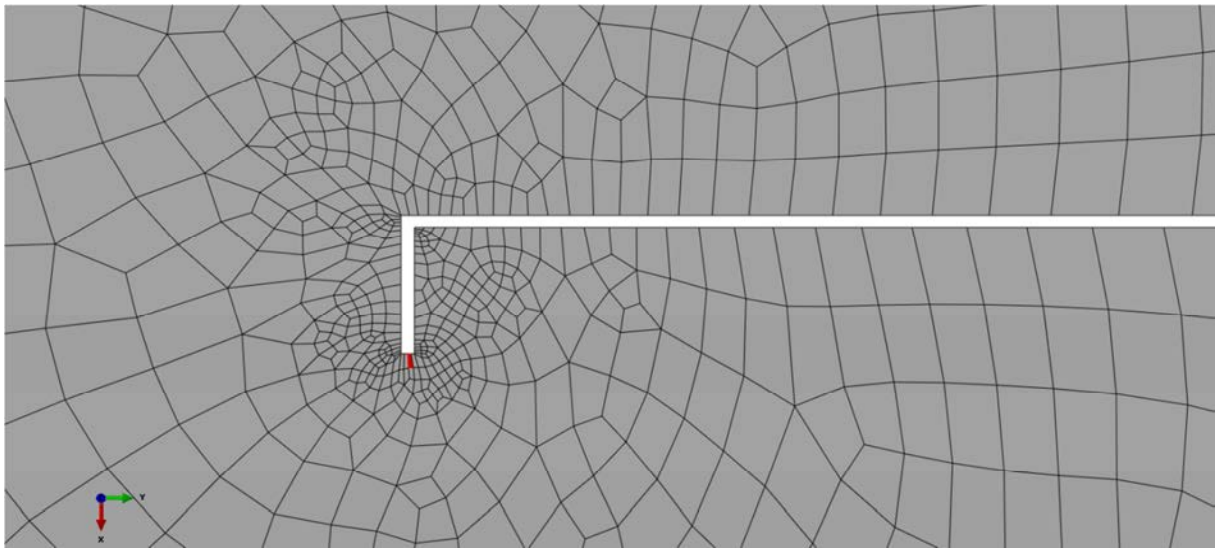

Figure 10-20. *Undeformed mesh at the bottom of the copper shell. The red element (element number 1218) shows the location of the largest equivalent creep strain at the bottom. Creep components versus time are plotted in Figure 10-25.*

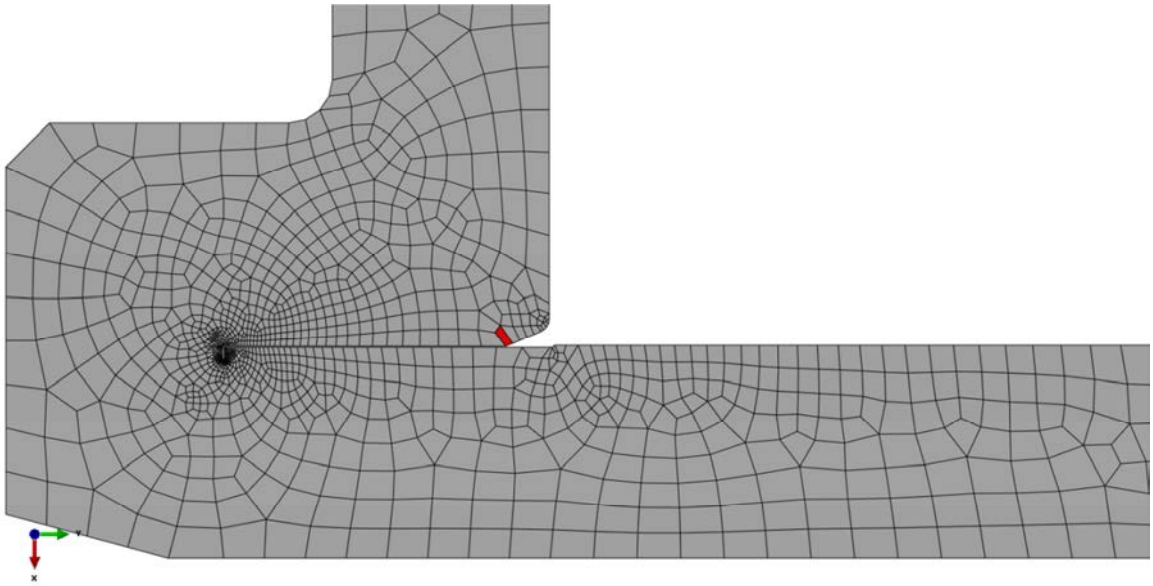

Figure 10-21. *Undeformed mesh at the bottom of the copper shell. The red element (element number 1040) shows the location of the largest equivalent creep strain for this region. Creep components versus time are plotted in Figure 10-28.*

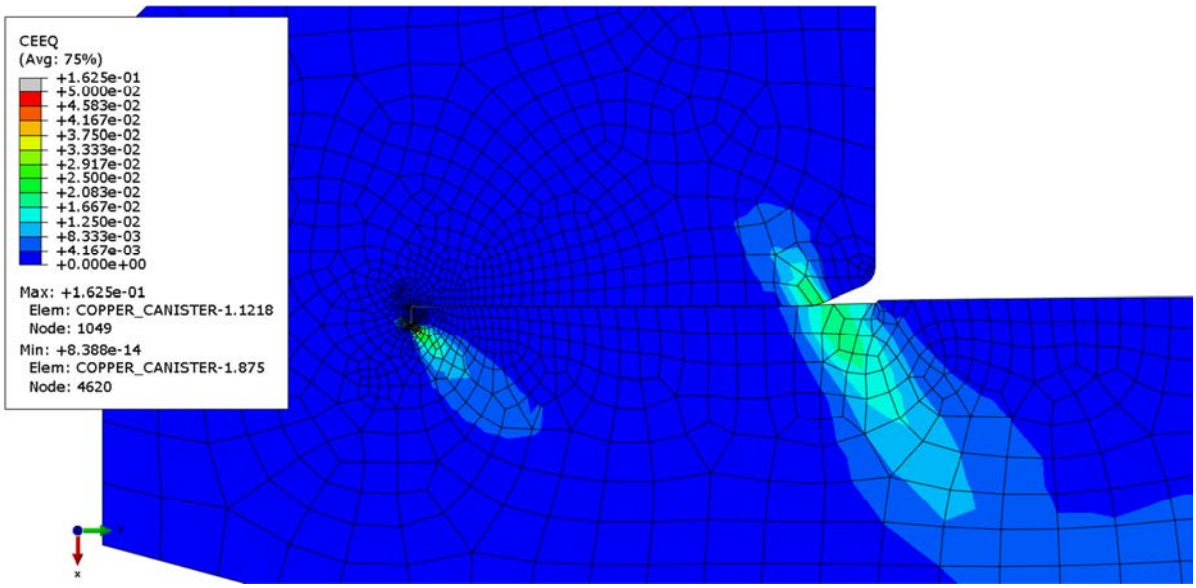

Figure 10-22. *Equivalent creep strain (CEEQ) at the bottom of the copper shell after 100 000 years, axi-symmetric analysis. This represents the situation after glaciations.*

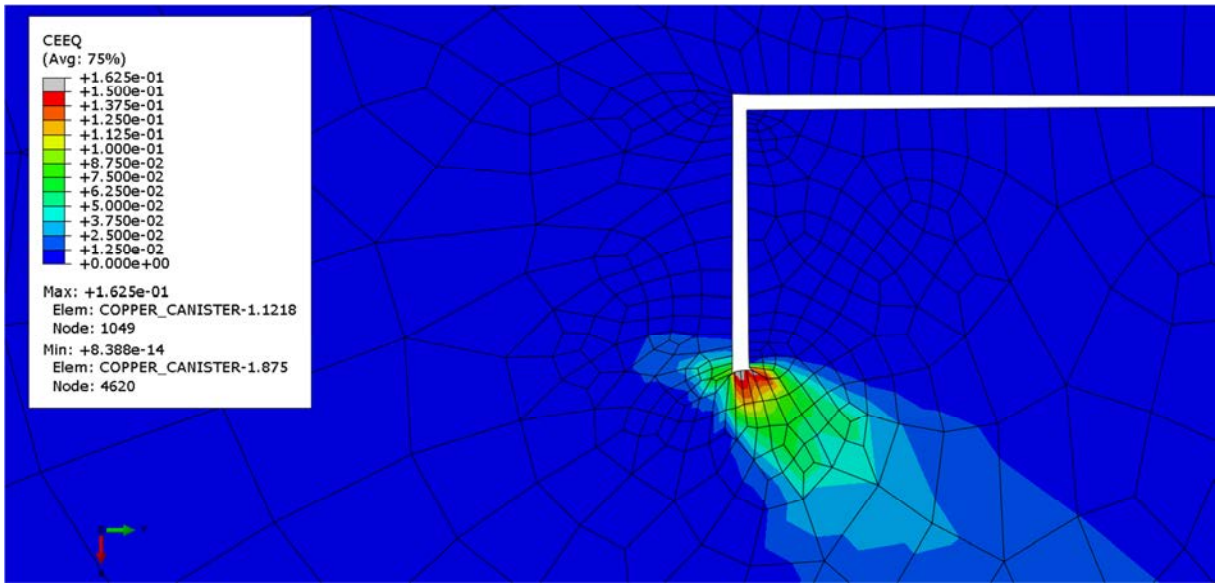

Figure 10-23. *Equivalent creep strain (CEEQ) at the bottom of the copper shell after 100 000 years, axi-symmetric analysis. This represents the situation after glaciations.*

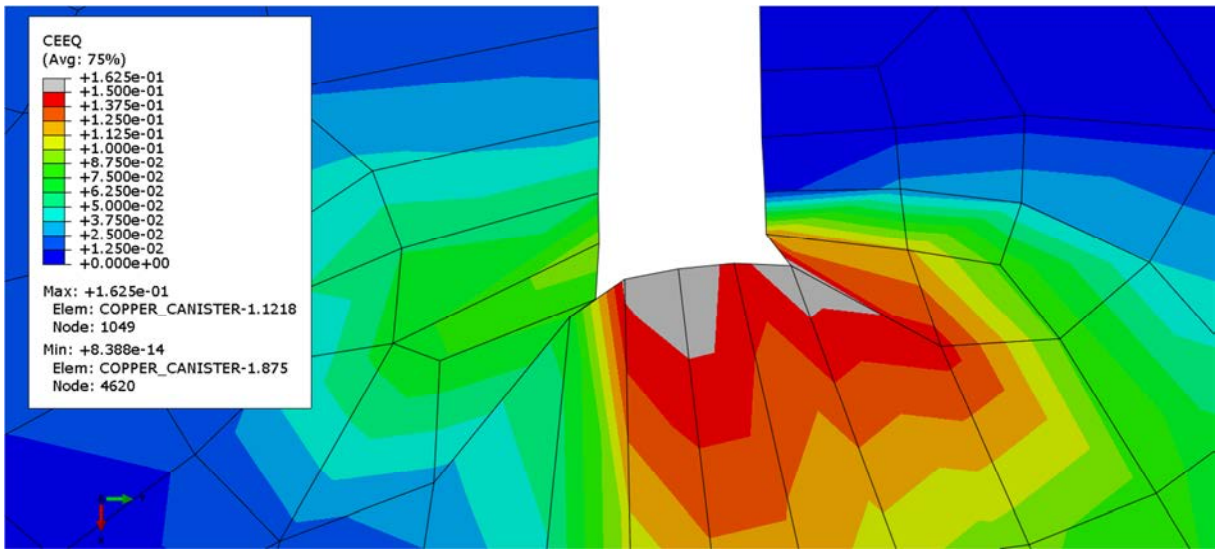

Figure 10-24 a. *Equivalent creep strain (CEEQ) at the bottom of the copper shell after 100 000 years, axi-symmetric analysis. This represents the situation after glaciations.*

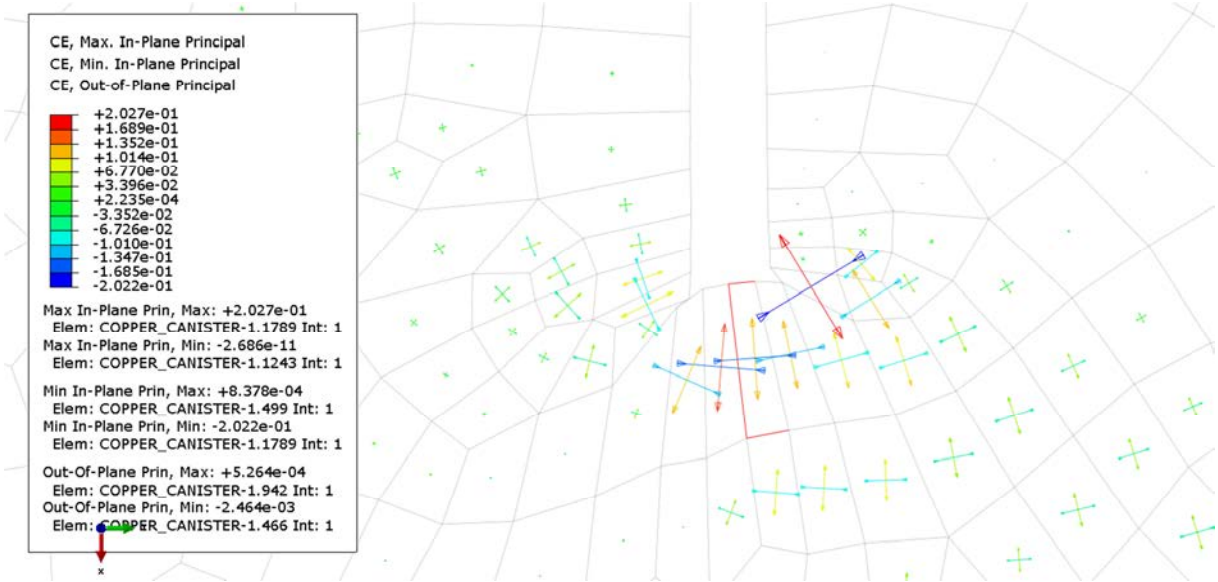

Figure 10-24 b. *Principal creep strain at the bottom of the copper shell after 100 000 years, axi-symmetric analysis. This represents the situation after glaciations. Blue arrow shows min principal creep strain and red arrow shows max principal strain (also indicated by the direction of the arrows).*

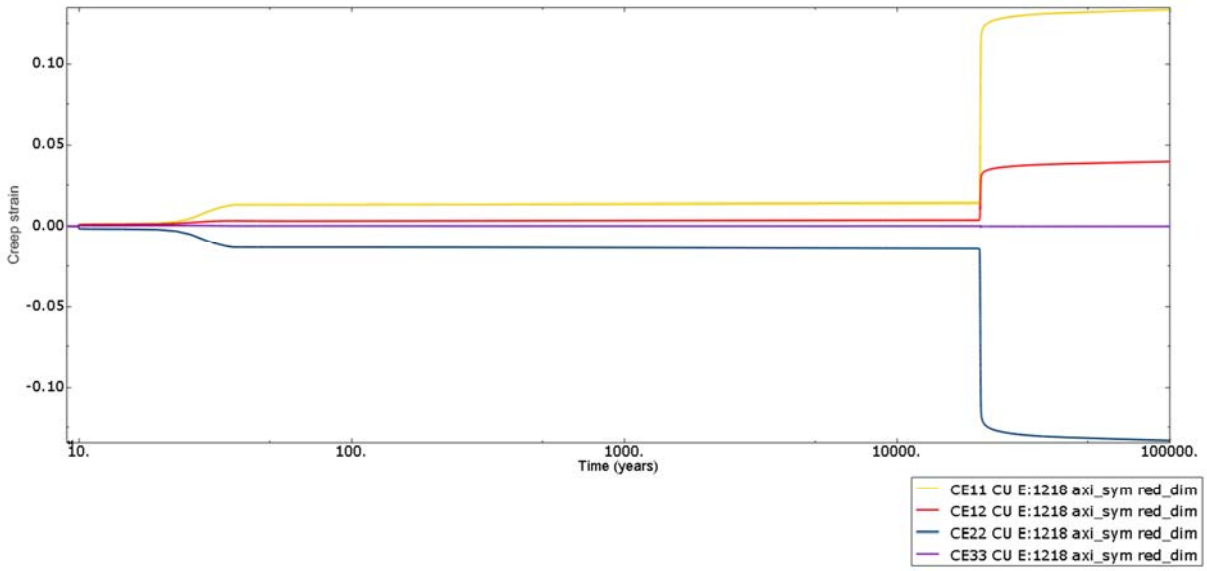

Figure 10-25. *Creep strain direct components versus time for element 1218 (see Figure 10-20), axi-symmetric analysis. CE11 (direct component in the radial direction) shows the largest magnitude.*

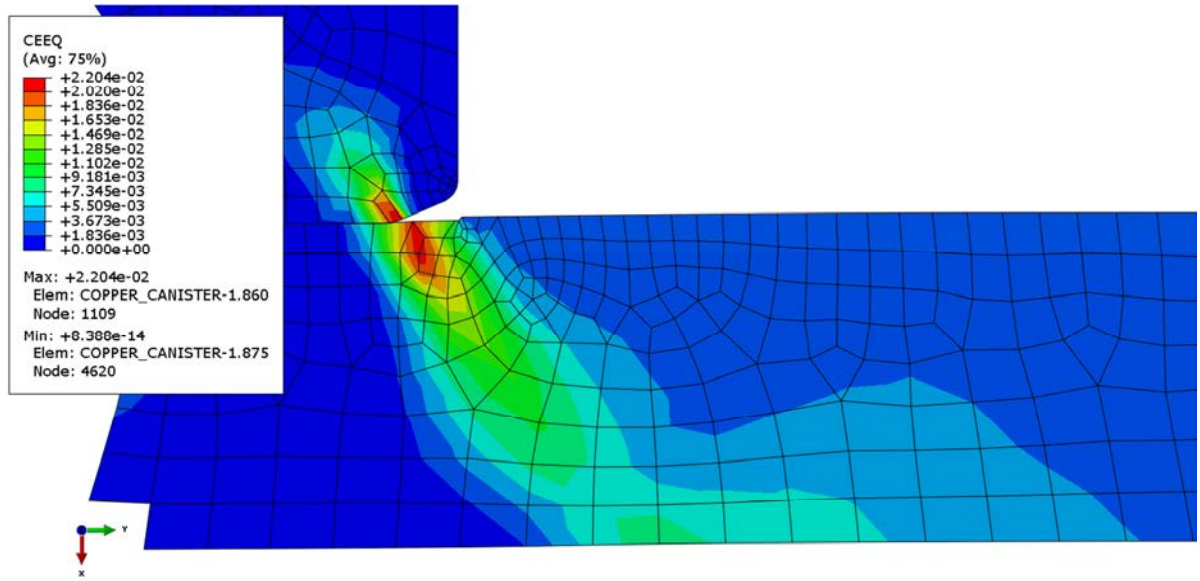

Figure 10-26. *Equivalent creep strain (CEEQ) at the bottom of the copper shell after 100 000 years, axi-symmetric analysis. This represents the situation after glaciations.*

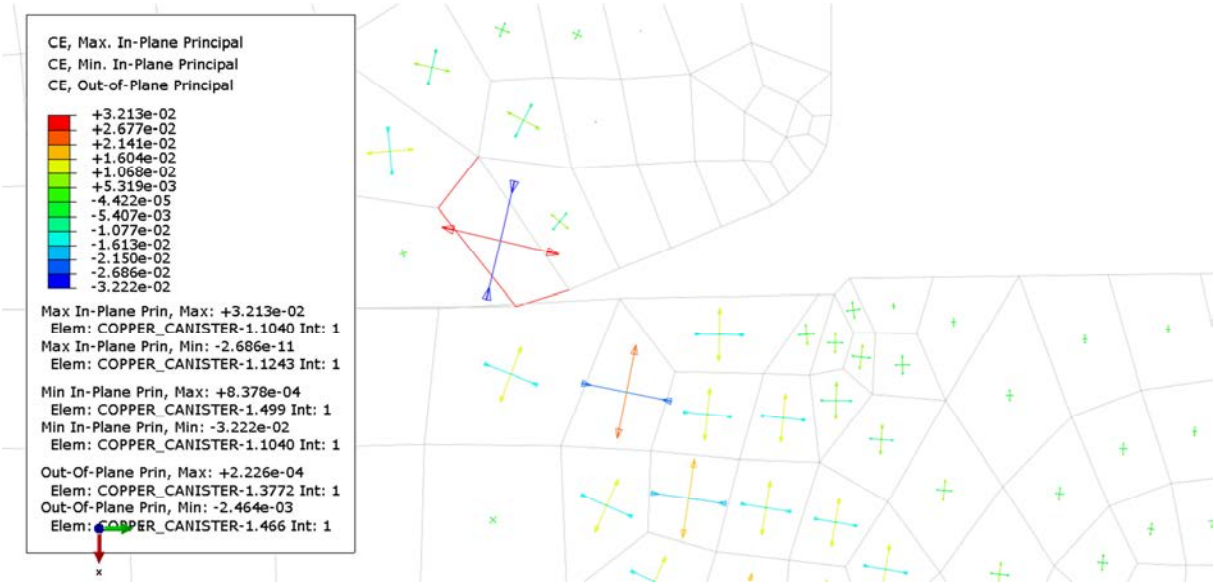

Figure 10-27. *Principal creep strain at the bottom of the copper shell after 100 000 years, axi-symmetric analysis. This represents the situation after glaciations. Blue arrow shows min principal creep strain and red arrow shows max principal strain (also indicated by the direction of the arrow.*

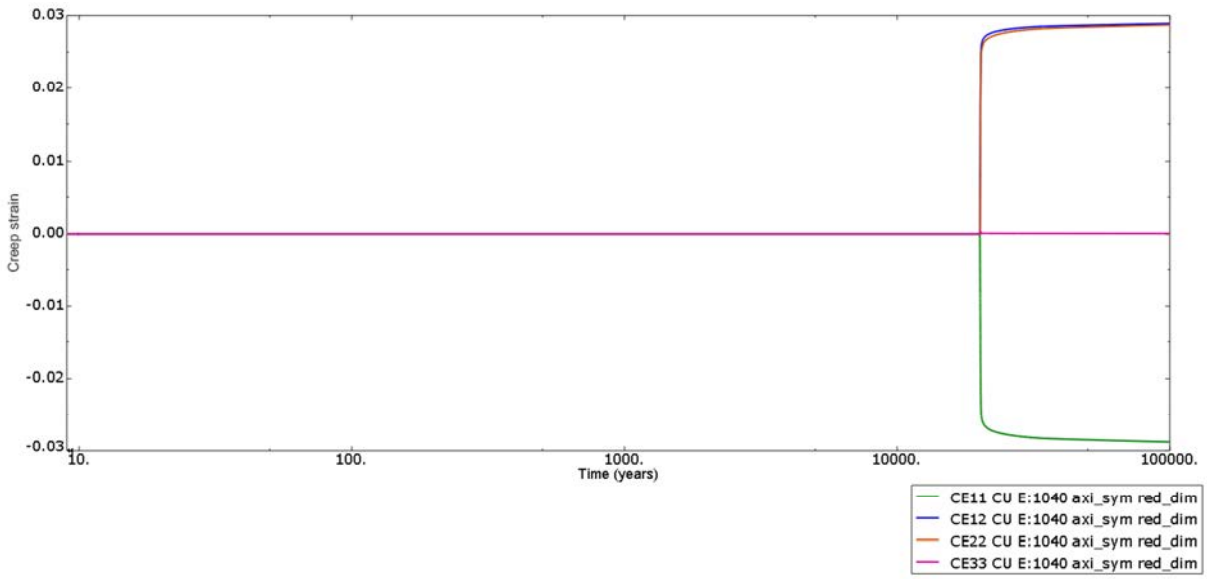

Figure 10-28. *Creep strain direct components versus time for element 1040 (see Figure 10-21), axi-symmetric analysis. CE12 (shearing component in the xy-plane) shows the largest magnitude.*

Axi-symmetric model worst case for the bottom area.
The worst case for the lower weld in the copper shell arises when the base plate is prescribed to zero displacements in a centric circle, see Figure 8-2, where the outer part of the copper shell implies maximum bending effect from the applied axial pressure on the copper lid causing the largest possible strains in the lower weld.

Figures 10-29 to 10-32 show results for the equivalent creep strain after 100 000 years (at the end of the process).

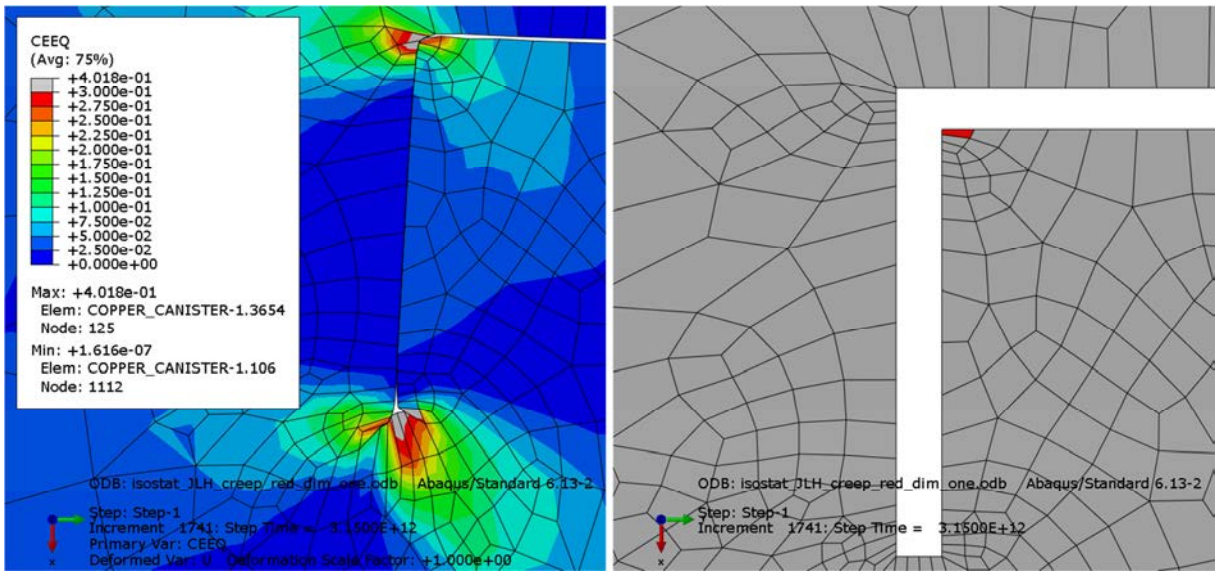

Figure 10-29. *Plot of equivalent creep strain close to the lower weld fof the copper shell at the end of the process. The right plot shows the element (3654) used for a history plot of creep strain components, Figure 10-31.*

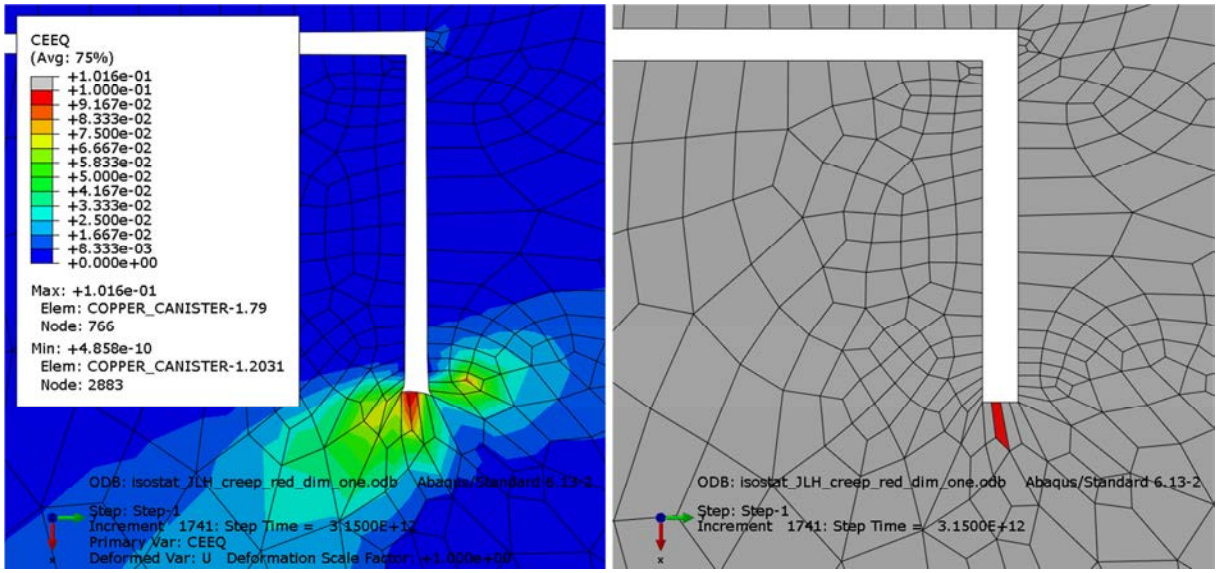

Figure 10-30. *Plot of equivalent creep strain close to the upper weld of the copper shell at the end of the process. The right plot shows the element (79) used for a history plot of creep strain components, Figure 10-32.*

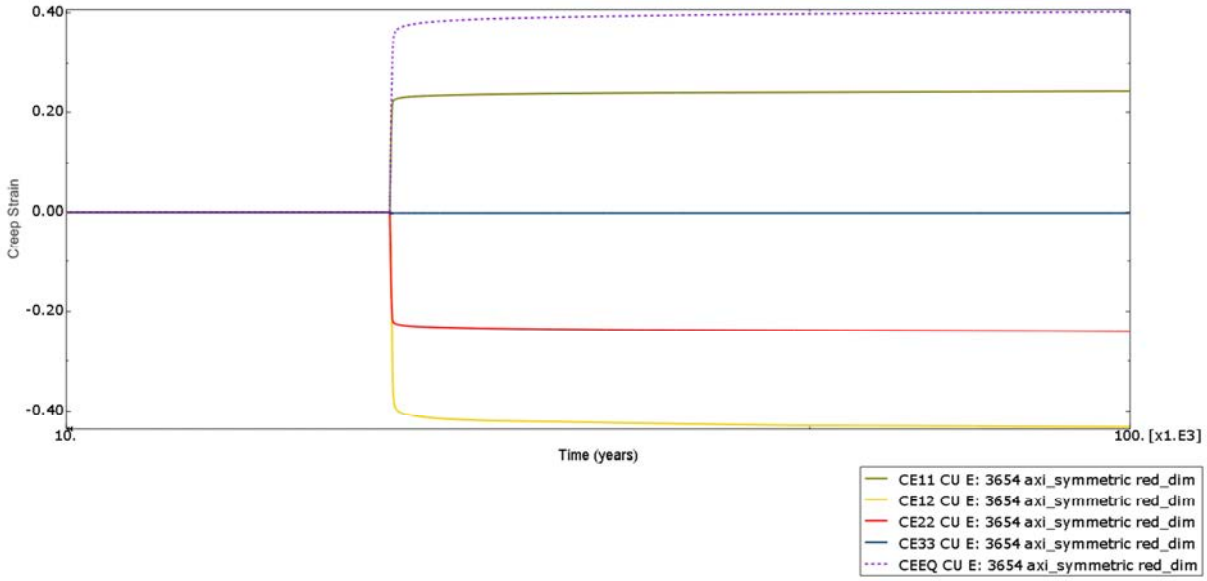

Figure 10-31. *Creep strain direct components versus time for element 3654 (see Figure 10-29), axi-symmetric analysis. CE12 (shearing component in the xy-plane) shows the largest magnitude.*

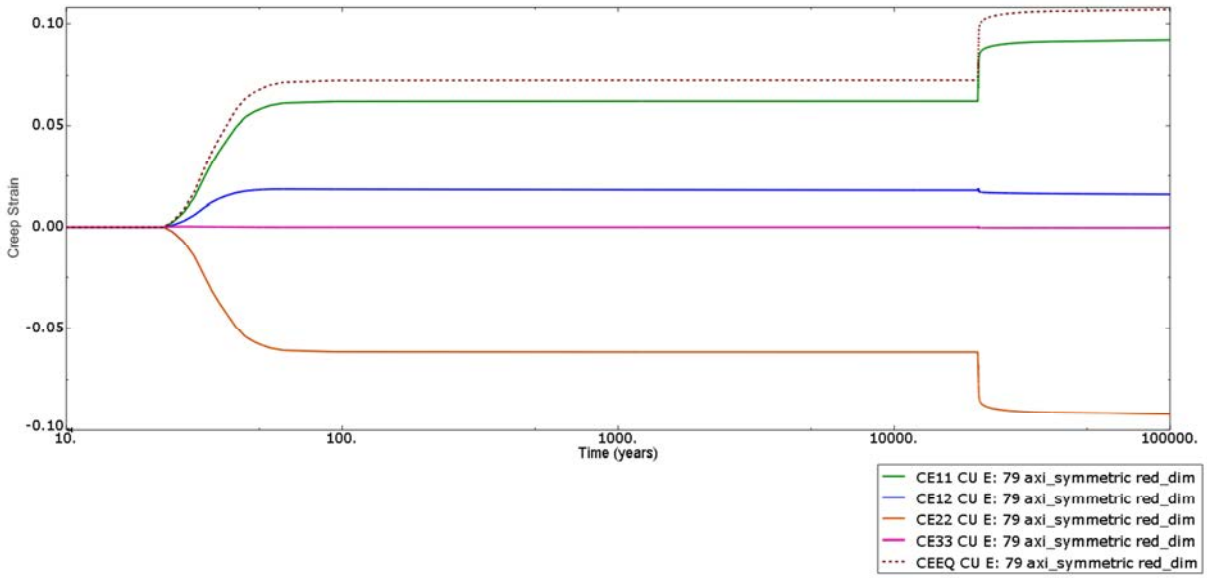

Figure 10-32. *Creep strain direct components versus time for element 79 (see Figure 10-30), axi-symmetric analysis. CE11 (direct strain component in the x-direction) shows the largest magnitude.*

10.2 3D model

The corresponding creep strain after 100 000 years in the copper shell from the 3D analysis is presented in Figure 10-33. It shows very similar results compared to the axi-symmetric analysis (Figure 10-1), but gives somewhat lower strain levels and also less affected areas are obtained, except for a local area in the root of the lid weld. Hence the use of the axi-symmetric model is pessimistic.

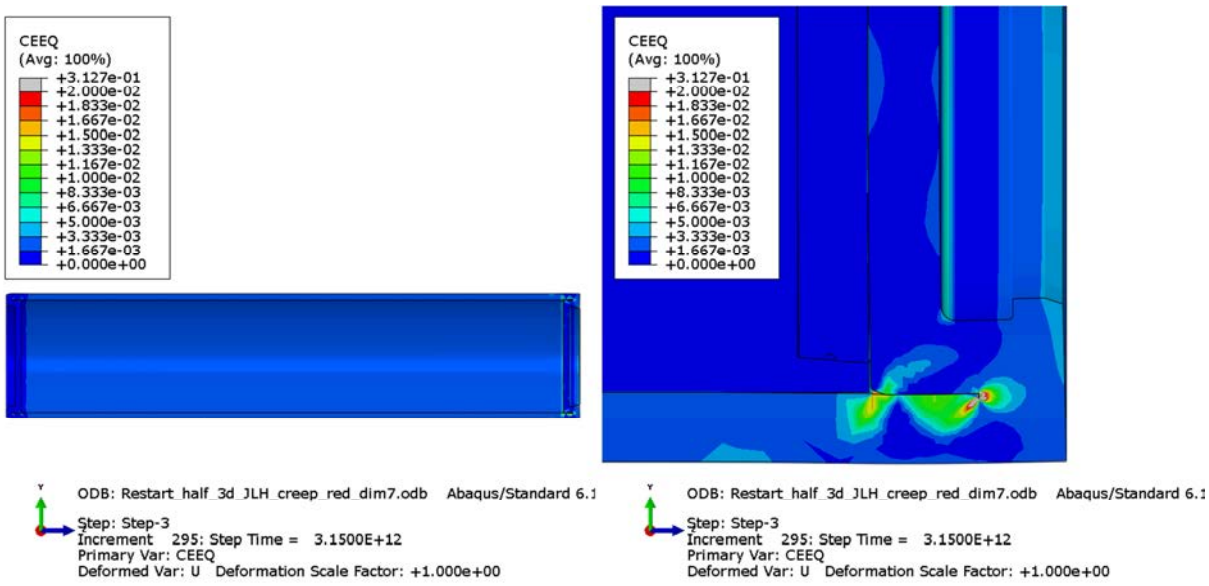

Figure 10-33. *Equivalent creep strain (CEEQ) in the copper shell after 100 000 years in the copper shell, 3D-analysis. This represents the situation after glaciations.*

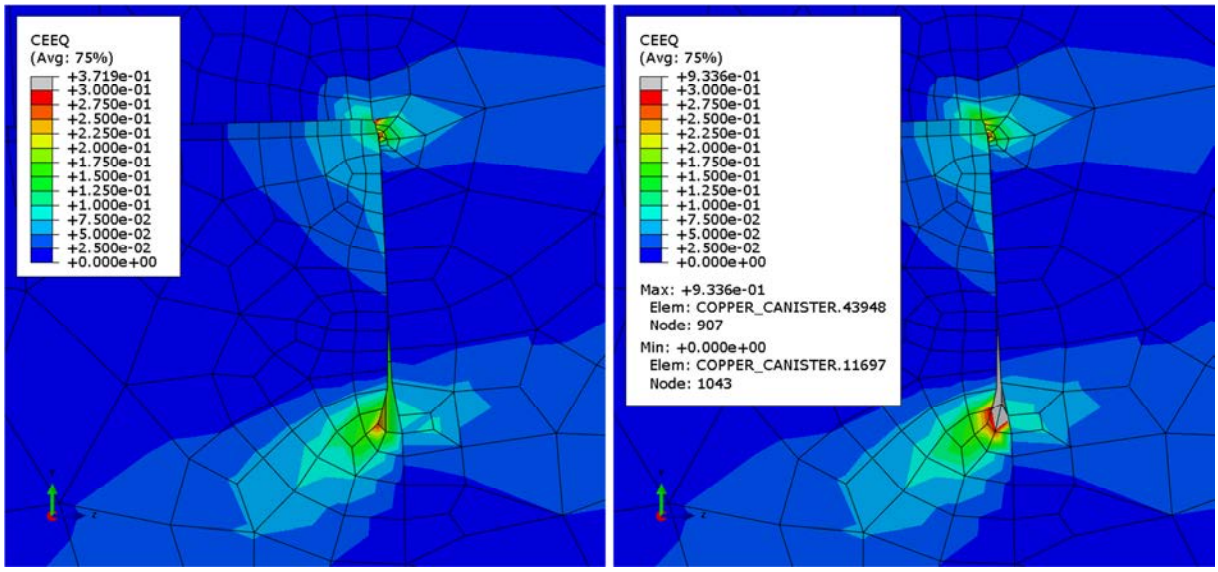

Figure 10-34. *Plot of equivalent creep strain (CEEQ)(3D).Left plot when distorted elements are removed and right plot without removing any elements. Figure 10-35 shows the ring of removed elements.*

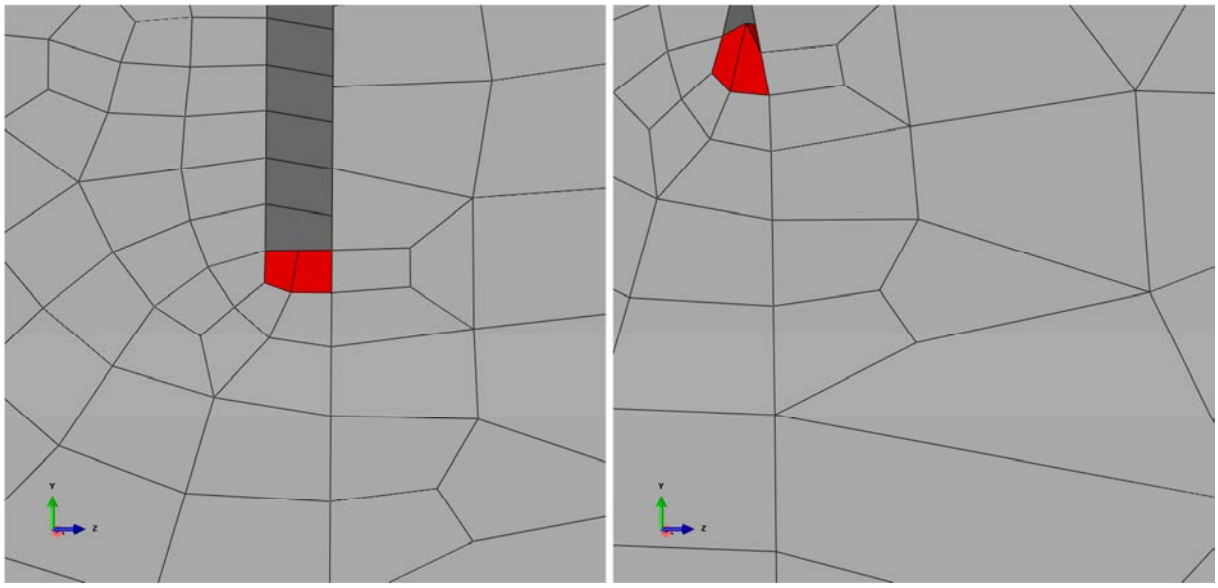

Figure 10-35. *Ring of elements removed before generating contour plot in Figure 10-34 (left plot (3D)). Left plot shows un-deformed elements and right plot deformed elements.*

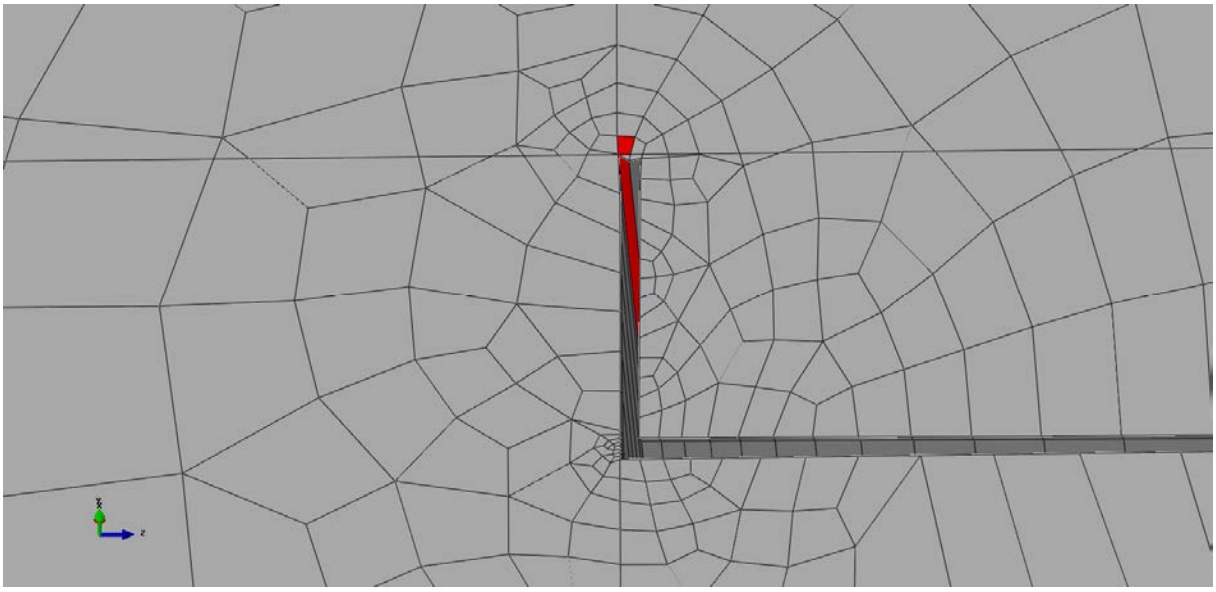

Figure 10-36. *Element 13887 having the maximum equivalent creep strain (CEEQ) after removing distorted elements. History plot of strain components, see Figure 10-39.*

Cast iron insert

The highest value for Mises stress, 550 MPa, occurs in the fillets, see Figure 10-37.

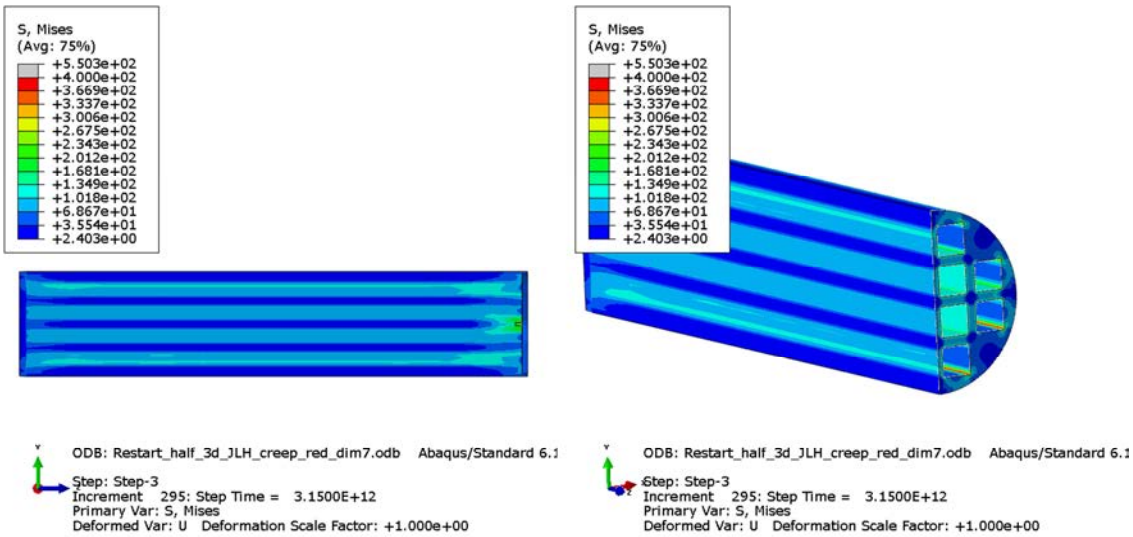

Figure 10-37. *Mises stress [MPa] in the insert at the end of the process.*

Steel lid

The steel lid has a large equivalent plastic strain (PEEQ) at the geometric discontinuity, 21.5 %; see Figure A1-25 but also in this region the dominating pressure is in compression, see Figure A1-28.

Steel channels (only 3D-analysis)

The steel channels show mainly an elastic response and the highest Mises stress occurs at the fillets and at the connection to the steel lid, se Figure 10-38.

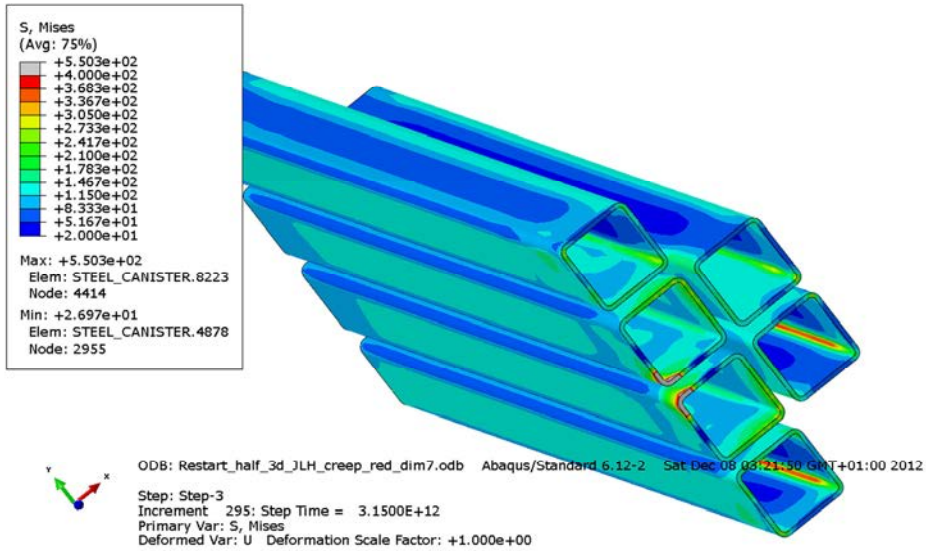

Figure 10-38. *Mises stress [MPa] for the steel channels at the end of the process.*

Copper shell

The maximum equivalent creep strain (CEEQ) is shown in Figures A1-8 and A1-10. The maximum magnitude, 61.4%, occurs for case isostat_JLH_creep_red_dim at the top weld, Figure A1-10. Figure A1-20 shows that the pressure is positive for the corresponding element. Comparing Figure A1-19 (showing results after applying the helium gas pressure) with A1-20 implies that the hydrostatic pressure at the weld corner changes from -159 MPa to almost zero. However, the equivalent creep strain is small after applying the helium gas pressure, see Figure A1-9.

10.3 Comparison axi-symmetric and 3D analyses

The visco-plastic strains (CE – creep strain) include normal plasticity and Figure 10-39 shows how the equivalent creep strain (CEEQ) develops for all axi-symmetric cases and also for the 3D-analysis. The figure shows the history response for the element having the maximum equivalent creep strain. The node position is at the root of the weld. As can be seen from the figure the traditional creep effect is rather small compared to the plastic response when the external load is changed. Most of the increase in strain magnitude occurs instantly when the load is increased. In comparison to a typical creep testing curve, see Figure 4-5 in Raiko et al. (2010) ,the creep fraction is only a few percent of the total strain.

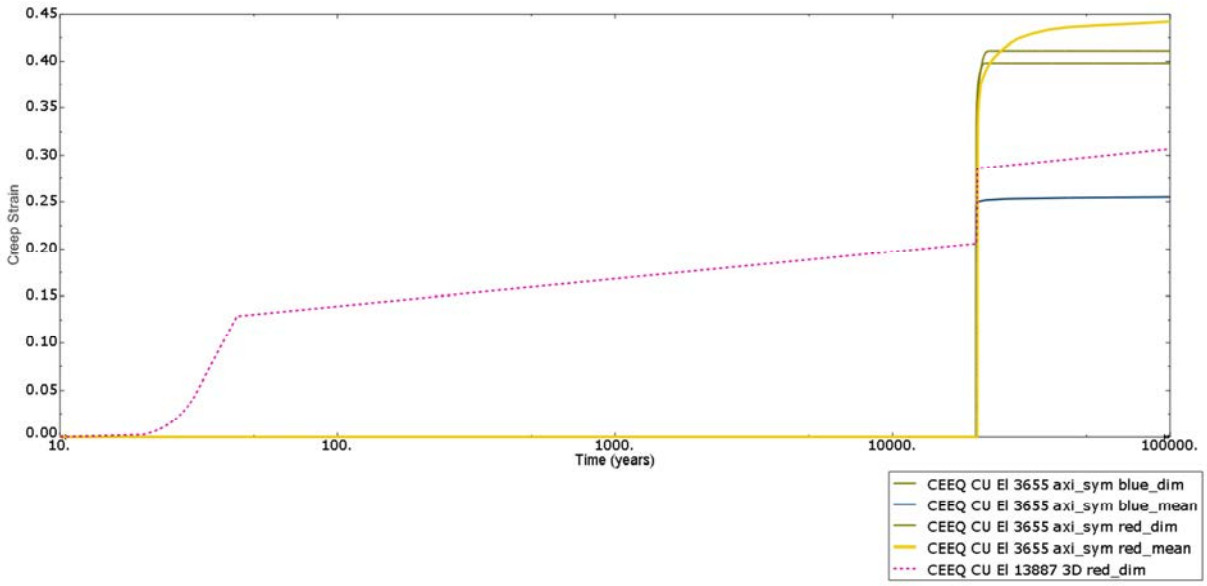

Figure 10-39. *Equivalent creep strain (CEEQ) for all cases. Highest value, about 70%, is achieved for case isostat_JLH_creep_red_mean. Most of the rise in strain comes instantaneously when the load is increased and only a few percent is traditional creep strain.*

11 Interpretation of contour plots

The FE-analyses calculates stresses and strains in each element at the integration points where the defined relation between stresses and strains is used. The obtained results are then presented as contour plots where the integration point values are extrapolated for each element to the nodal points and then eventually averaged. The default rule is that the averaging is performed for nodal values. The extent to which values are averaged at nodes within each region is controlled by the averaging threshold (default is 75% and is shown at the legend table) as follows:

$$\text{relative nodal variation} = \frac{(\text{maximum at node} - \text{minimum at node})}{(\text{maximum within region} - \text{minimum within region})}$$

If the relative nodal variation for each node included in the plot is less than the averaging threshold, values of contributing elements are averaged at that node. If the relative nodal variation exceeds the setting, the values are not averaged.

The lower the averaging threshold value is, the more the displayed values depict the individual element results. Conversely, a higher averaging threshold produces a smoother effect with fewer noticeable discontinuities at element boundaries and lower maximum magnitude.

At regions with large gradients the choice of averaging threshold affects the produced plots significantly but with small gradients the threshold value has very small influence on the plots.

For the performed analyses, the peak values for stresses and strains are localized around the crack tip which has a geometric discontinuity. This results in large gradients and in most cases heavily distorted elements affecting the corresponding contour plots. To have more reliable results a much finer mesh is required together with a correct geometric definition (at the moment the crack tip is modelled with sharp corners implying discontinuity in the geometry). It seems reasonable to neglect results from theses highly distorted elements, especially since the element size is very small, see Figures 10-34 to 10-35 which are examples of results from the 3D analysis. Figures 10-34 shows the result when one highly distorted element is removed before generating the contour plot. Highly distorted elements could create unrealistic results for values extrapolated from the integration points to the element nodes.

12 Uncertainties

The obtained results are based on several assumptions regarding loads and material properties. Also the discretization in the computer model will affect the results. Some of these influencing factors are addressed below.

- Strain rate effects in the copper and iron will affect the results. For the copper shell, the strain rate effect has been included in all reported analyses.
- All experiments used for material calibration have a spread which will imply a range for the properties defining each material model.
- Element mesh is rather fine but nevertheless it is too coarse in some regions, especially at the welds and regions with geometric discontinuities. A more refined mesh will probably increase the maximum stress and strain levels. Fortunately, the use of non-linear material properties (such as plasticity and creep) will decrease the sensitivity to the used mesh. The used mesh has been judged to be accurate enough considering also the required computer resources to obtain the results. Since several models have been executed with different mesh densities it has been possible to make a comparison and the conclusion is that the mesh in a global sense is accurate except at geometrical discontinues.
- The chosen boundary conditions at the copper shell base probably imply stresses/strains higher than would be the case with the buffer included in the analyses.

13 Evaluation and conclusions

The study aimed to simulate the complete time history of stresses and strains in the canister due to external and internal loads such as helium gas pressure, buffer swelling pressure from the saturation phase and overburden from glaciations based on an assumed evolution of these loads. A few general conclusions from the performed simulations are listed below:

- The temperature is assumed to increase for 20-30 years due to heat generation in the spent fuel and then the temperature declines. During the same time interval (20- 50 years) the swelling pressure is also assumed to increase and at the glaciations, which is assumed to occur after about 20,000 years the external pressure increases significantly. The external pressure will increase the pressure between the copper shell and the insert while the temperature decreases the pressure since the copper shell expands more than the iron. When the temperature drops, the pressure between the copper shell and the insert increases.
- The different models behave in a very similar way where an axi-symmetric approach represents the stress/strain distribution accurately. The axi-symmetric approach allows a much finer mesh without having extremely long computer time.
- The stiffness of the insert could be approximated with an axi-symmetric approach but the stress and strain distribution in the insert requires a 3D interpretation.

The results obtained from creep analyses could be summarized as:

- The magnitude of the external pressure has the highest impact on the results but also increased temperature is important to consider since the yield surface depends on the temperature.
- Despite the differences in the assumptions regarding temperature- and pressure development, the dominant factor for the creep strain is the high external pressure during glaciations.
- The creep from the internal processes, before external loads are applied, case c) and d), is very small and of minor importance.
- High creep strains occur locally in the weld roots due to external pressure. The maximum equivalent creep strain in the copper shell occurs at the discontinuities at the upper weld (using boundary conditions simulating a worst case for the upper weld, see Figure 8-2) and is very local. The lower weld is less stressed even when boundary conditions simulating a worst case for the lower weld are used. The magnitude will depend on the width and shape of the slit and postulated discontinuity in relation to the mesh but the current mesh at least shows that despite local effects the strains will be low. It should be noted that the maximum strain is caused by compressive stresses, see Figures 13-1 and 13-2 which show the ratio between pressure and Mises stress (p/q). The maximum plastic strains in the insert occur at the lid where the geometry has a discontinuity.

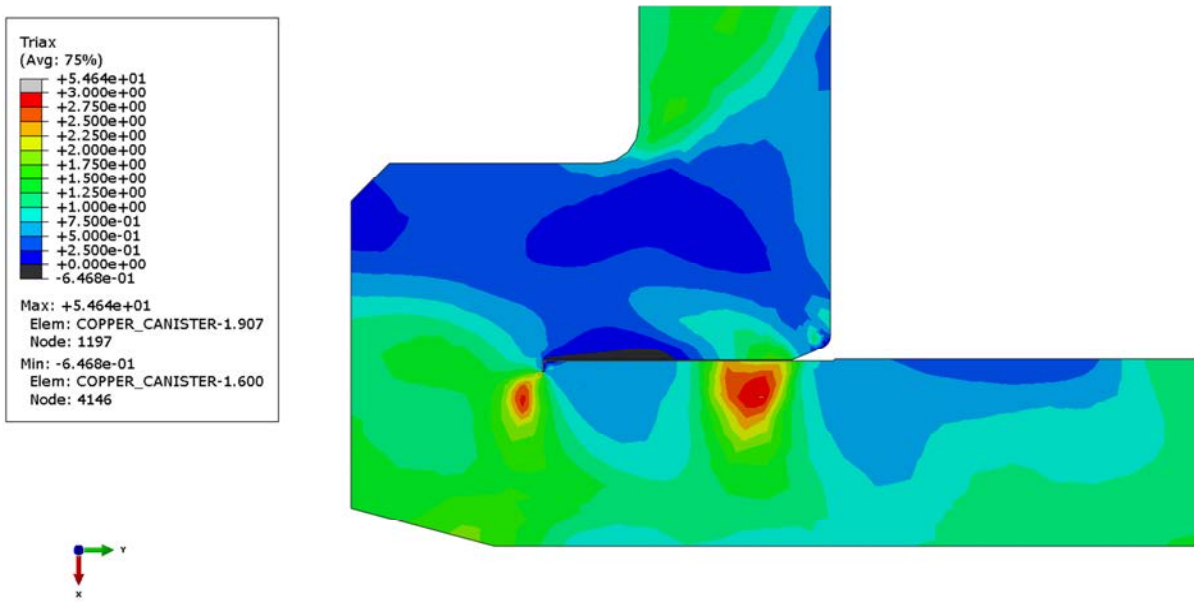

Figure 13-1. *Plot of ratio p/q (pressure divided by Mises stress) at the bottom of the copper shell, axi-symmetric case at the end of the process.*

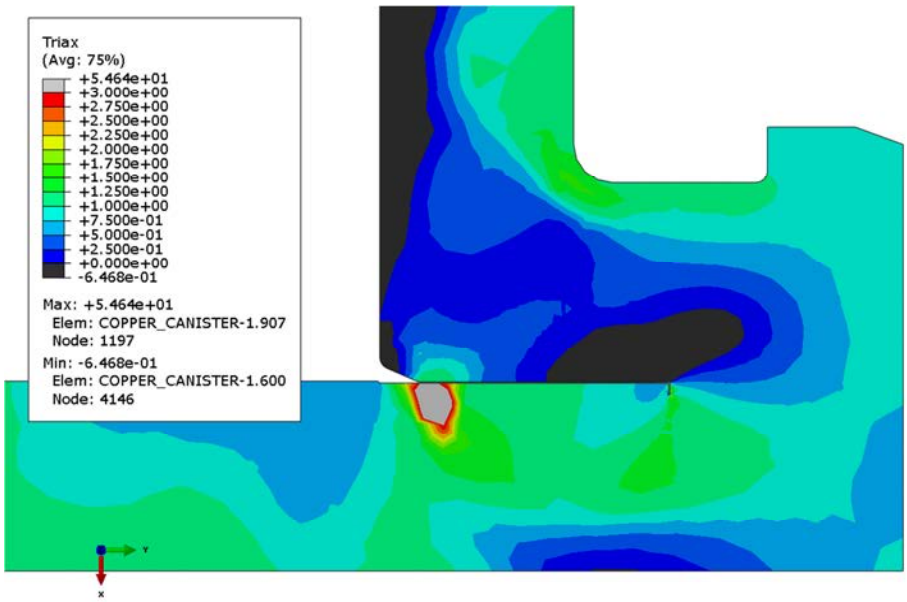

Figure 13-2. *Plot of ratio p/q (pressure divided by Mises stress) at the top of the copper shell, axi-symmetric case at the end of the process.*

- The total strain is represented by CEEQ. The creep effect defined as the long term deformation seems to be small during the whole time period analyzed and shows small variations despite differences in the assumed temperature evolution.
- Comparing obtained results after applying the helium gas pressure with long term results show that the long term results imply the highest stress and strain levels, see e.g. Figures A1-9, A1-10, A1-20 and A1-21. Another observation is that the hydrostatic negative pressure (corresponds to tension) is greater after applying the gas pressure than after long time but the corresponding equivalent creep strain is still low for this case.

References

SKB's (Svensk Kärnbränslehantering AB) publications can be found at www.skb.se/publications.
References to SKB's unpublished documents are listed separately at the end of the reference list.
Unpublished documents will be submitted upon request to document@skb.se.

ABAQUS Manuals, 2012. Version 6.12.1. Dassault Systèmes Simulia Corp.

Andersson-Östling H C M, Sandström R, 2009. Survey of creep properties of copper intended for nuclear waste disposal. SKB TR-09-32, Svensk Kärnbränslehantering AB.

Hökmark H, Lönnqvist M, Fälth B, 2010. THM-issues in repository rock. Thermal, mechanical, thermo-mechanical and hydro-mechanical evolution of the rock at the Forsmark and Laxemar sites. SKB TR-10-23, Svensk Kärnbränslehantering AB.**Jin L-Z, Sandström R, 2008.** Creep of copper canisters in power-law breakdown. Computational Materials Science 43, 403–416.

Raiko H, Sandström R, Rydén H, Johansson M, 2010. Design analysis report for the canister. SKB TR-10-28, Svensk Kärnbränslehantering AB.

Sandström R, Andersson H C M, 2008. Creep in phosphorus alloyed copper during power-law breakdown. Journal of Nuclear Materials 372, 76–88.

Sandström R, Hallgren J, Burman G, 2009. Stress strain flow curves for Cu-OFP. SKB R-09-14, Svensk Kärnbränslehantering AB.

SKB, 2010. Design, production and initial state of the canister. SKB TR 10-14, Svensk Kärnbränslehantering AB.

SSABDirekt, 2008. Steelfacts Domex 355 MC. Available at https://steelfactssvc.ssab.com/steelfact/strain.aspx?product=DOMEX355MC [2014-03-02].

SS-EN 10025-2:2004. Varmvalsade konstruktionsstål – Del 2: Tekniska leveransbestämmelser för olegerade stål (Hot rolled products of structural steels – Part 2: Technical delivery conditions for non-alloy structural steels). Stockholm: Swedish Standards Institute.

Unpublished documents

SKBdoc id, version	Title	Issuer, year
1201865 ver 1.0	Dragprovning av gjutjärn. (In Swedish.)	KTH, 2009
1203875 ver 1.0	Ritningsförteckning för kapselkomponenter. (In Swedish.)	SKB, 2009
1333208 ver 2.0	Inre övertryck i kapseln. (In Swedish.)	SKB, 2012
1333256 ver 2.0	Svar på begäran om kompletteringar angående kapselfrågor. (In Swedish.)	SKB, 2012

Appendix 1 – Isostat_JLH_creep_red_dim

Plots showing temperature and pressure contours and history.

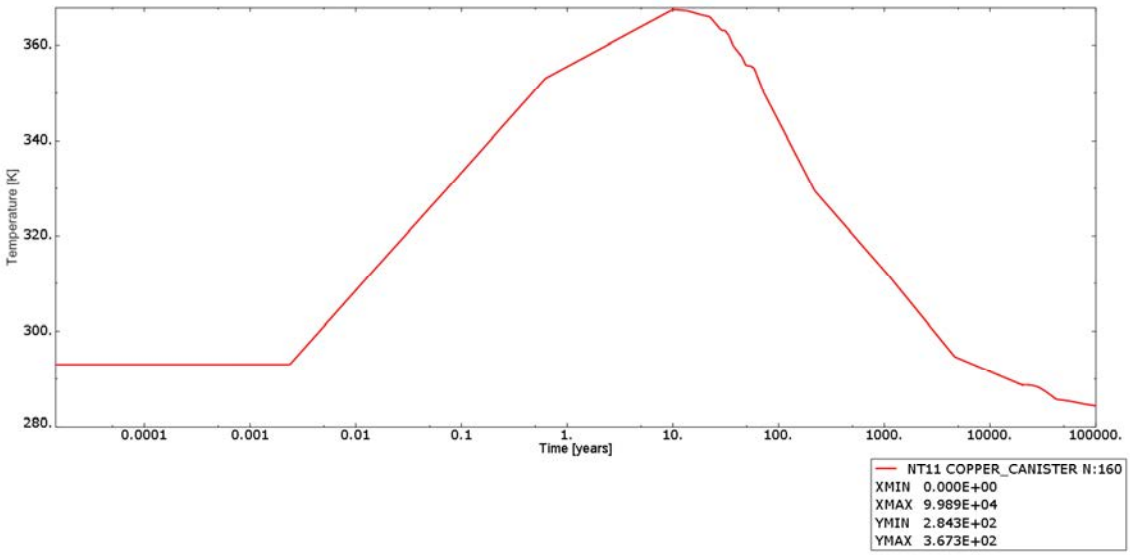

Figure A1-1. *Plot showing the temperature history. Time is in years, temperature is in Kelvin.*

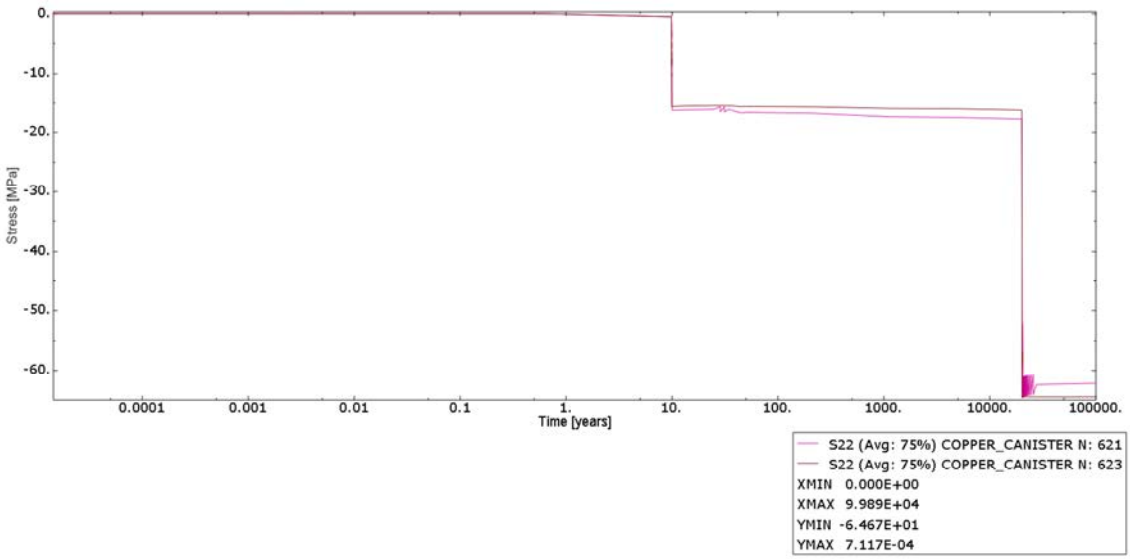

Figure A1-2. *Plot showing the applied pressure at the top lid of the copper shell.Time is in years and stress is in MPa.*

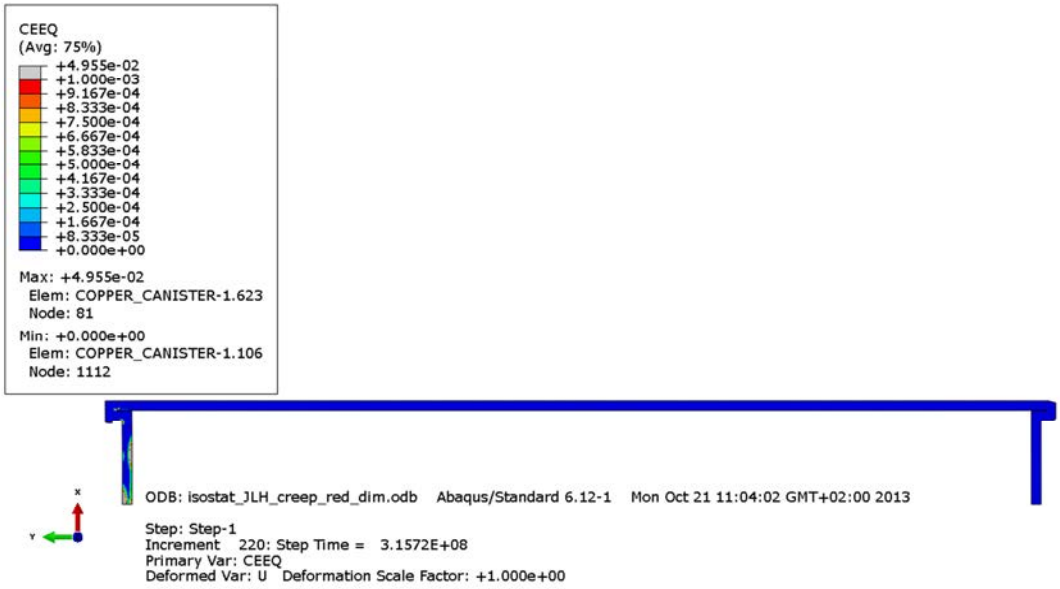

Figure A1-3. *Plot showing equivalent creep strain after 10 years.Gas pressure is applied. Distorted elements removed.*

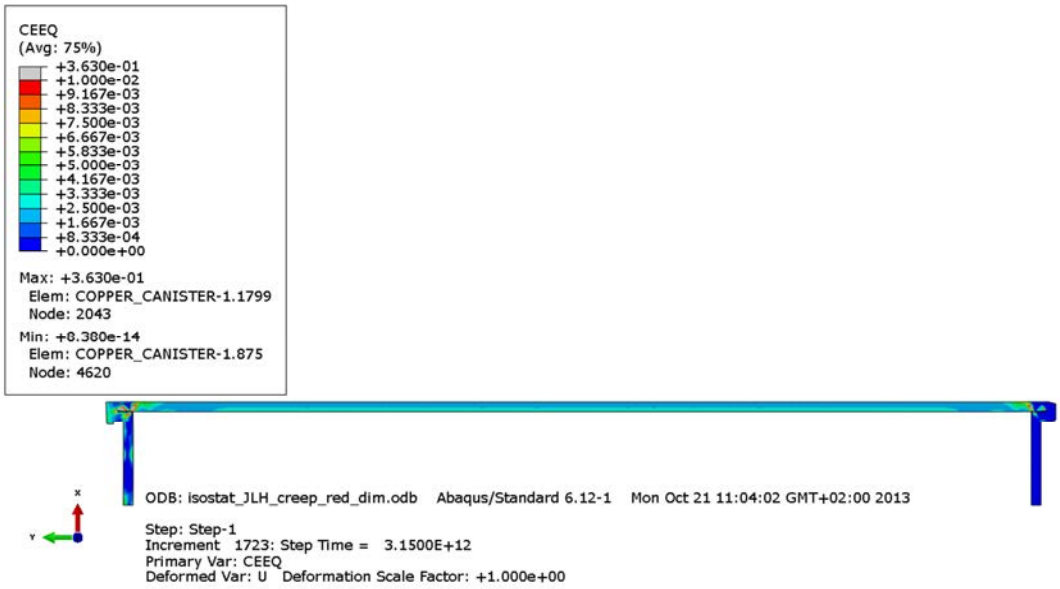

Figure A1-4. *Plot showing the equivalent creep strain after 100,000 years. Distorted elements removed.*

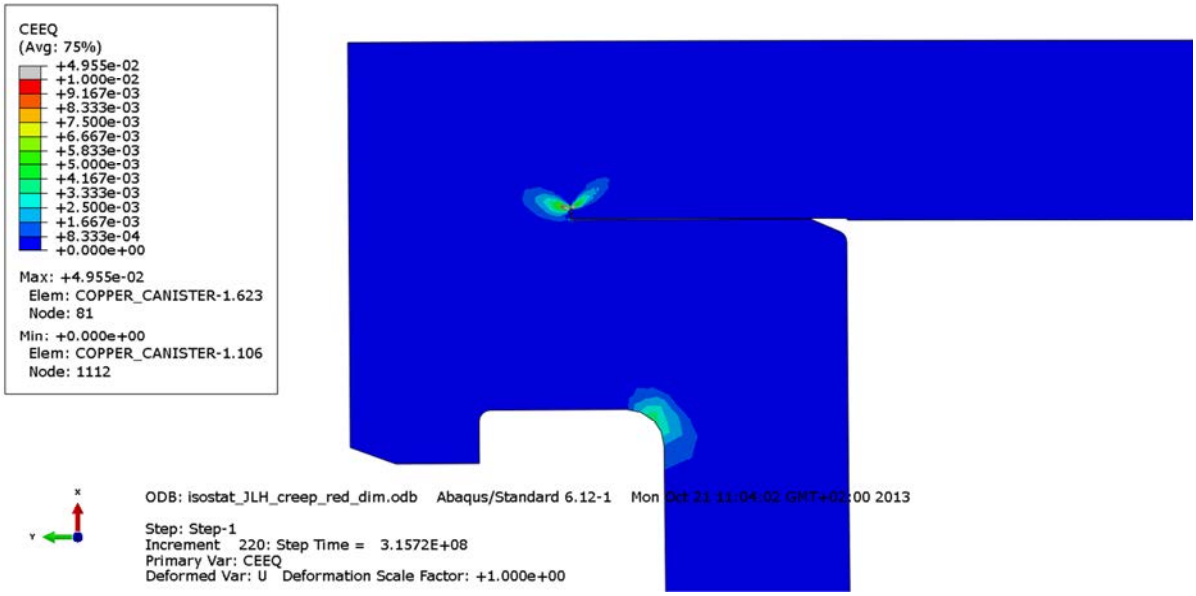

Figure A1-5. *Plot showing the equivalent creep strain at the top weld of the copper shell after 10 years. Gas pressure is applied. Distorted elements removed.*

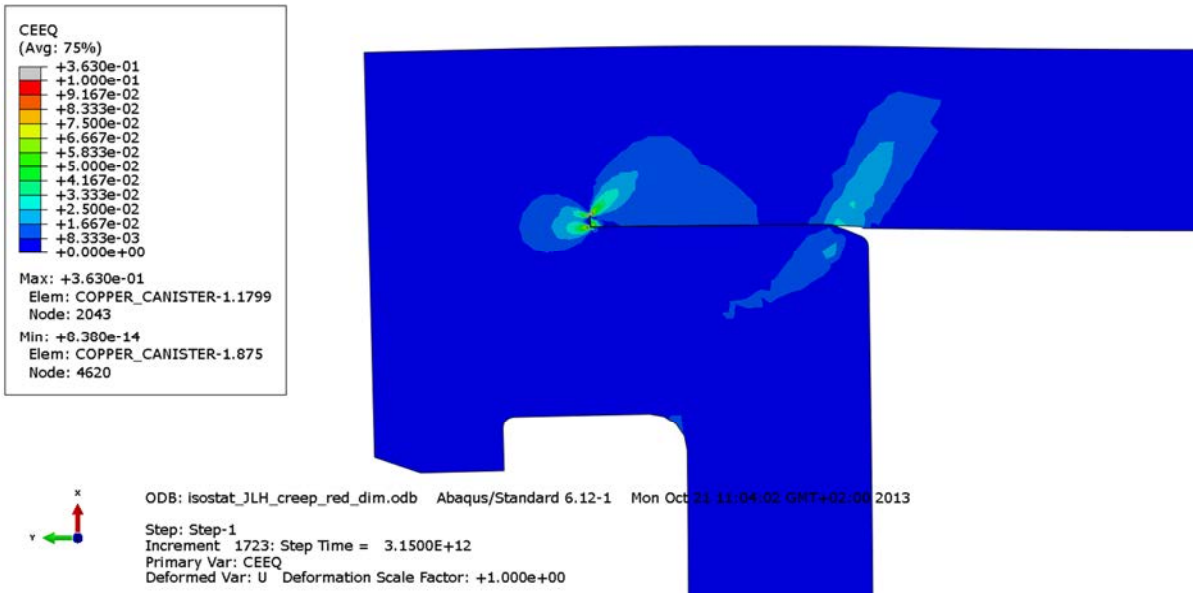

Figure A1-6. *Plot showing the equivalent creep strain at the top weld of the copper shell after 100,000 years. Note the localized strain concentration. Distorted elements removed.*

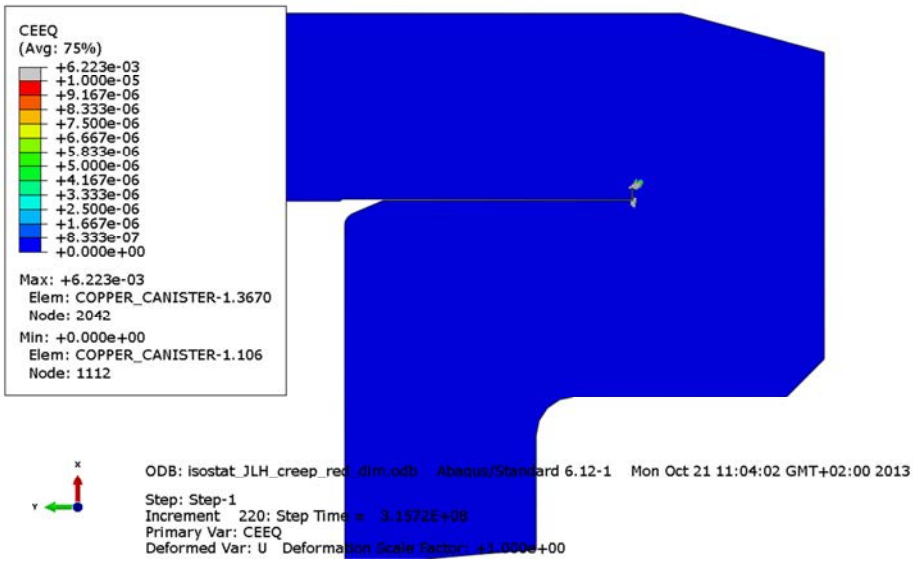

Figure A1-7. *Plot showing the equivalent creep strain at the bottom weld of the copper shell after 10 years. Gas pressure is applied. Distorted elements removed.*

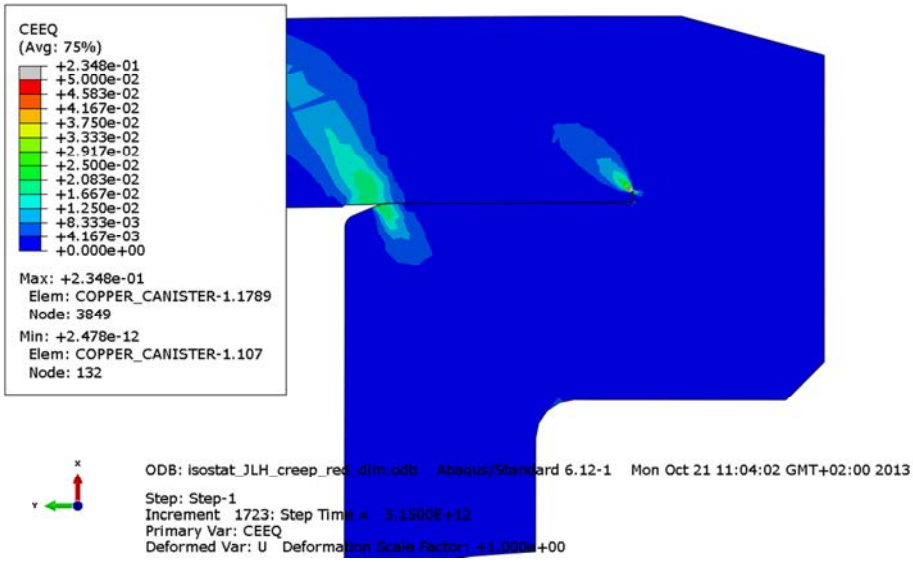

Figure A1-8. *Plot showing the equivalent creep strain at the bottom weld of the copper shell after 100,000 years. CEEQ>5% is localized to the crack tip. Distorted elements removed.*

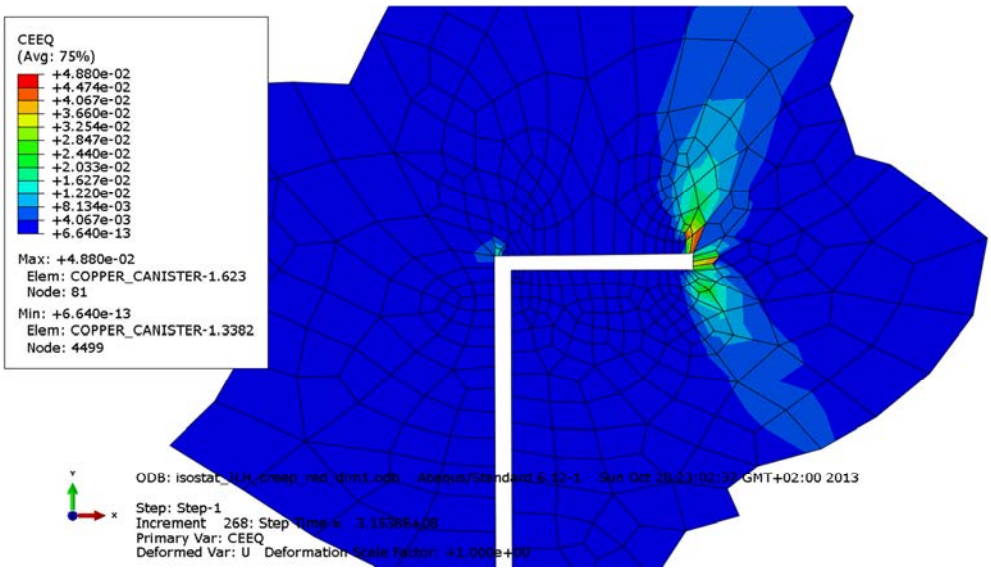

Figure A1-9. *Plot showing the equivalent creep strain at the copper shell top weld after 10 years. Gas pressure is applied.*

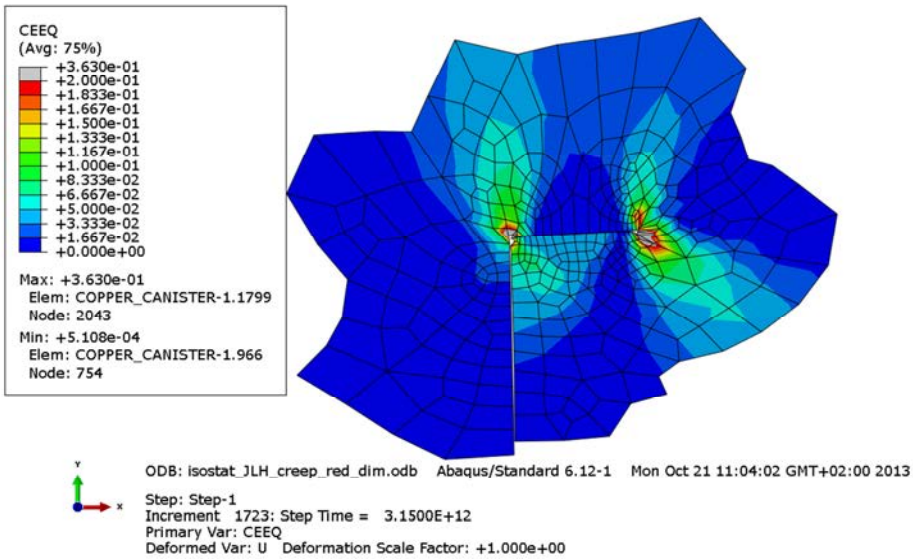

Figure A1-10. *Plot showing the equivalent creep strain at the copper shell top weld after 100,000 year. Distorted elements removed.*

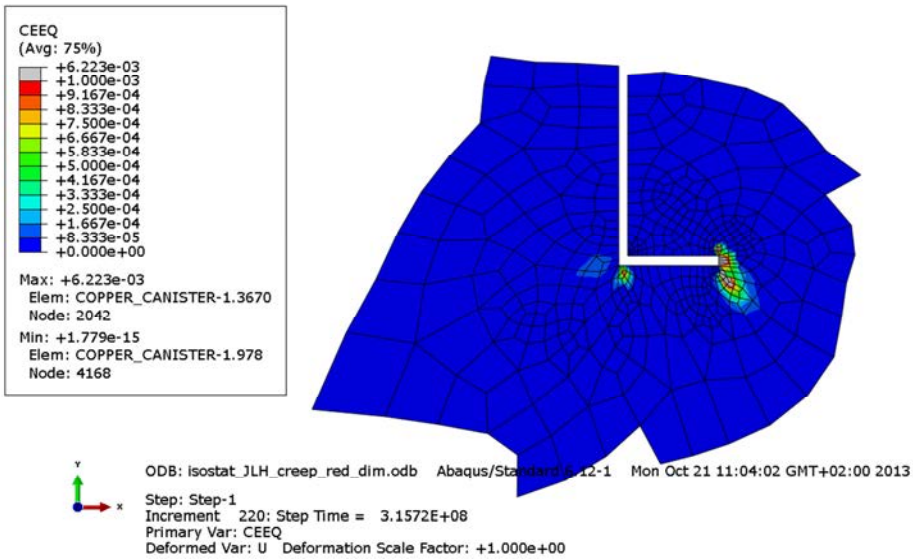

Figure A1-11. *Plot showing the equivalent creep strain at the copper shell bottom weld after 10 years. Gas pressure is applied.*

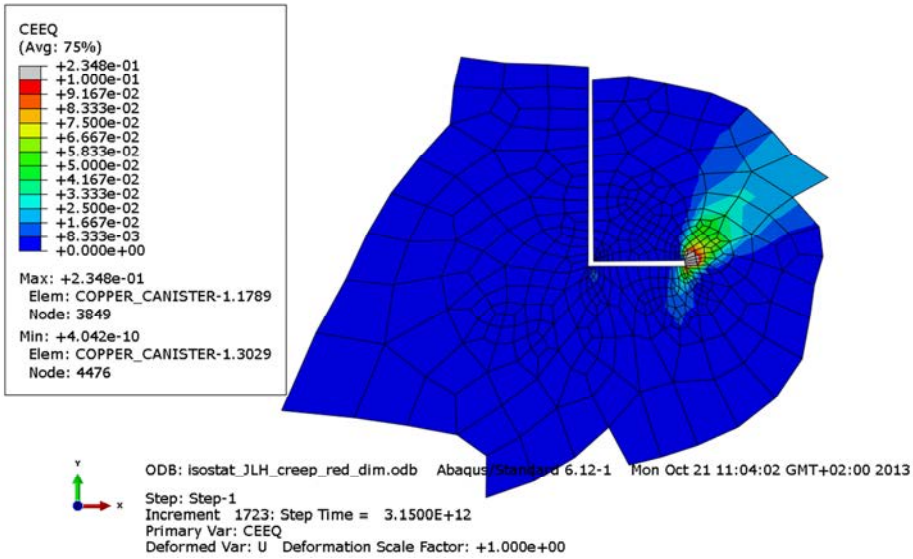

Figure A1-12. *Plot showing the equivalent creep strain at the copper shell bottom weld after 100,000 years.*

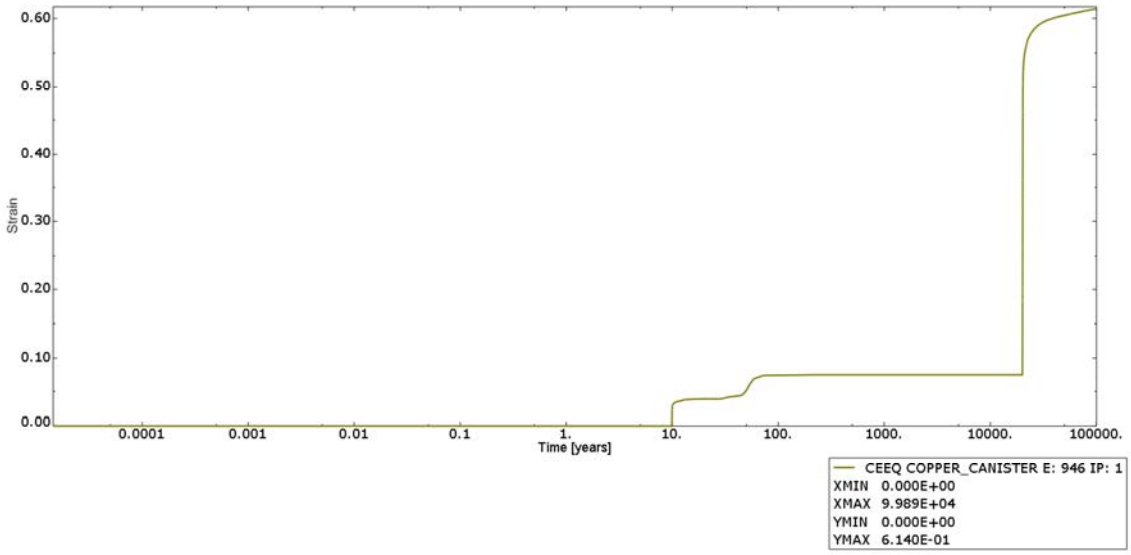

Figure A1-13. *Plot showing the history of equivalent creep strain in the element having the maximum magnitude. Time is in years and strain is dimensionless.*

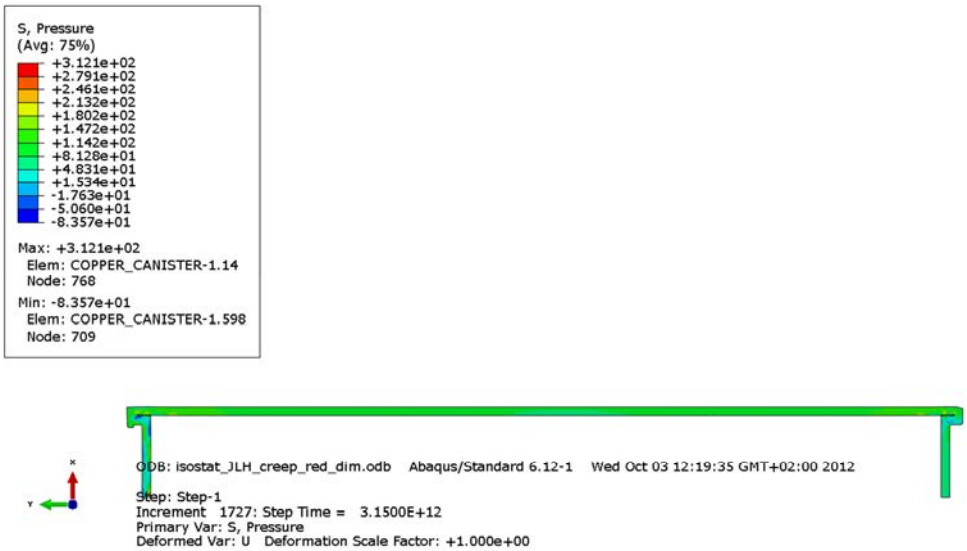

Figure A1-14. *Plot showing the pressure stress in the copper shell after 10 years. Gas pressure is applied.*

Figure A1-15. *Plot showing the pressure stress in the copper shell after 100,000 years.*

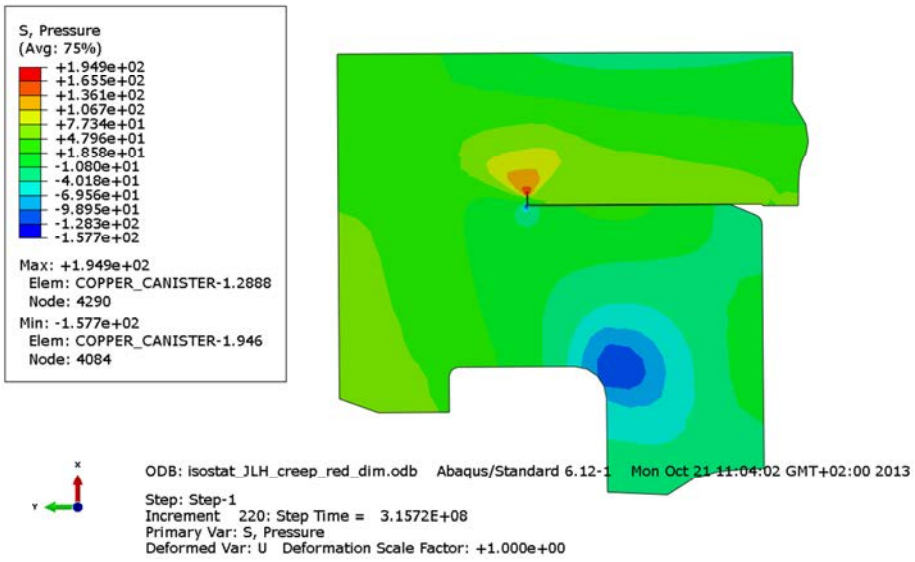

Figure A1-16. *Plot showing the pressure stress at the copper shell top weld after 10 years. Gas pressure is applied.*

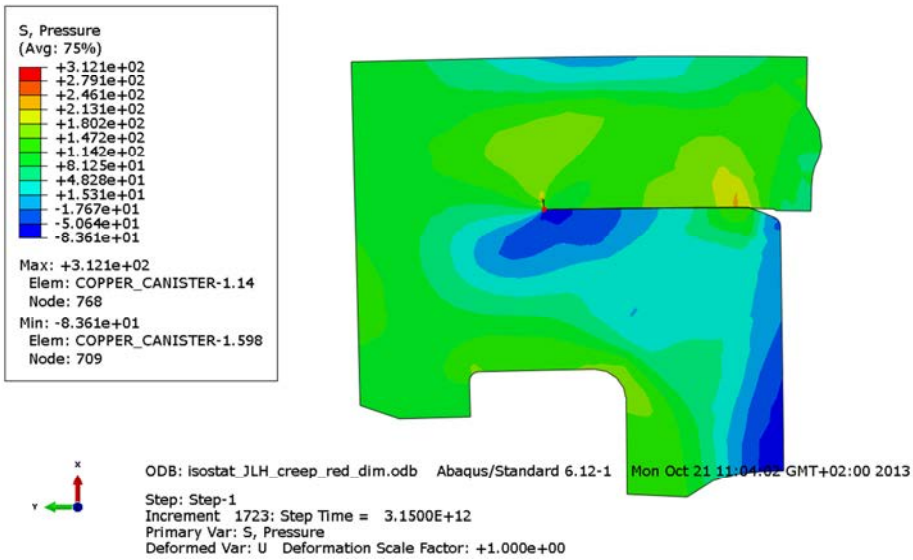

Figure A1-17. *Plot showing the pressure stress at the copper shell top weld after 100,000 years.*

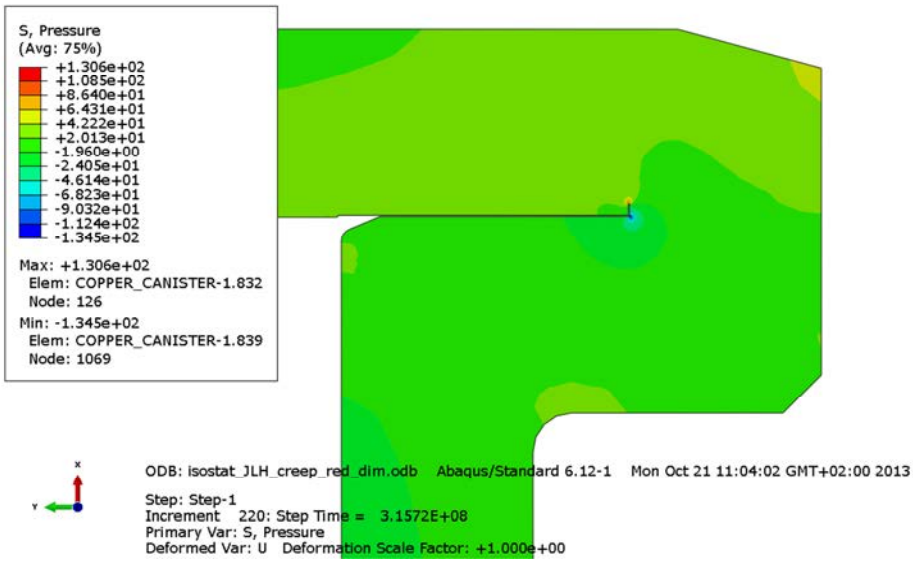

Figure A1-18. *Plot showing the pressure stress at the copper shell bottom weld after 10 years. Gas pressure is applied.*

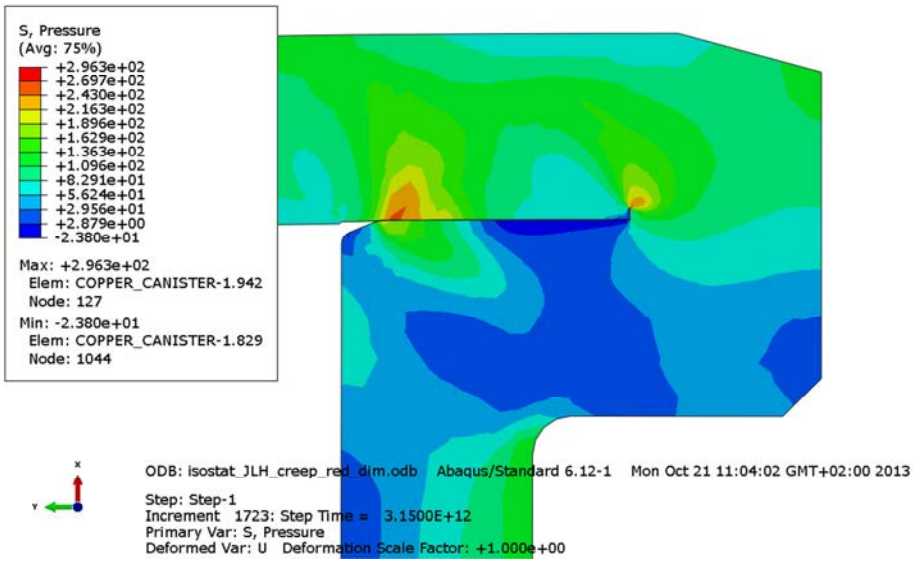

Figure A1-19. *Plot showing the pressure stress at the copper shell bottom weld after 100,000 years.*

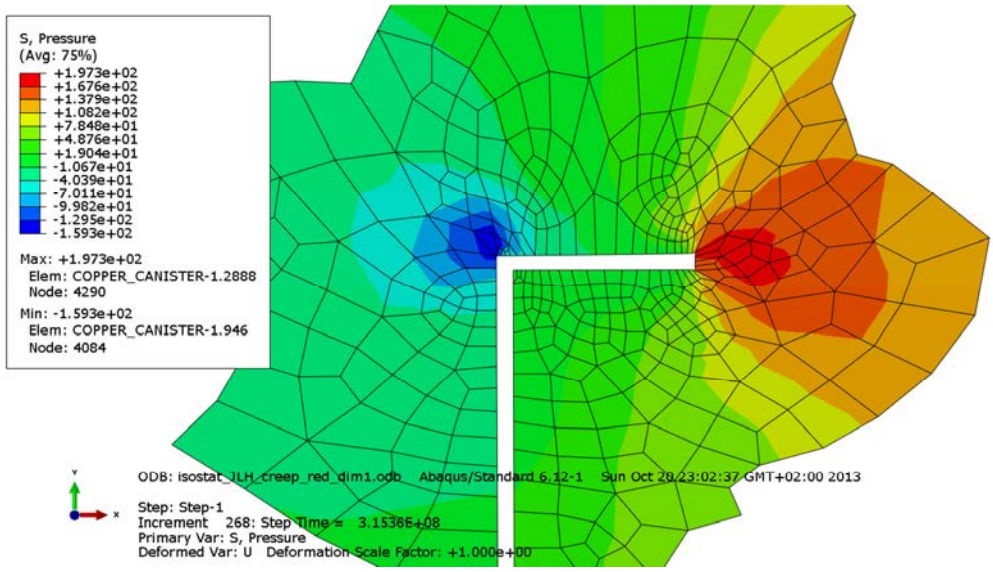

Figure A1-20. *Plot showing the pressure stress at the copper shell top weld after 10 years. Gas pressure is applied.*

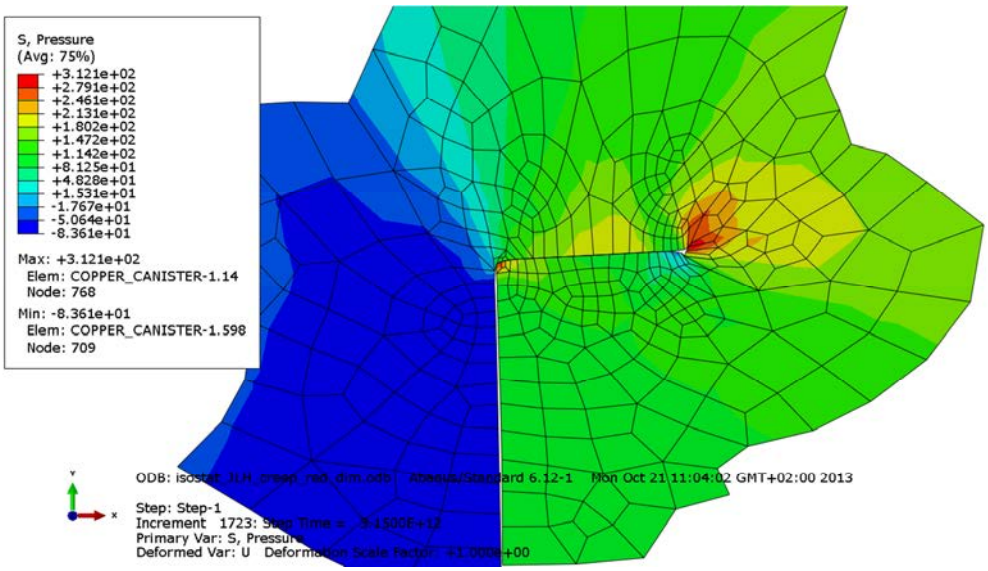

Figure A1-21. *Plot showing the pressure stress at the copper shell top weld after 10,000 years.*

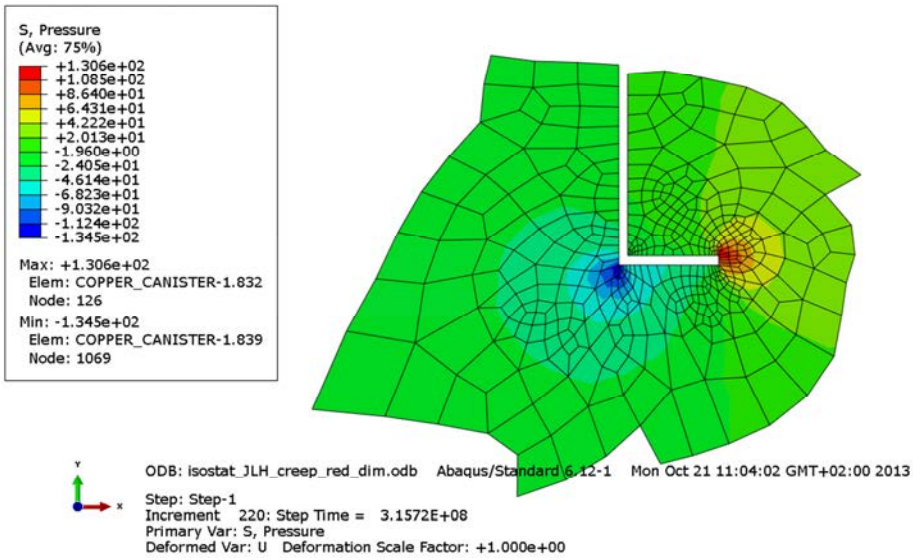

Figure A1-22. *Plot showing the pressure stress at the copper shell bottom weld after 10 years. Gas pressure is applied.*

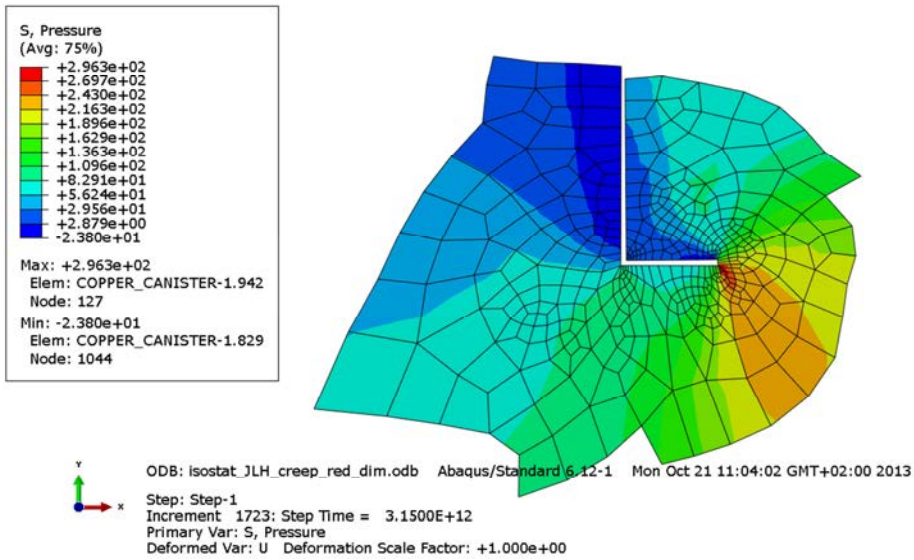

Figure A1-23. *Plot showing the pressure stress at the copper shell bottom weld after 100,000 years.*

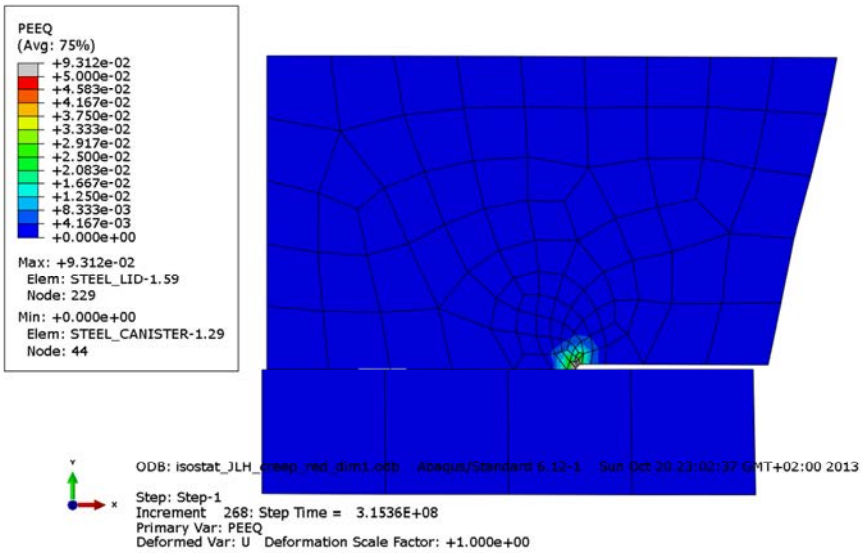

Figure A1-24. *Plot showing the equivalent plastic strain at the steel lid after 10 years; see also Fig 4.3 for understanding of the detail. Gas pressure is applied.*

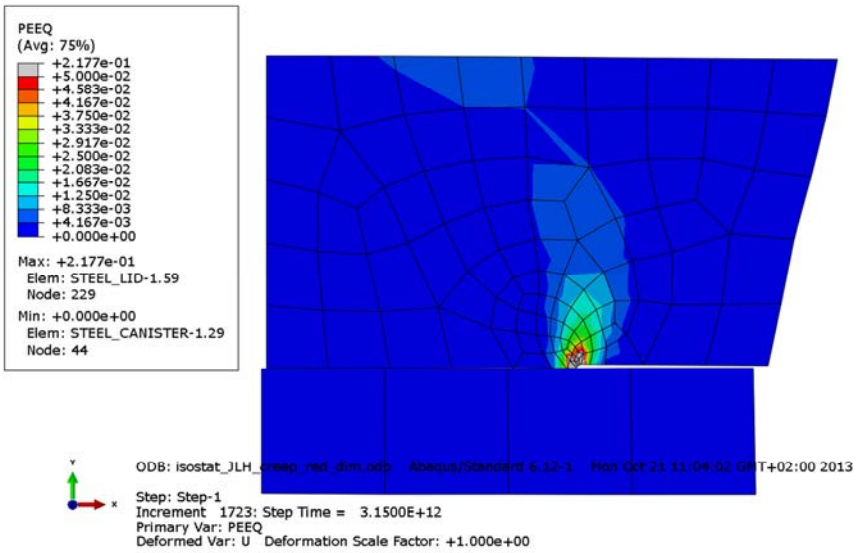

Figure A1-25. *Plot showing the equivalent plastic strain at the steel lid after 100,000 years; see also Fig 4.3 for understanding of the detail.*

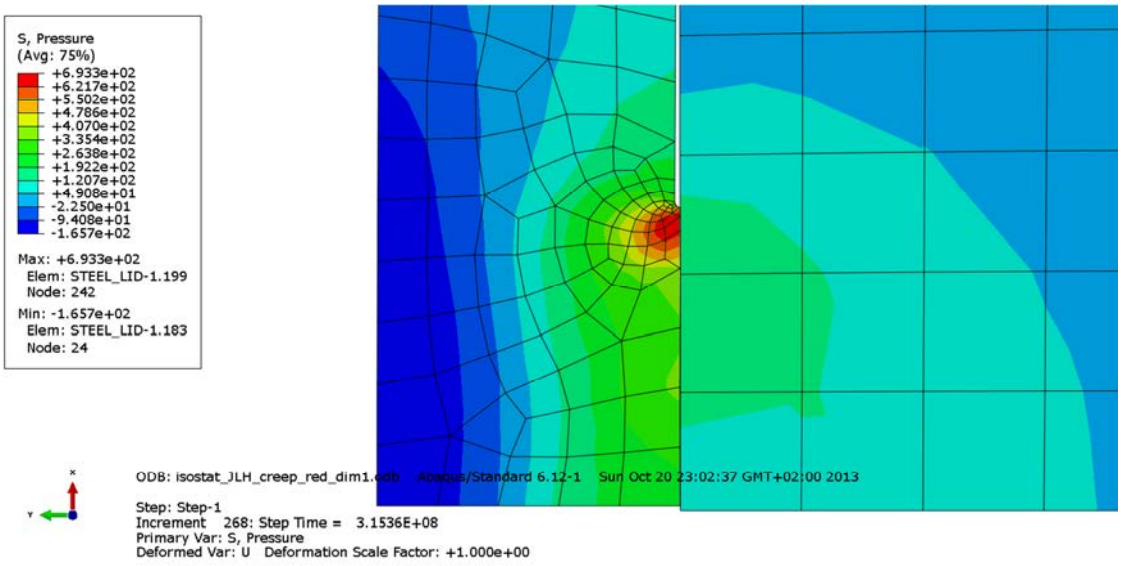

Figure A0-1-26. *Plot showing the pressure stress at discontinuity of insert after 10 years. Gas pressure is applied.*

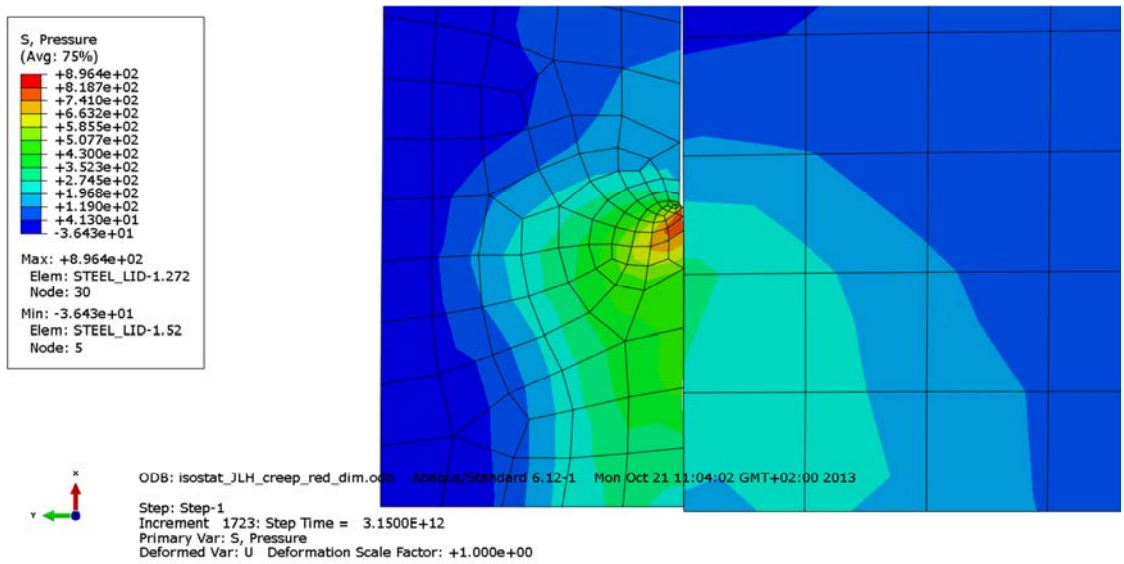

Figure A1-27. *Plot showing the pressure stress at discontinuity of insert after 100,000 years.*

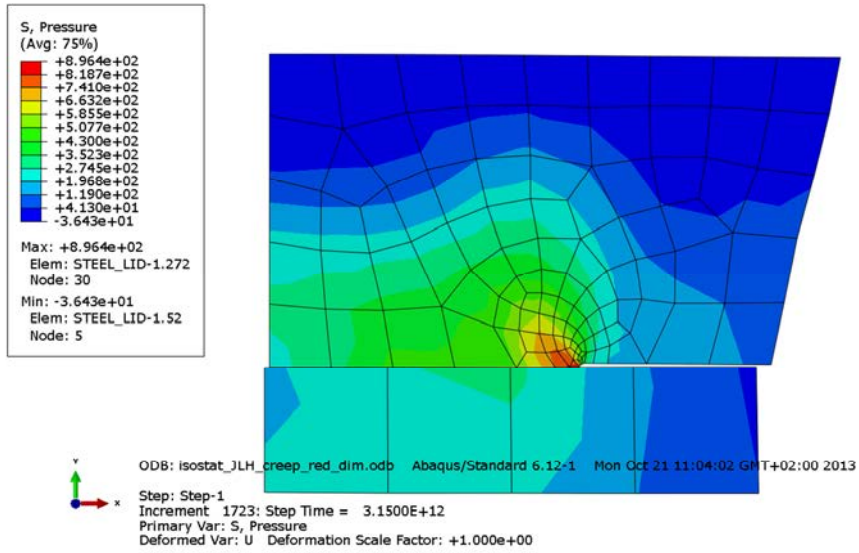

Figure A1-28. *Plot showing the pressure stress at the steel lid after 100,000 years; see also Fig 4.3 for understanding of the detail.*

Appendix 2 – Isostat_JLH_creep_red_mean

Plots showing temperature and pressure contours and history.

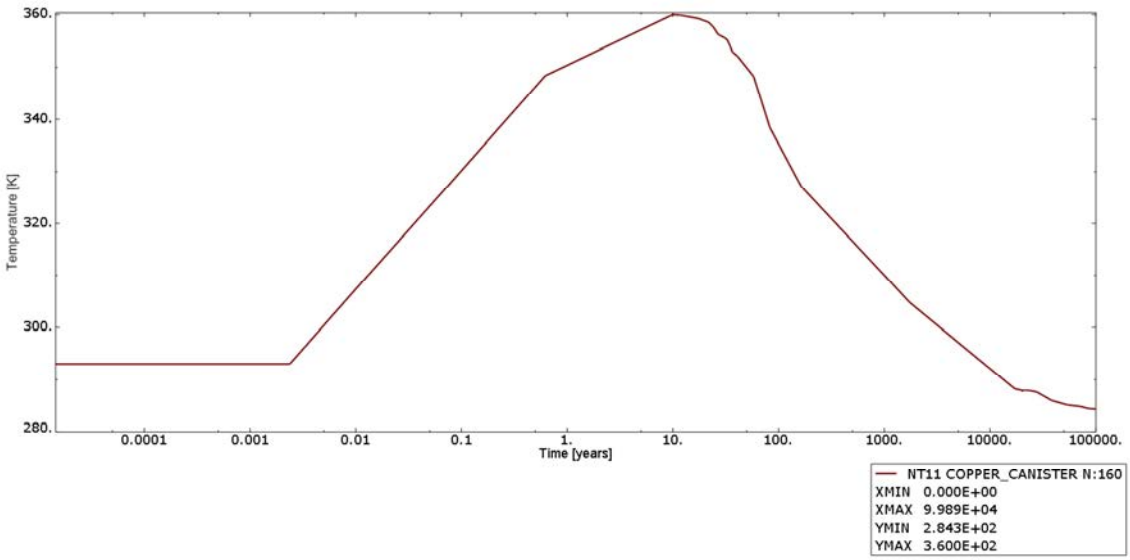

Figure A2-1. *Plot showing the temperature history. Time is in years, temperature is in Kelvin.*

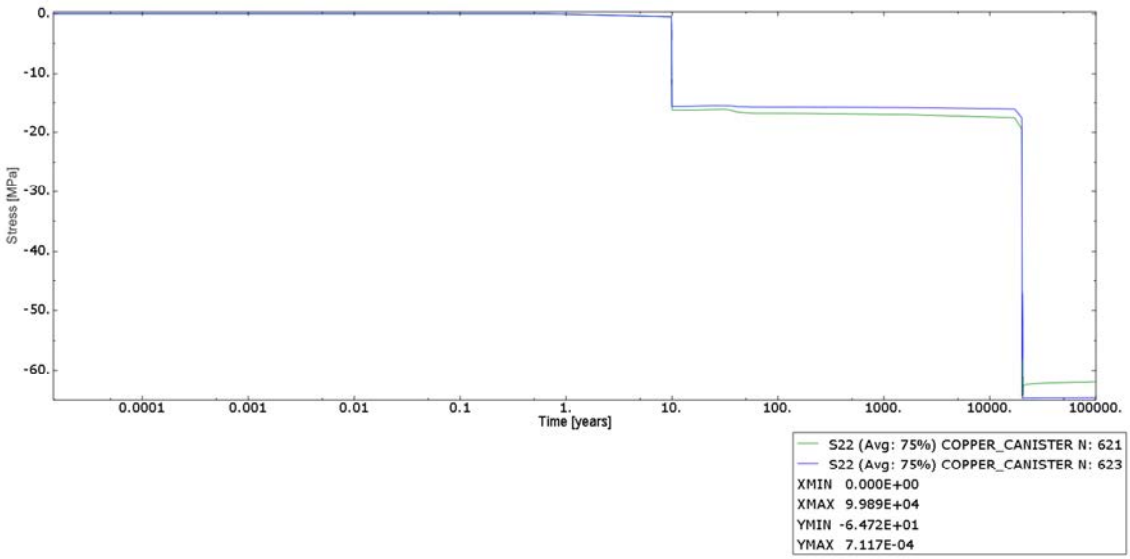

Figure A2-2. *Plot showing the applied pressure at the top lid of the copper shell. Time is in years and stress is in MPa.*

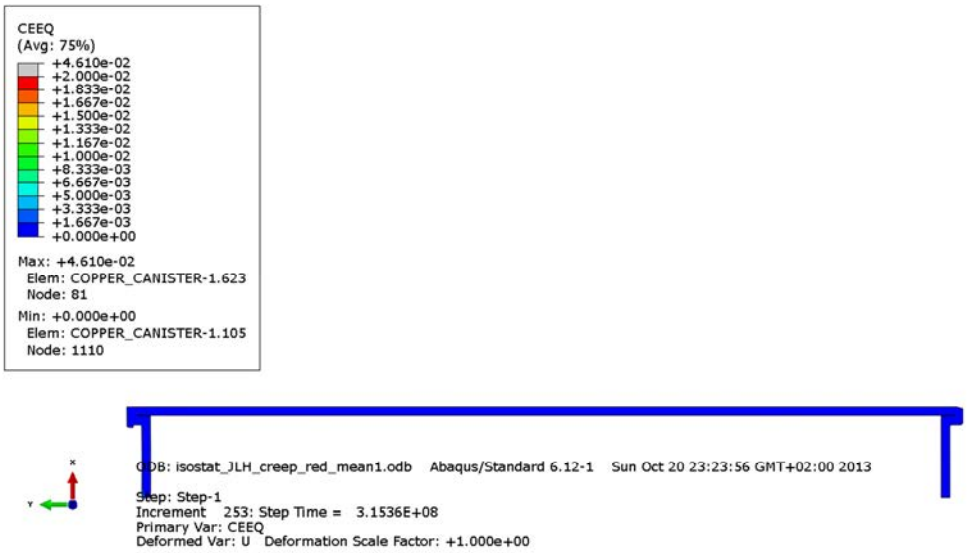

Figure A2-3. *Plot showing the equivalent creep strain after 10 years. Gas pressure is applied.*

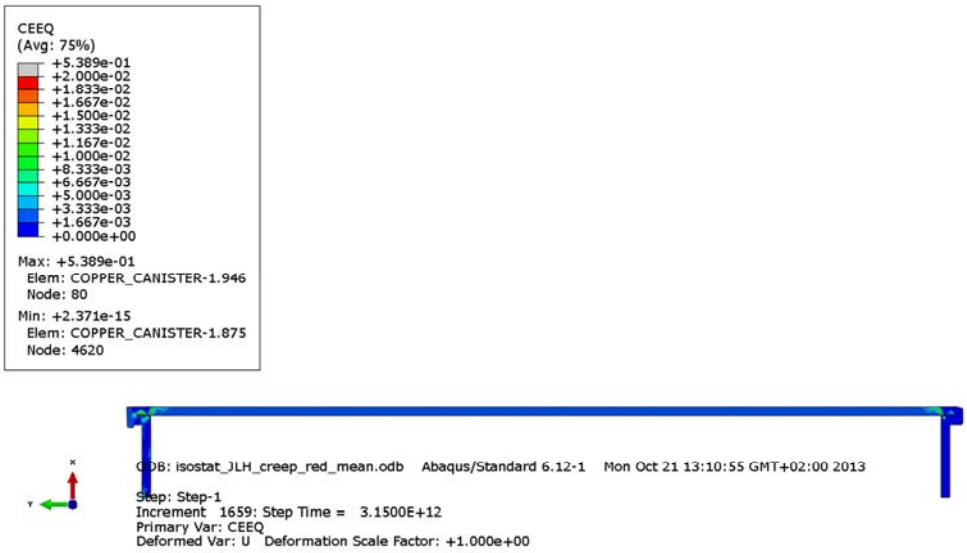

Figure A2-4. *Plot showing the equivalent creep strain after 100,000 years.*

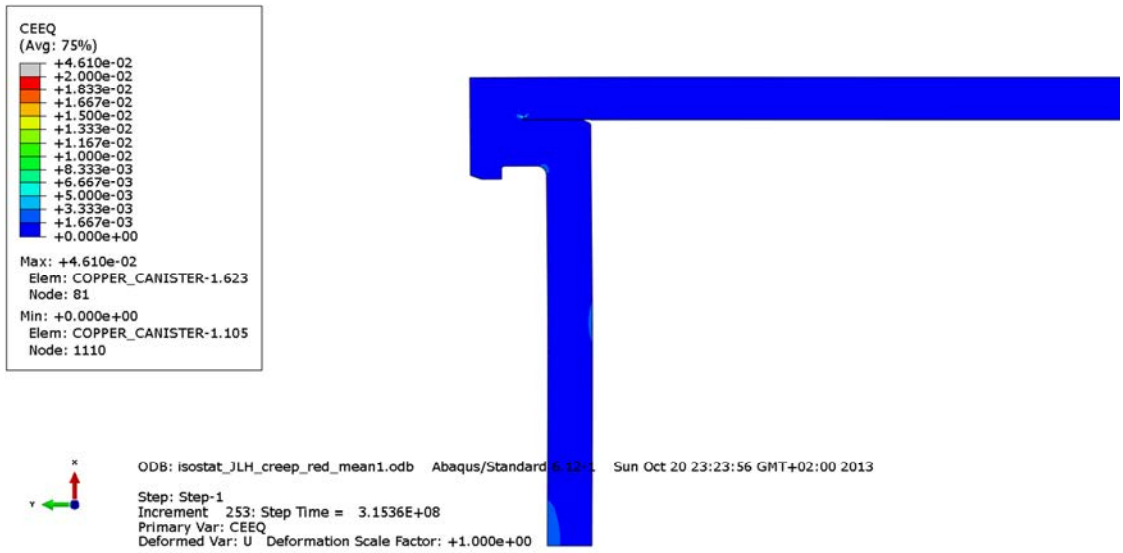

Figure A2-5. *Plot showing the equivalent creep strain at the top weld of the copper shell after 10 years. Gas pressure is applied.*

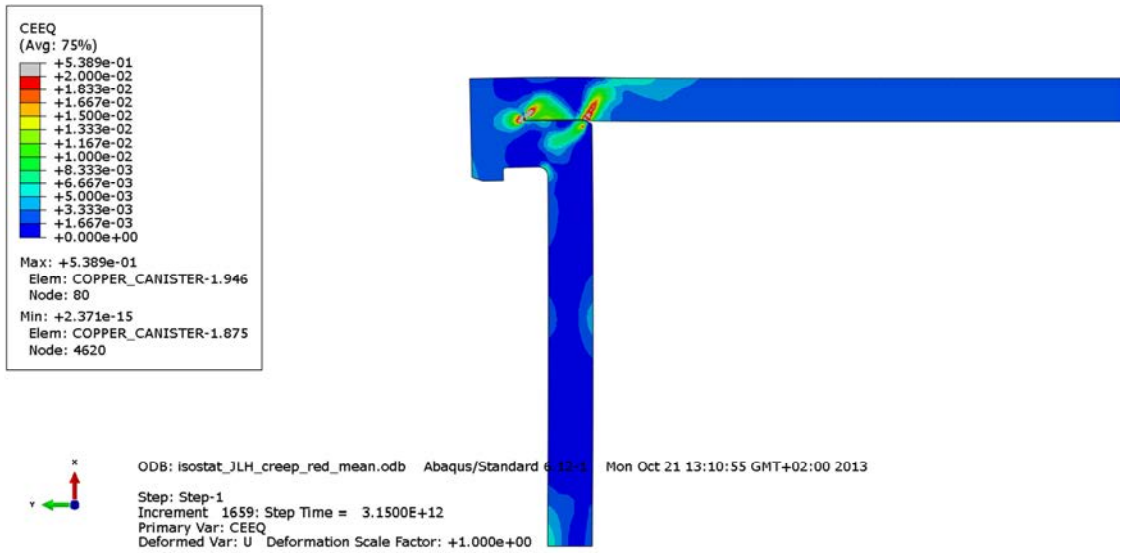

Figure A2-6. *Plot showing the equivalent creep strain at the top weld of the copper shell after 100,000 years.*

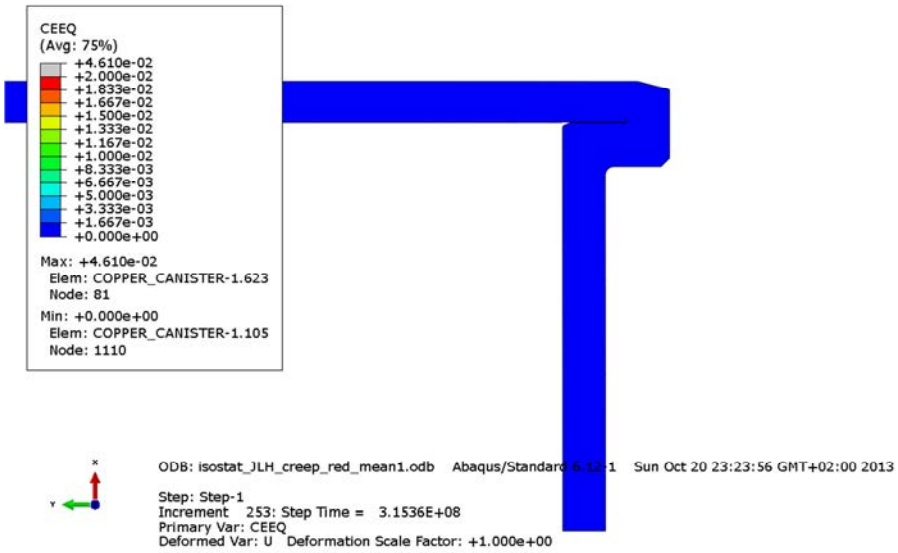

Figure A2-7. *Plot showing the equivalent creep strain at the bottom weld of the copper shell after 10 years. Gas pressure is applied.*

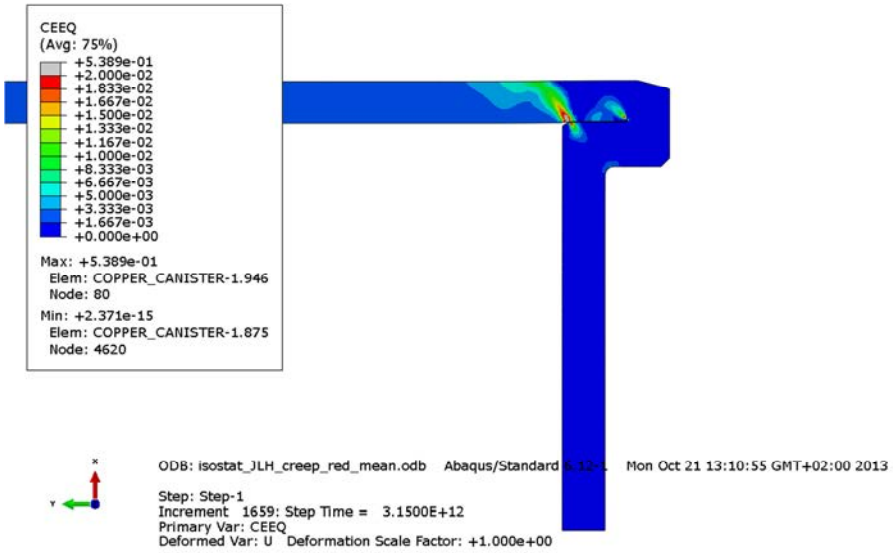

Figure A2-8. *Plot showing the equivalent creep strain at the bottom weld of the copper shell after 100,000 years.*

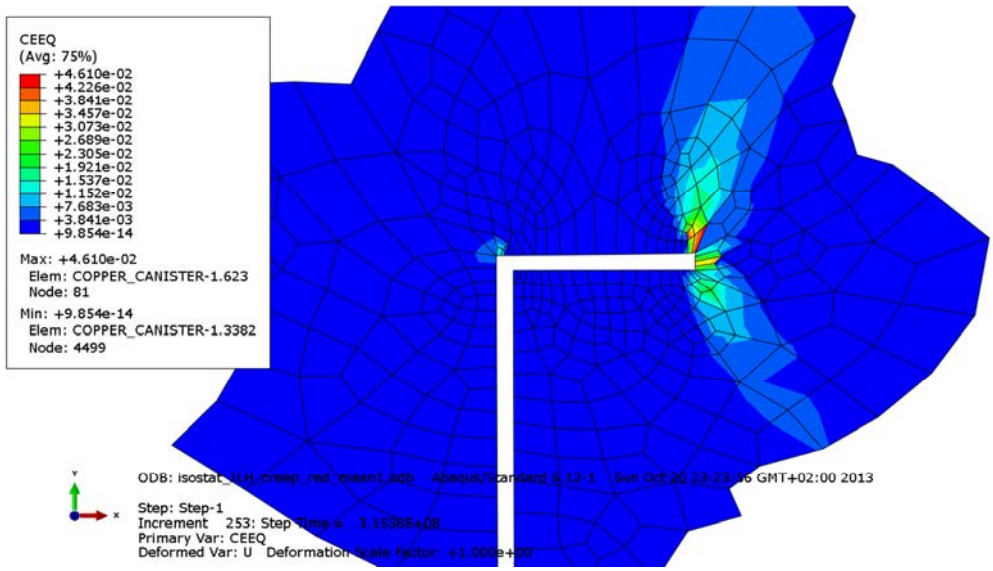

Figure A2-9. *Plot showing the equivalent creep strain at the copper shell top weld after 10 years. Gas pressure is applied.*

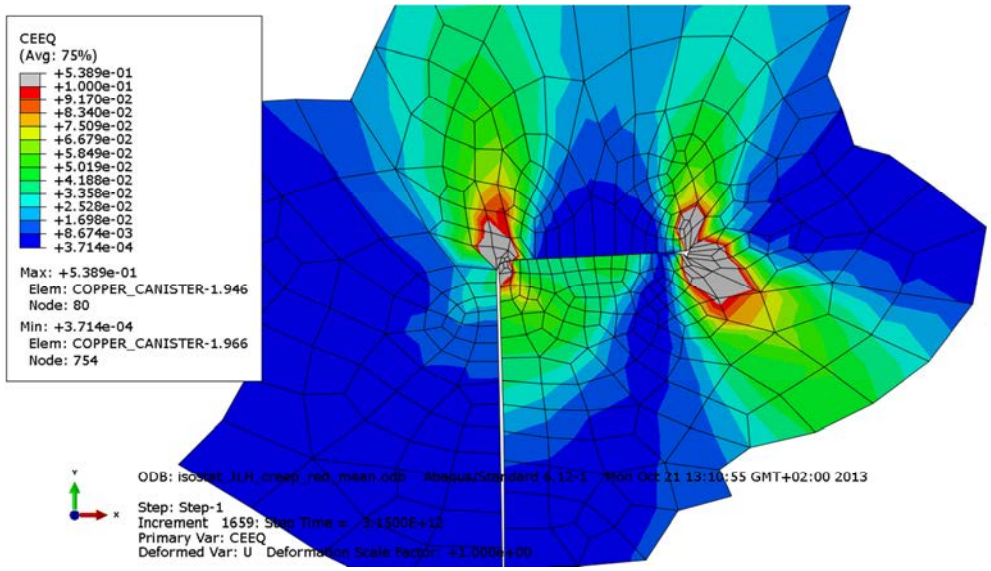

Figure A2-10. *Plot showing the equivalent creep strain at the copper shell top weld after 100,000 years.*

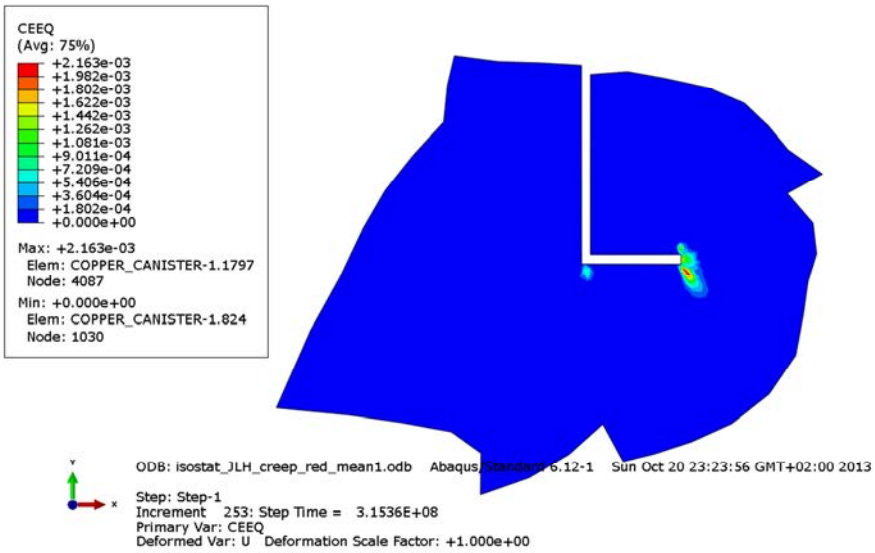

Figure A2-11. *Plot showing the equivalent creep strain at the copper shell bottom weld after 10 years. Gas pressure is applied.*

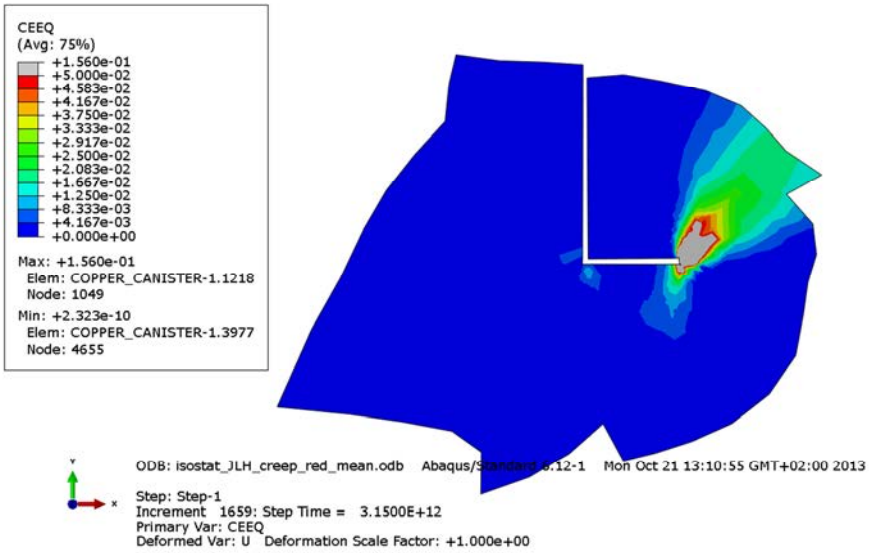

Figure A2-12. *Plot showing the equivalent creep strain at the copper shell bottom weld after 100,000 years.*

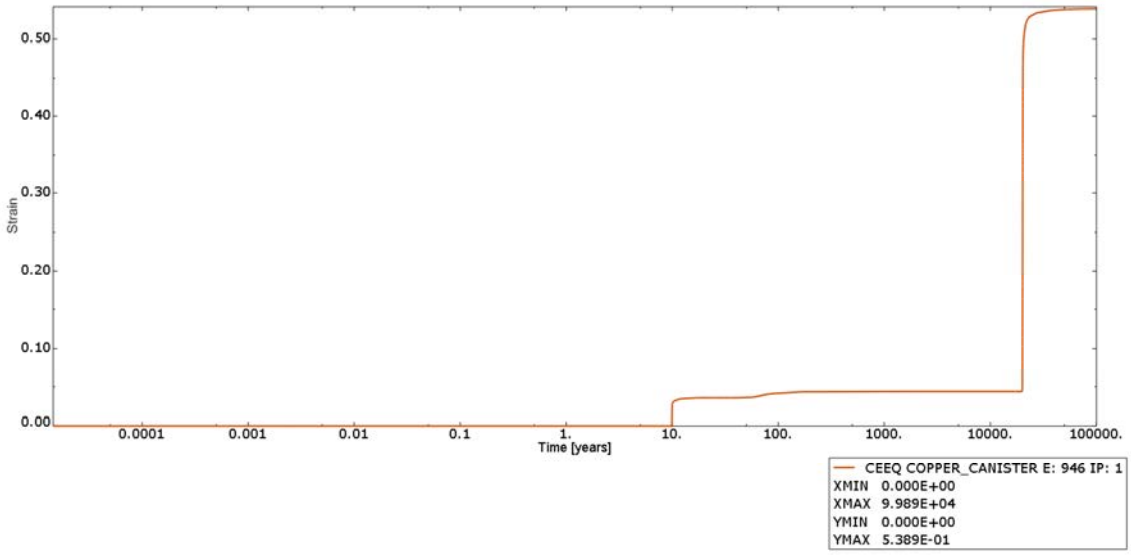

Figure A2-13. *Plot showing the history of equivalent creep strain in the element having the maximum magnitude. Time is in years and strain is dimensionless.*

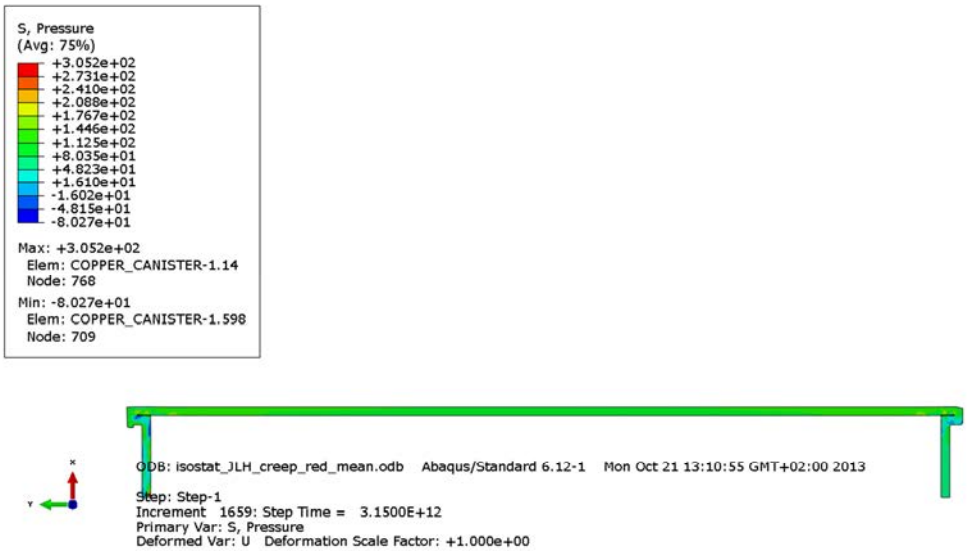

Figure A2-14. *Plot showing the pressure stress in the copper shell after 10 years. Gas pressure is applied.*

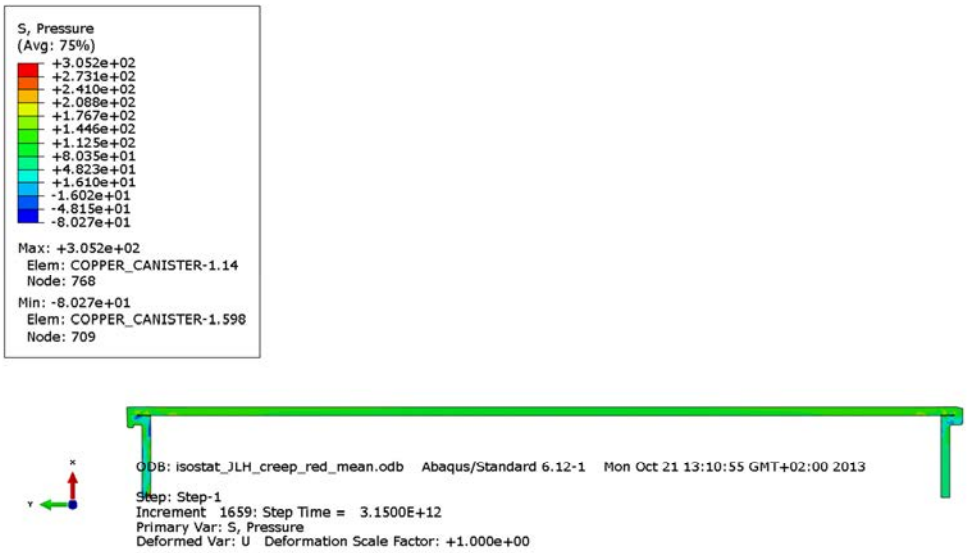

Figure A2-15. *Plot showing the pressure stress in the copper shell after 100,000 years.*

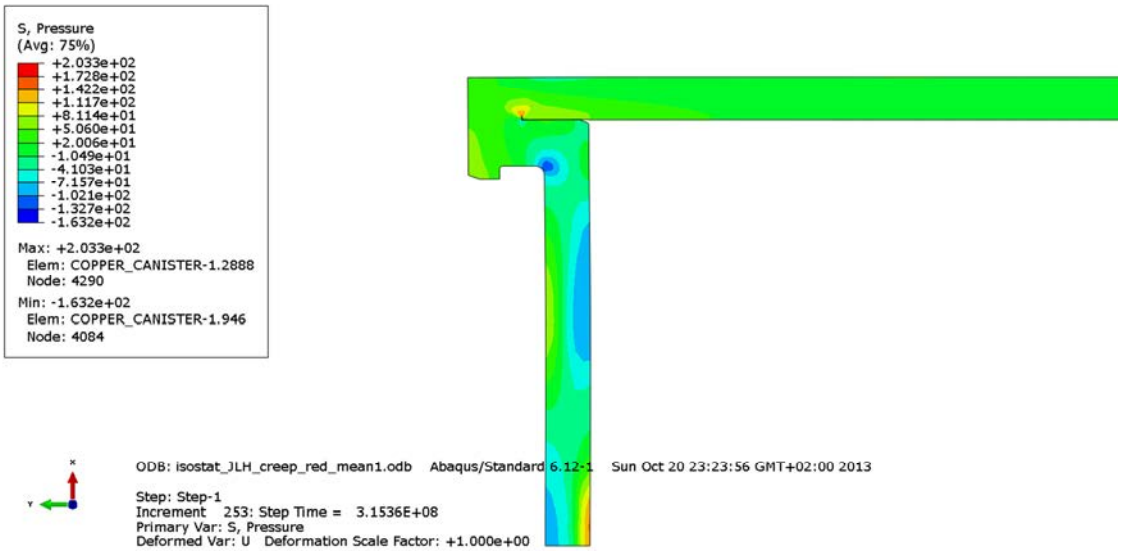

Figure A2-16. *Plot showing the pressure stress at the copper shell top weld after 10 years. Gas pressure is applied.*

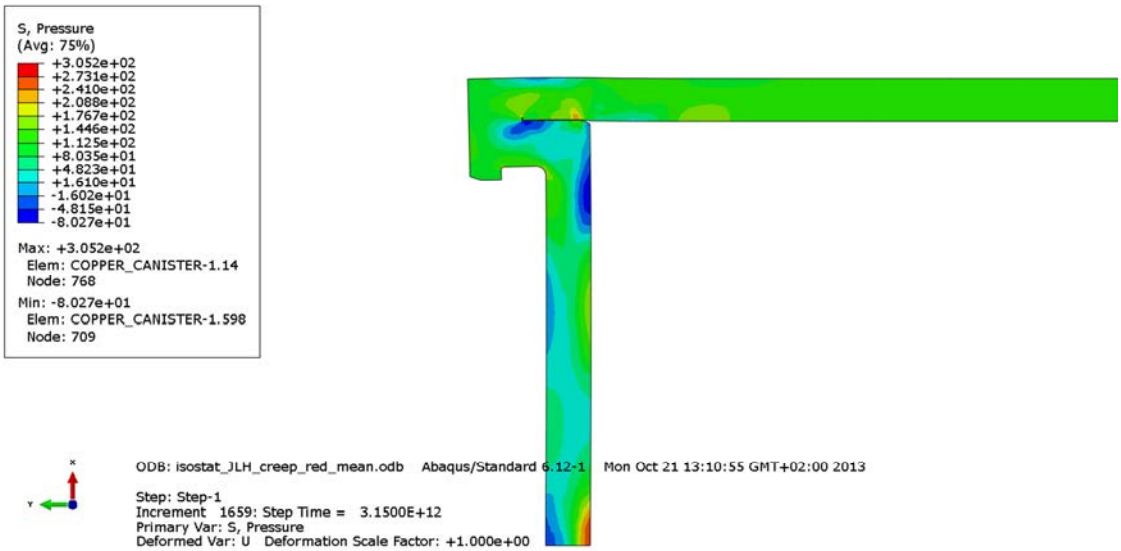

Figure A2-17. *Plot showing the pressure stress at the copper shell top weld after 100,000 years.*

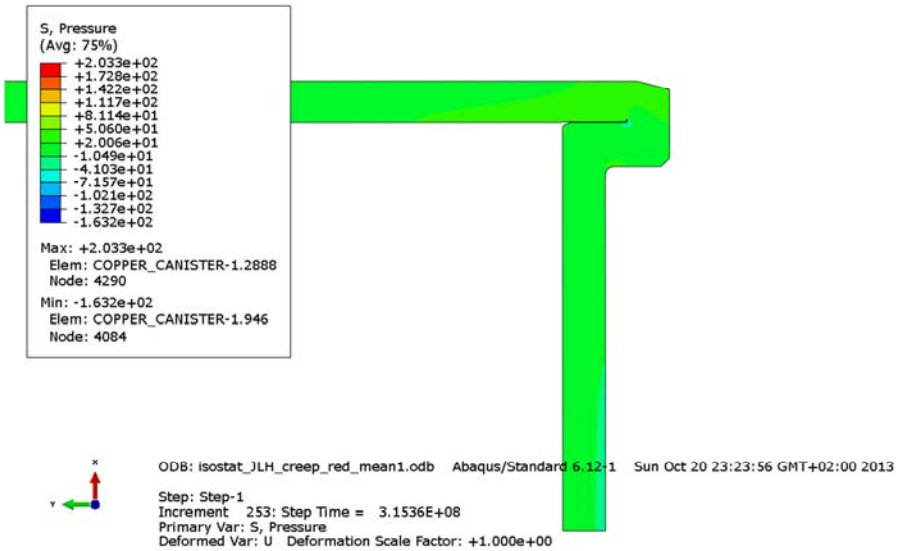

Figure A2-18. *Plot showing the pressure stress at the copper shell bottom weld after 10 years. Gas pressure is applied.*

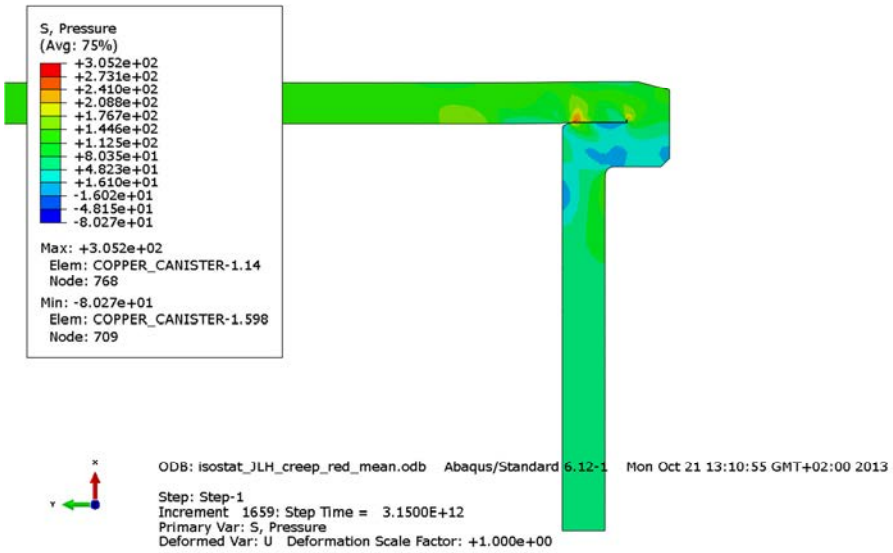

Figure A2-19. *Plot showing the pressure stress at the copper shell bottom weld after 100,000 years.*

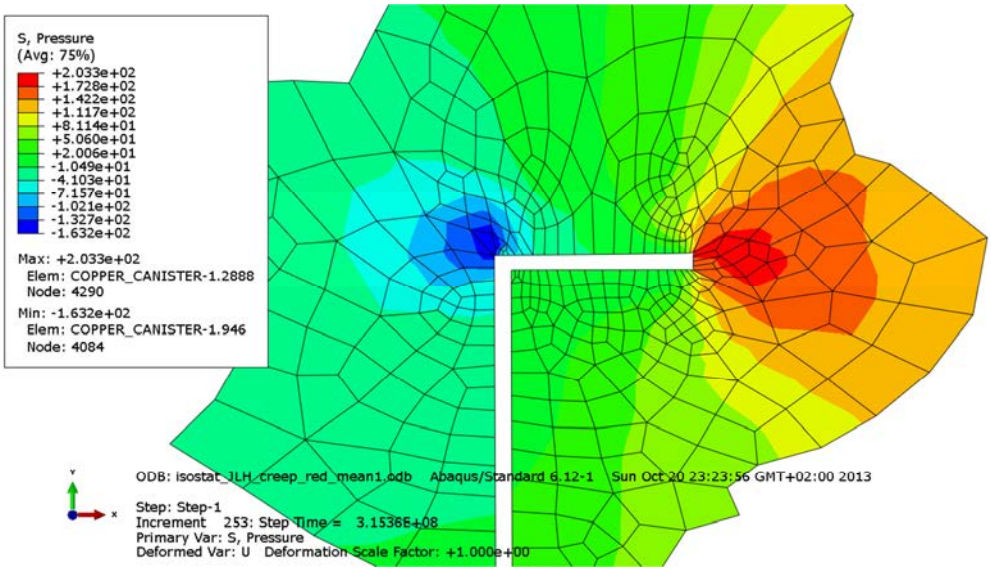

Figure A2-20. *Plot showing the pressure stress at the copper shell top weld after 10 years. Gas pressure is applied.*

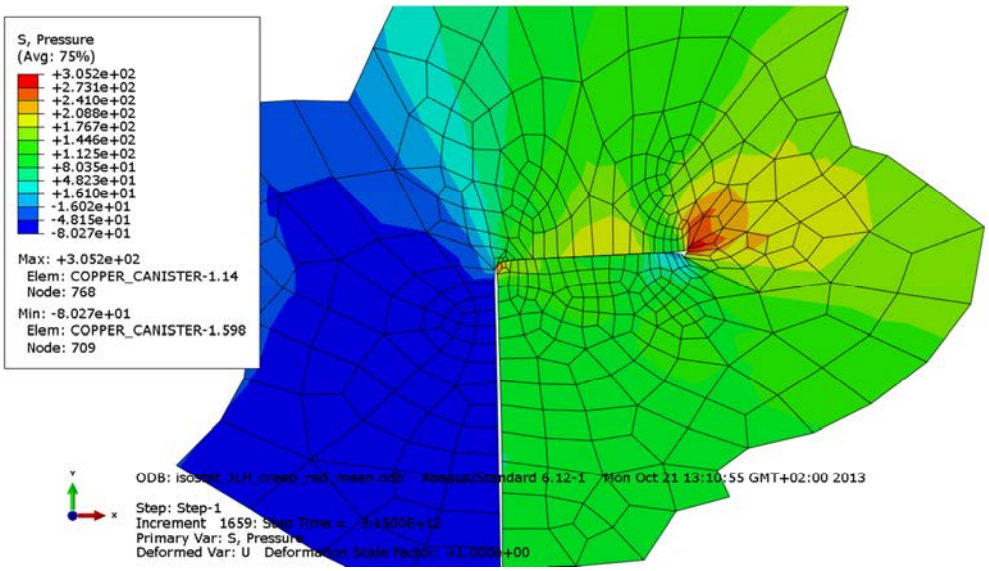

Figure A2-21. *Plot showing the pressure stress at the copper shell top weld after 10,000 years.*

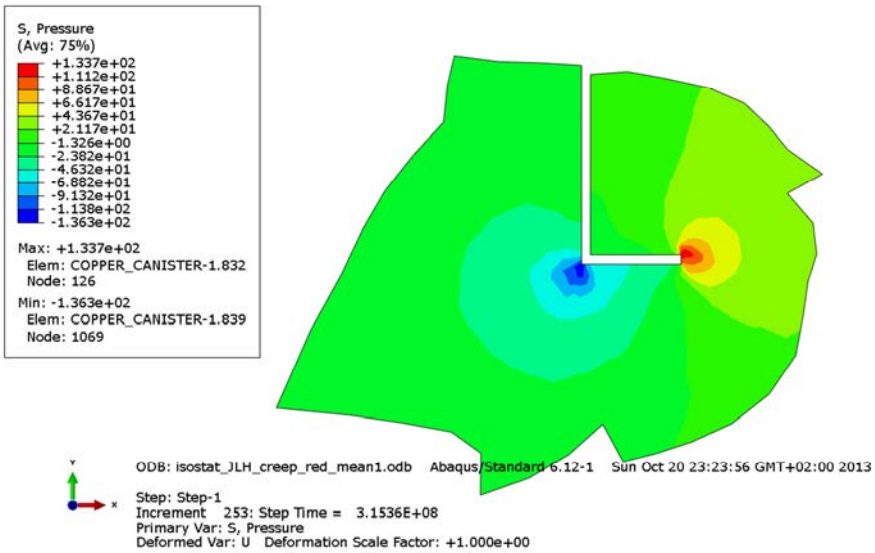

Figure A2-22. *Plot showing the pressure stress at the copper shell bottom weld after 10 years. Gas pressure is applied.*

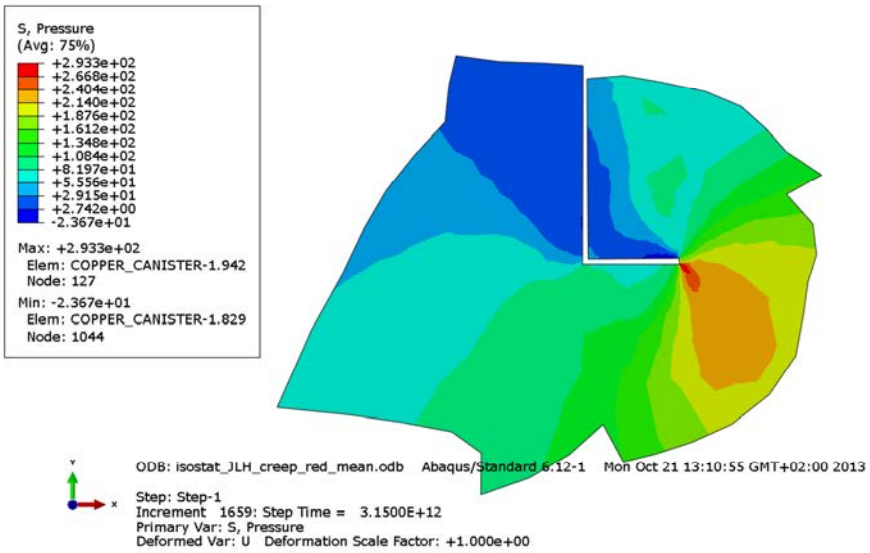

Figure A2-23. *Plot showing the pressure stress at the copper shell bottom weld after 100,000 years.*

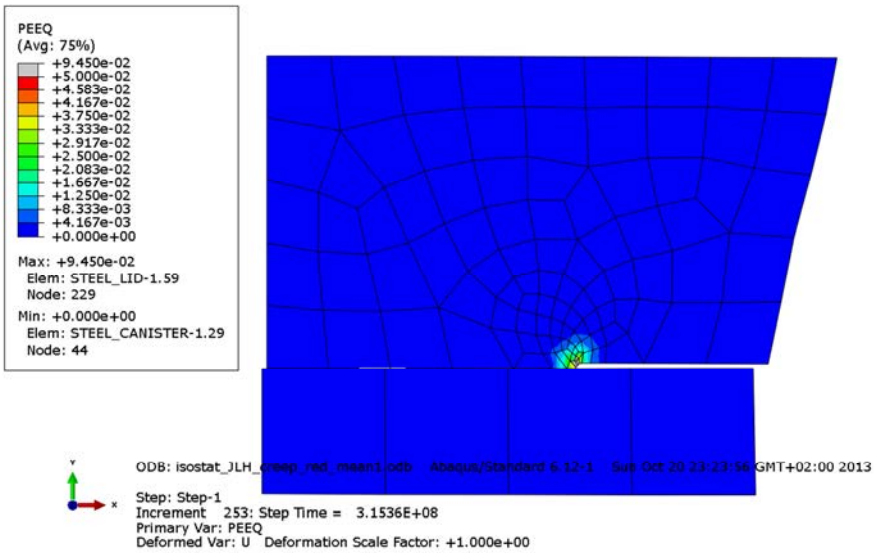

Figure A2-24. *Plot showing the equivalent plastic strain at the steel lid after 10 years; see also Fig 4.3 for understanding of the detail. Gas pressure is applied.*

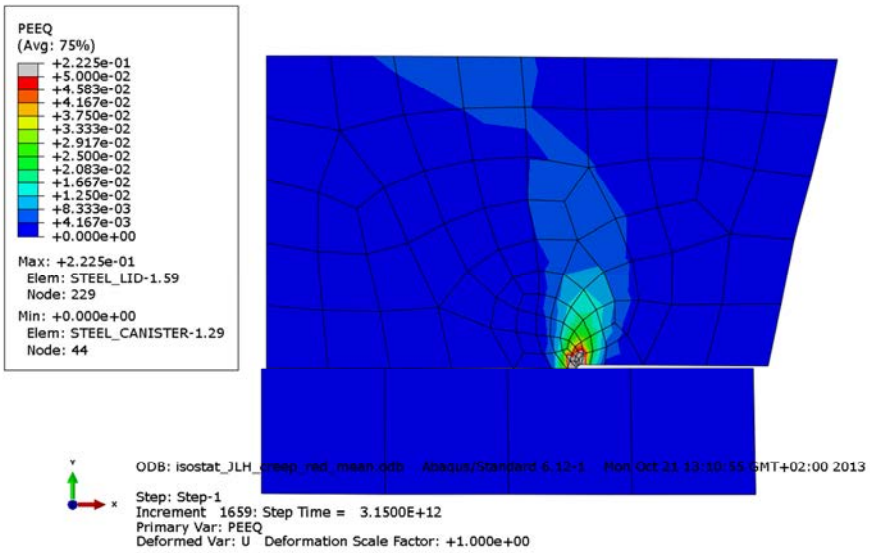

Figure A2-25. *Plot showing the equivalent plastic strain at the steel lid after 100,000 years; see also Fig 4.3 for understanding of the detail.*

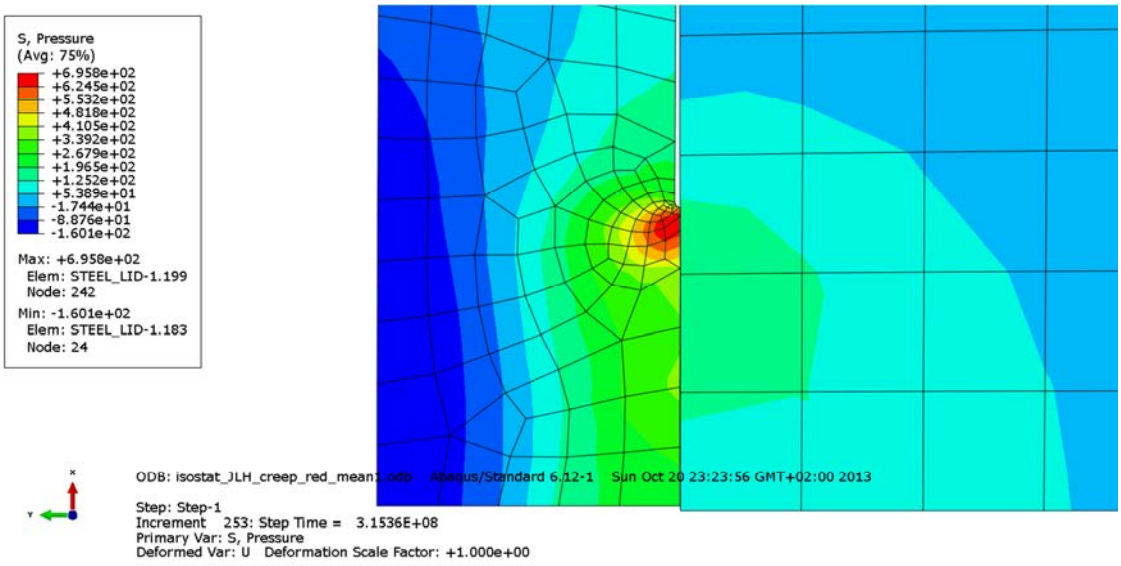

Figure A2-26. *Plot showing the pressure stress at discontinuity of insert after 10 years. Gas pressure is applied.*

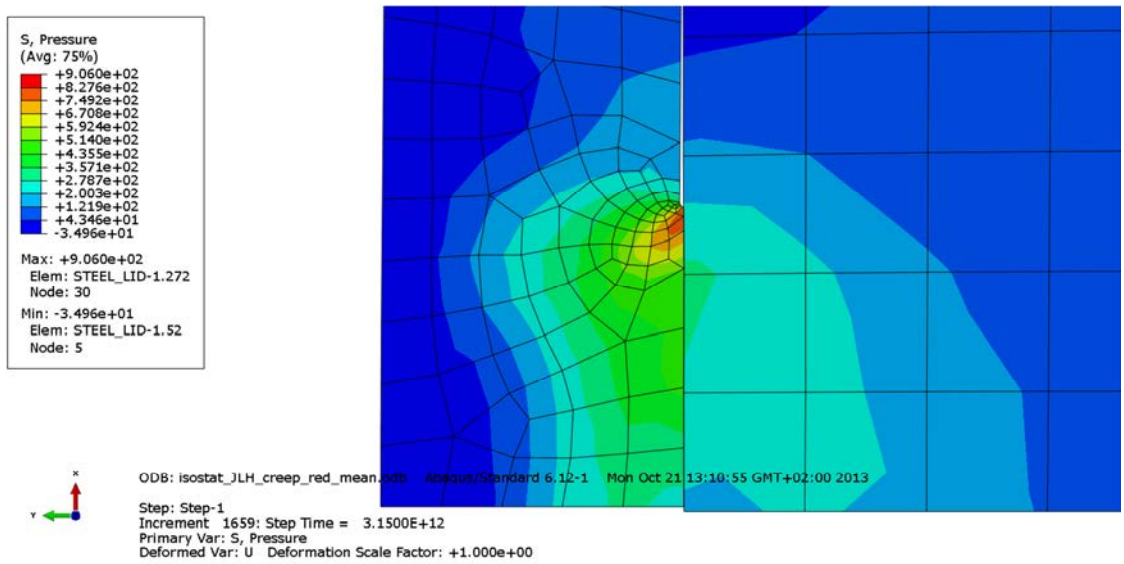

Figure A2-27. *Plot showing the pressure stress at discontinuity of insert after 100,000 years.*

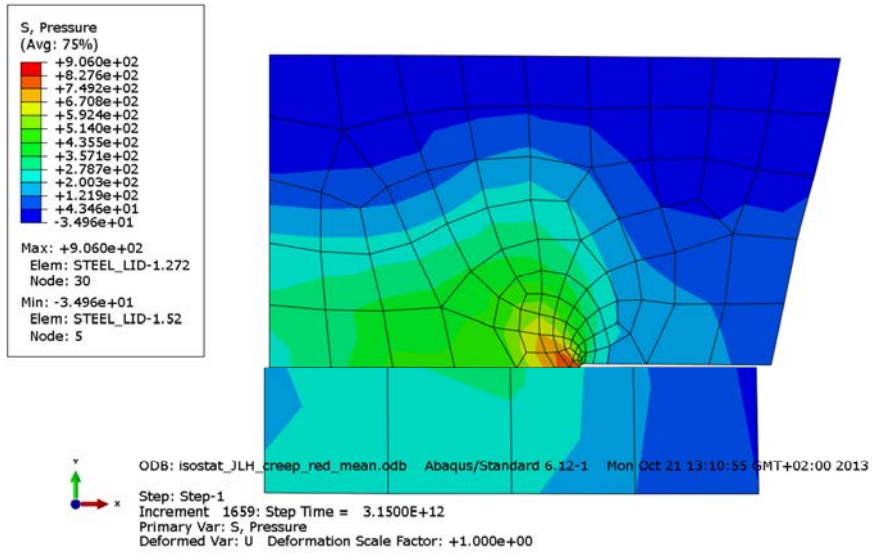

Figure A2-28. *Plot showing the pressure stress at the steel lid after 100,000 years; see also Fig 4.3 for understanding of the detail.*

Appendix 3 – Isostat_JLH_creep_blue_dim

Plots showing temperature and pressure contours and history.

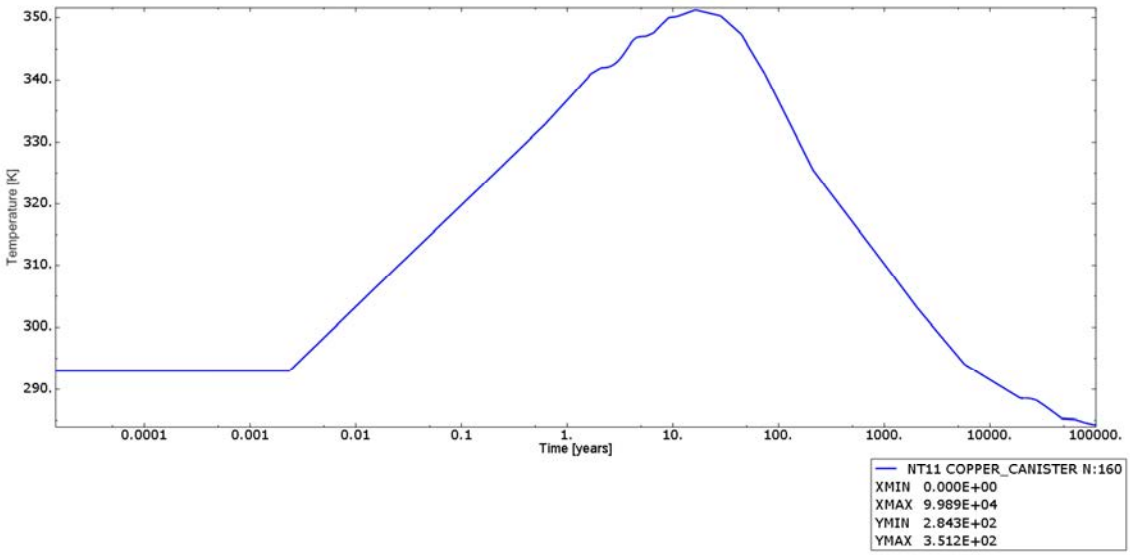

Figure A3-1. *Plot showing the temperature history. Time is in years, temperature is in Kelvin.*

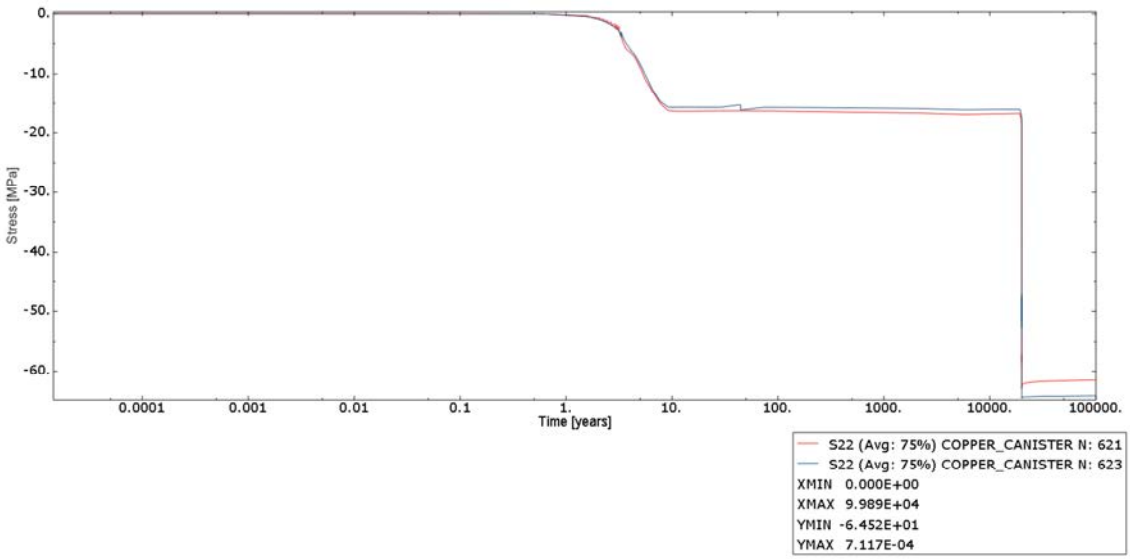

Figure A3-2. *Plot showing the applied pressure at the top lid of the copper shell. Time is in years and stress is in MPa.*

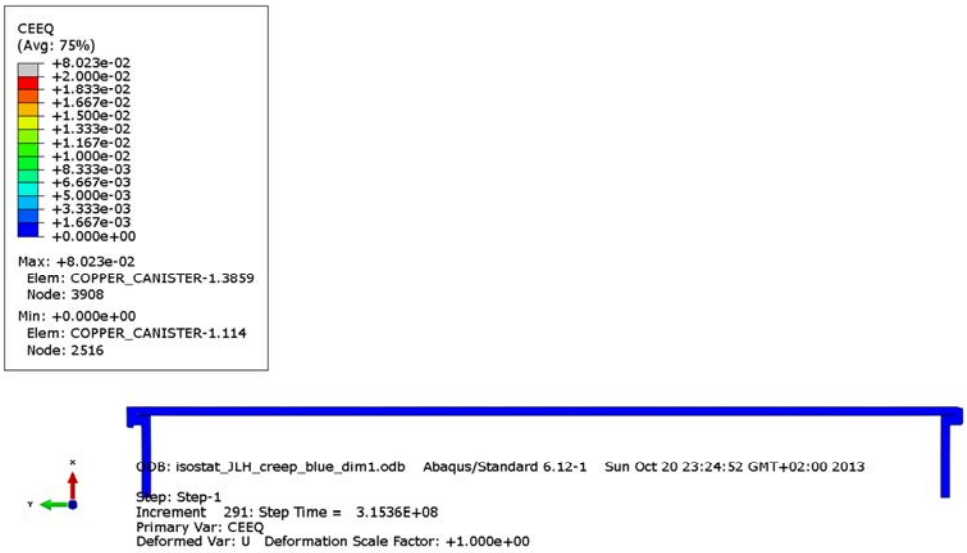

Figure A3-3. *Plot showing the equivalent creep strain after 10 years. Gas pressure is applied.*

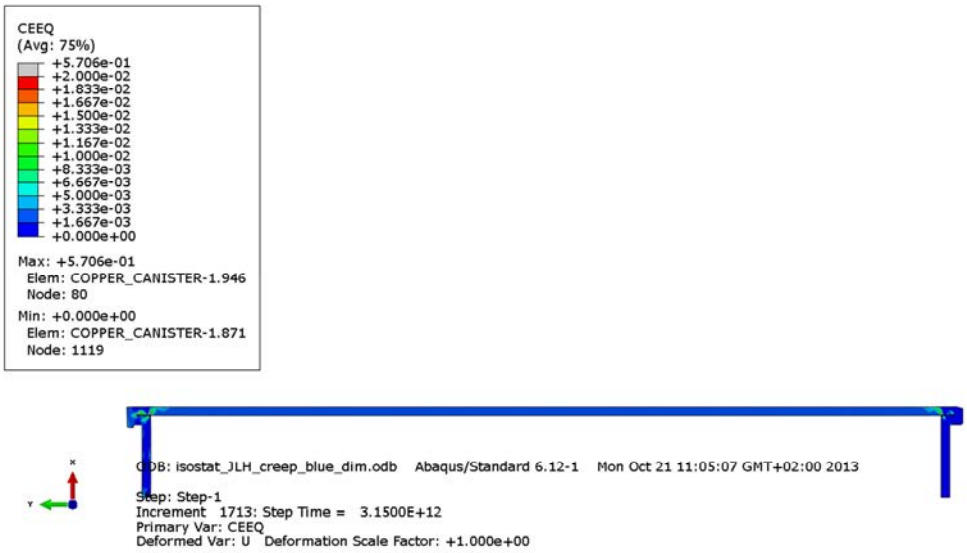

Figure A3-4. *Plot showing the equivalent creep strain after 100,000 years.*

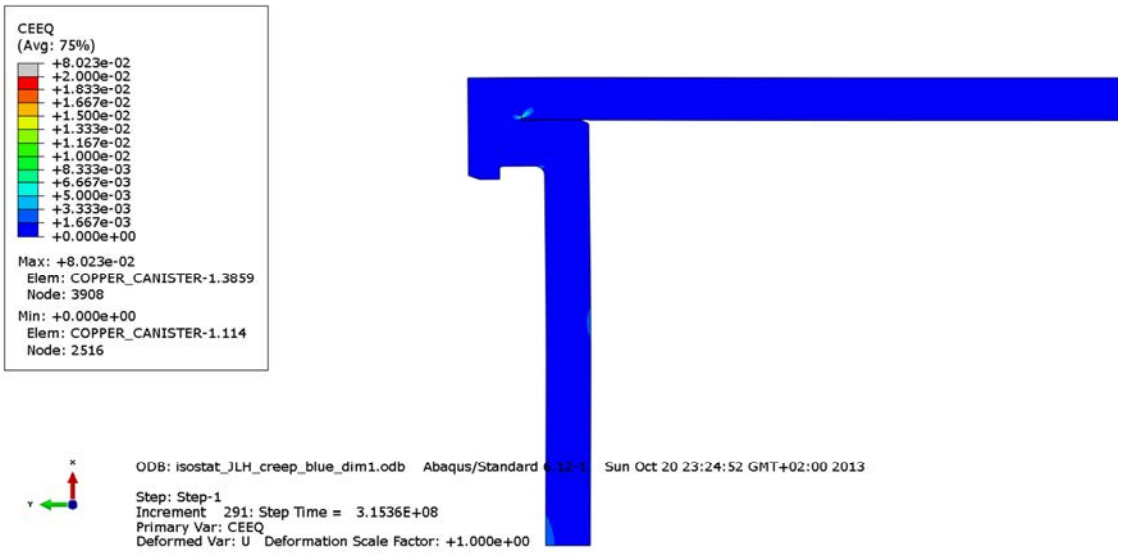

Figure A3-5. *Plot showing the equivalent creep strain at the top weld of the copper shell after 10 years. Gas pressure is applied.*

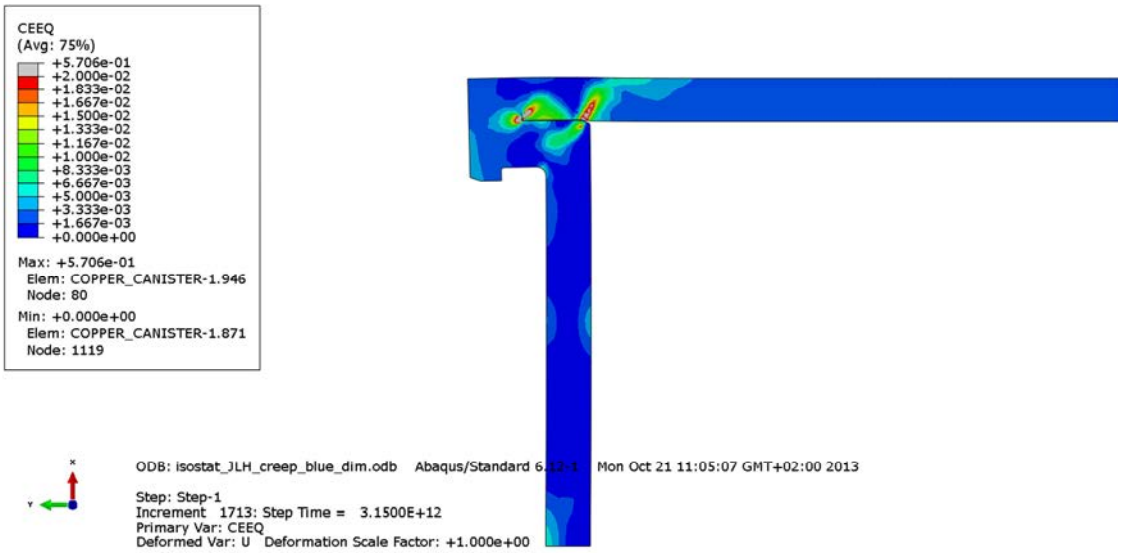

Figure A3-6. *Plot showing the equivalent creep strain at the top weld of the copper shell after 100,000 years.*

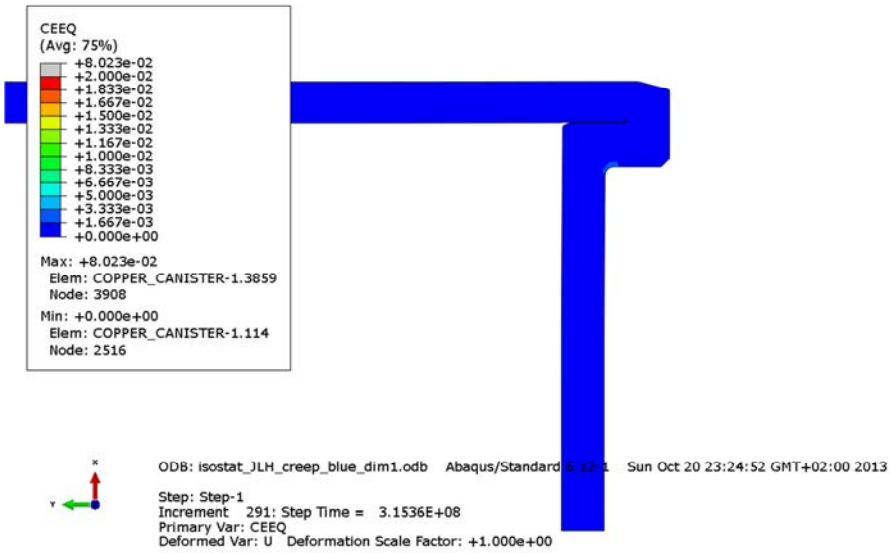

Figure A3-7. *Plot showing the equivalent creep strain at the bottom weld of the copper shell after 10 years. Gas pressure is applied.*

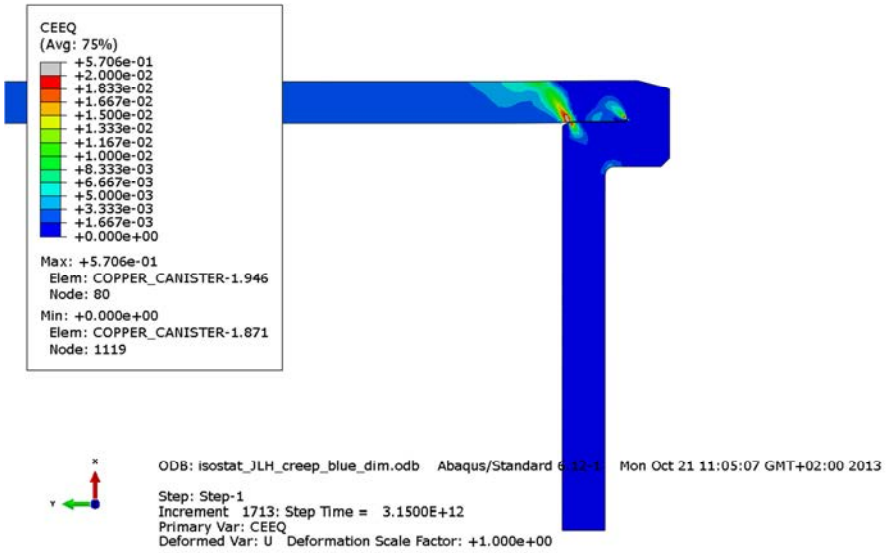

Figure A3-8. *Plot showing the equivalent creep strain at the bottom weld of the copper shell after 100,000 years.*

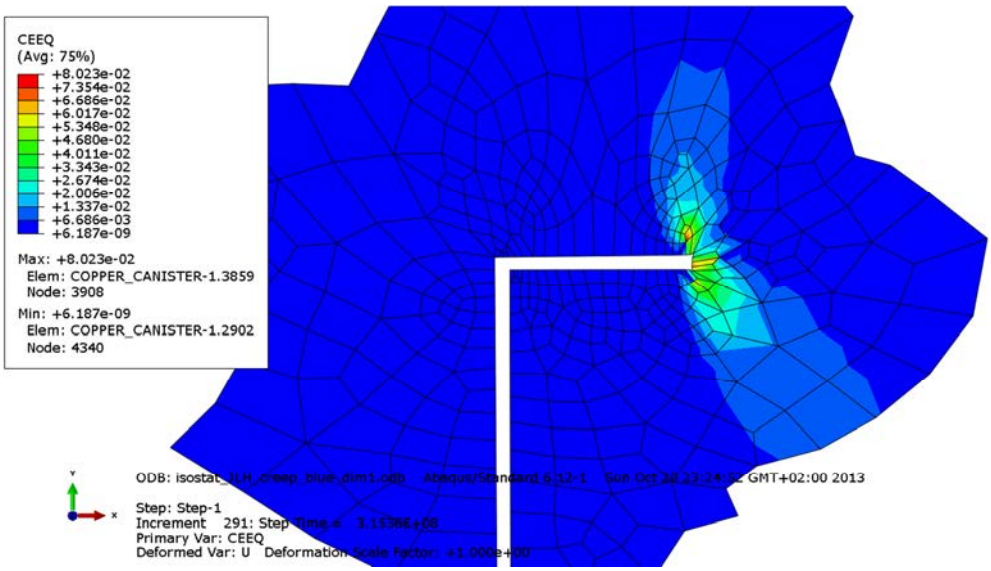

Figure A3-9. *Plot showing the equivalent creep strain at the copper shell top weld after 10 years. Gas pressure is applied.*

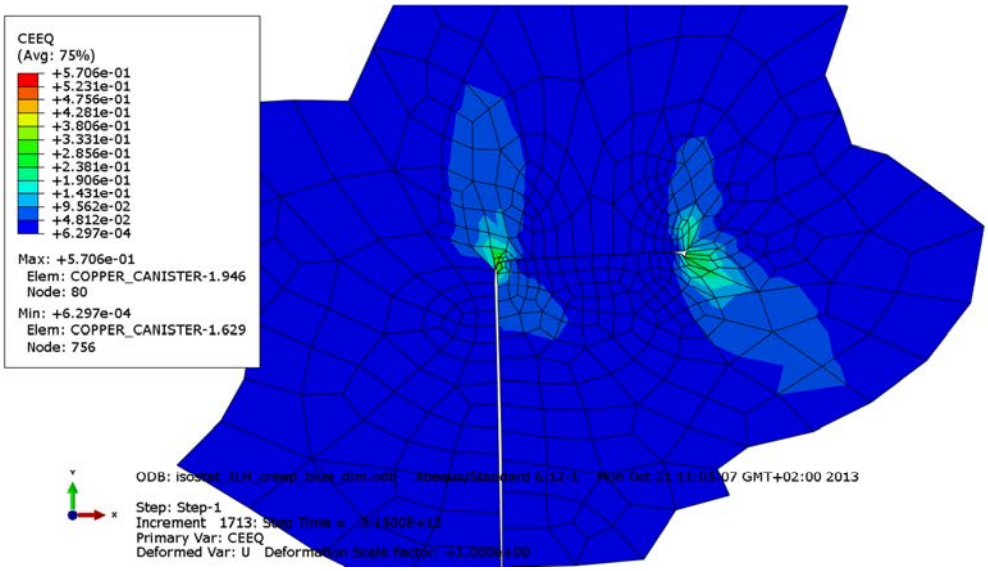

Figure A3-10. *Plot showing the equivalent creep strain at the copper shell top weld after 100,000 years.*

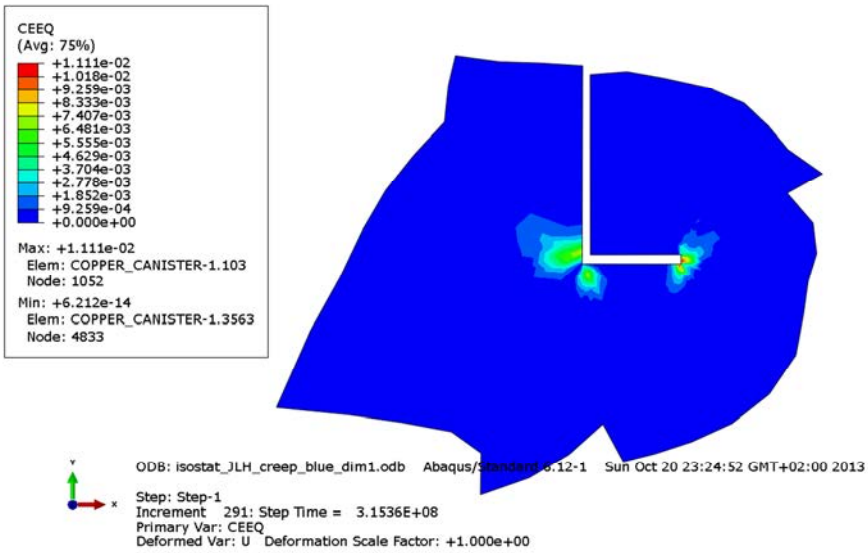

Figure A3-11. *Plot showing the equivalent creep strain at the copper shell bottom weld after 10 years. Gas pressure is applied.*

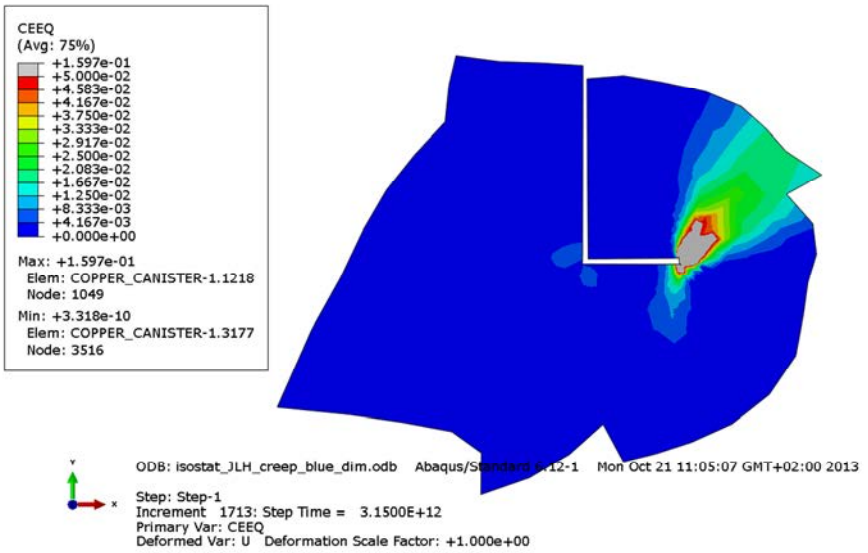

Figure A3-12. *Plot showing the equivalent creep strain at the copper shell bottom weld after 100,000 years.*

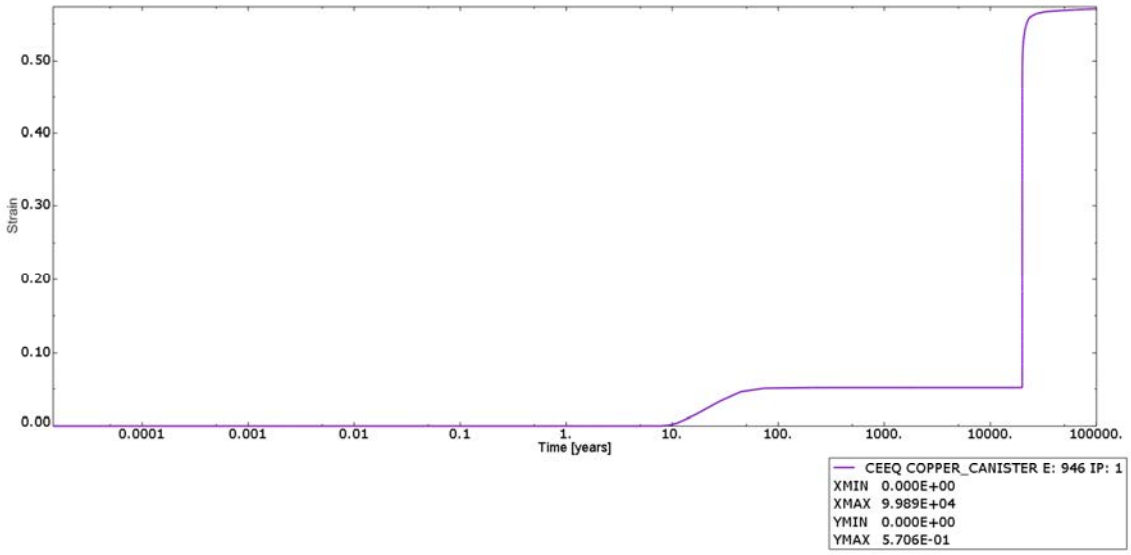

Figure A3-13. *Plot showing the history of equivalent creep strain in the element having the maximum magnitude. Time is in years and strain is dimensionless.*

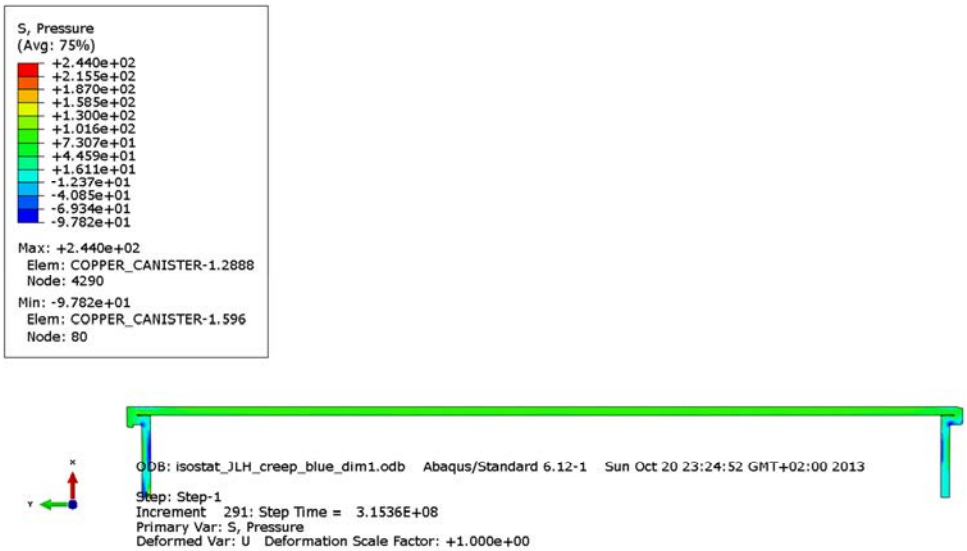

Figure A3-14. *Plot showing the pressure stress in the copper shell after 10 years. Gas pressure is applied.*

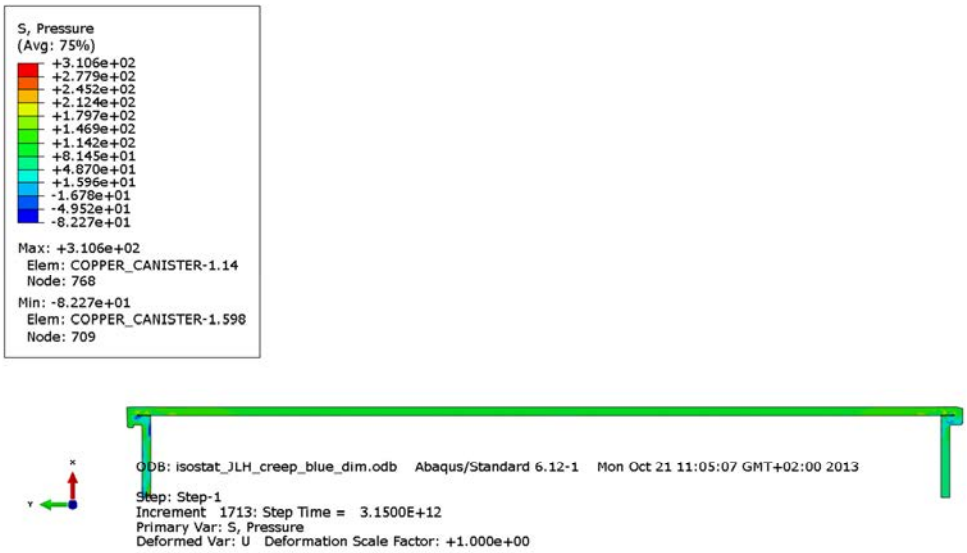

Figure A3-15. *Plot showing the pressure stress in the copper shell after 100,000 years.*

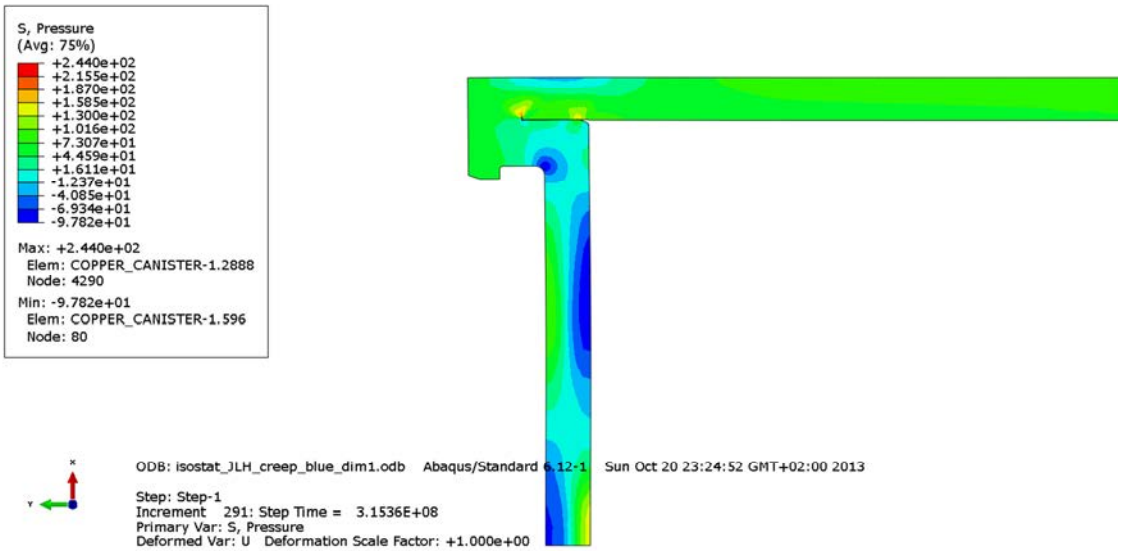

Figure A3-16. *Plot showing the pressure stress at the copper shell top weld after 10 years. Gas pressure is applied.*

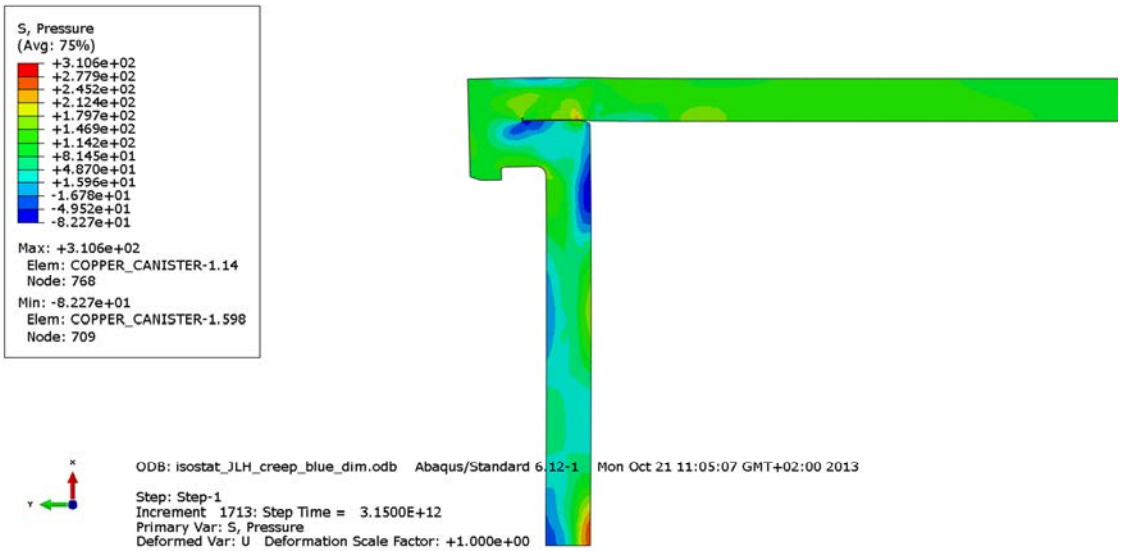

Figure A3-17. *Plot showing the pressure stress at the copper shell top weld after 100,000 years.*

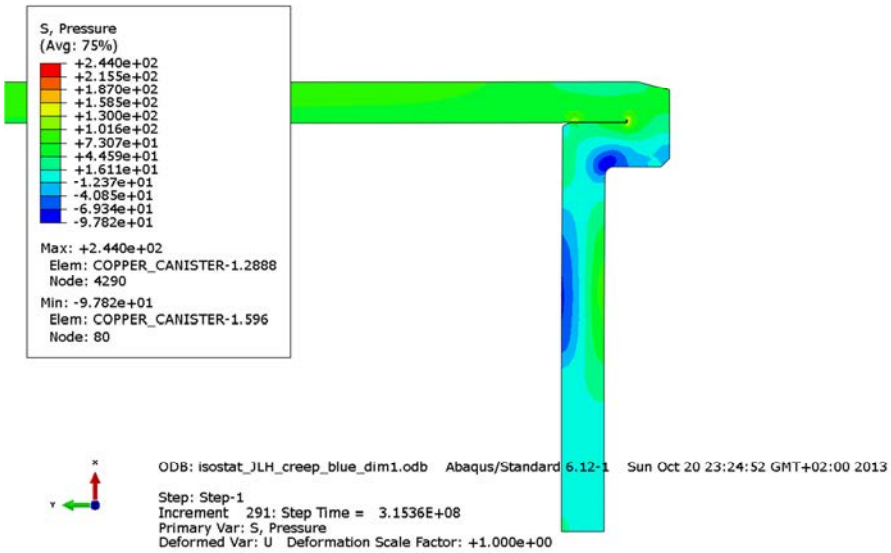

Figure A3-18. *Plot showing the pressure stress at the copper shell bottom weld after 10 years. Gas pressure is applied.*

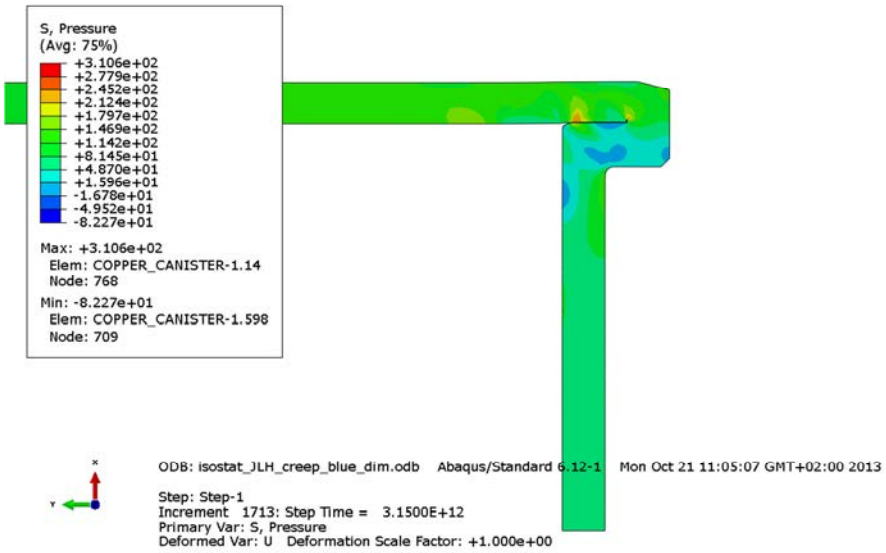

Figure A3-19. *Plot showing the pressure stress at the copper shell bottom weld after 100,000 years.*

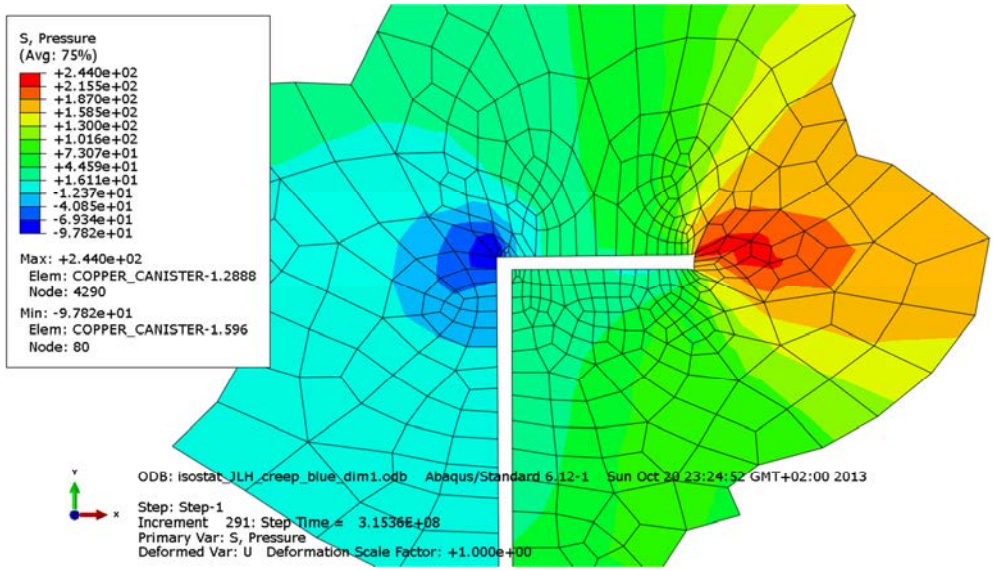

Figure A3-20. Plot showing the pressure stress at the copper shell top weld after 10 years. Gas pressure is applied.

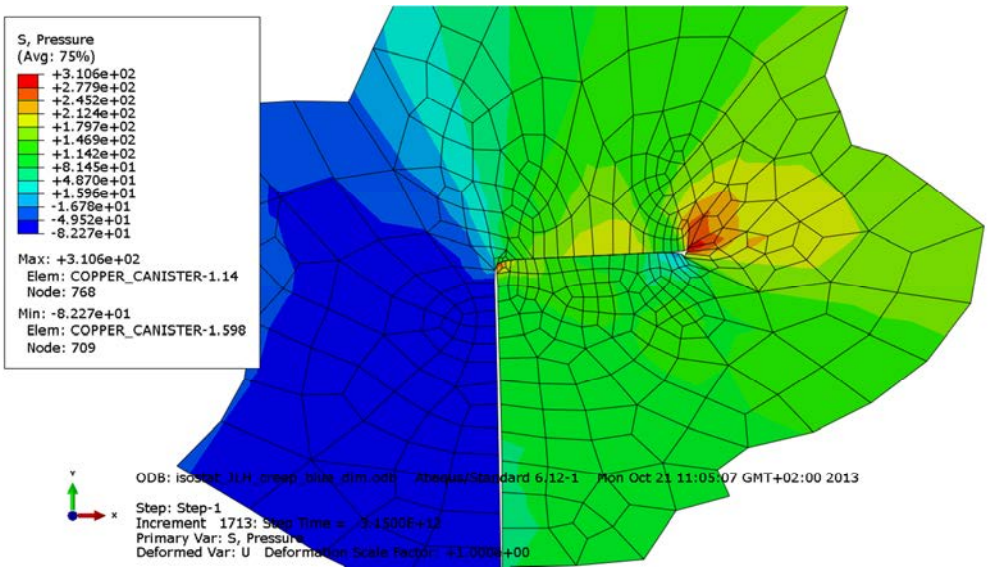

Figure A3-21. *Plot showing the pressure stress at the copper shell top weld after 10,000 years.*

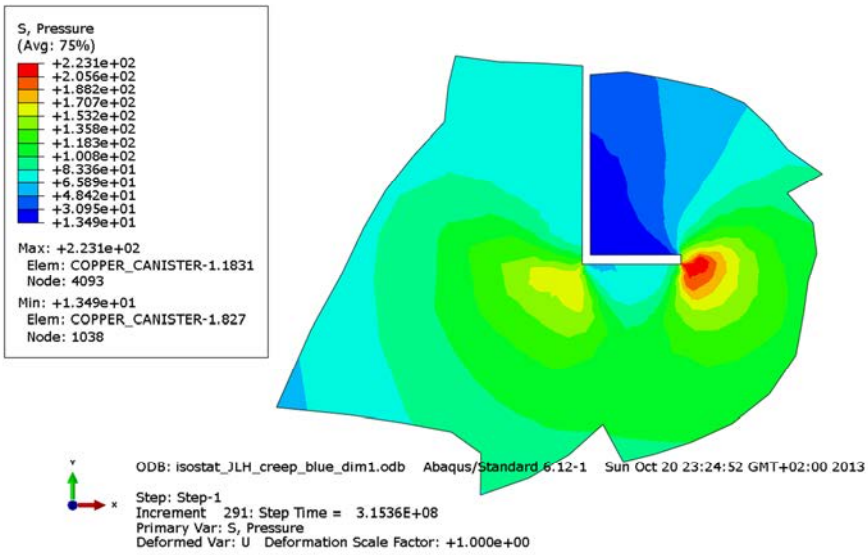

Figure A3-22. *Plot showing the pressure stress at the copper shell bottom weld after 10 years. Gas pressure is applied.*

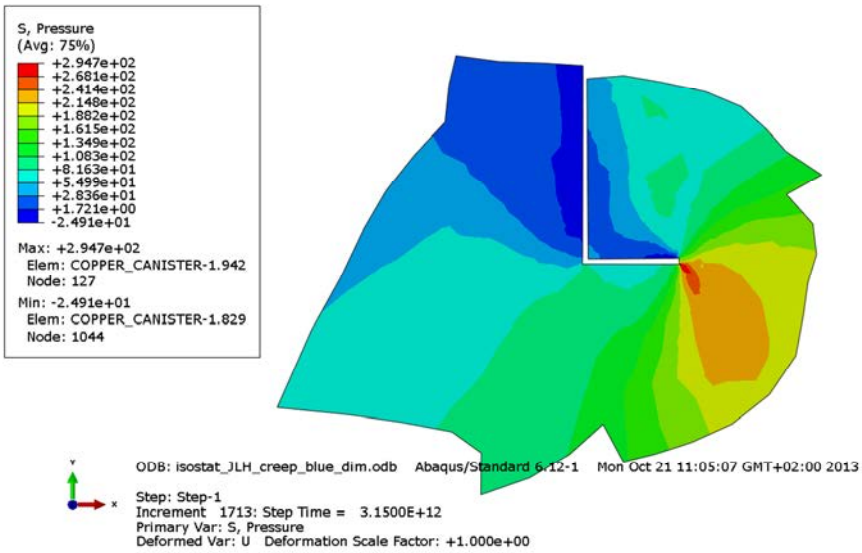

Figure A3-23. *Plot showing the pressure stress at the copper shell bottom weld after 100,000 years.*

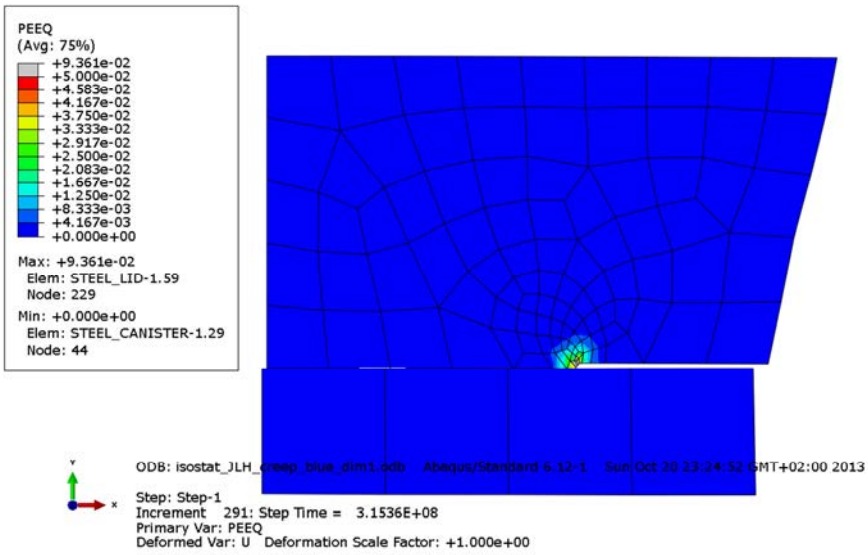

Figure A3-24. *Plot showing the equivalent plastic strain at the steel lid after 10 years; see also Fig 4.3 for understanding of the detail. Gas pressure is applied.*

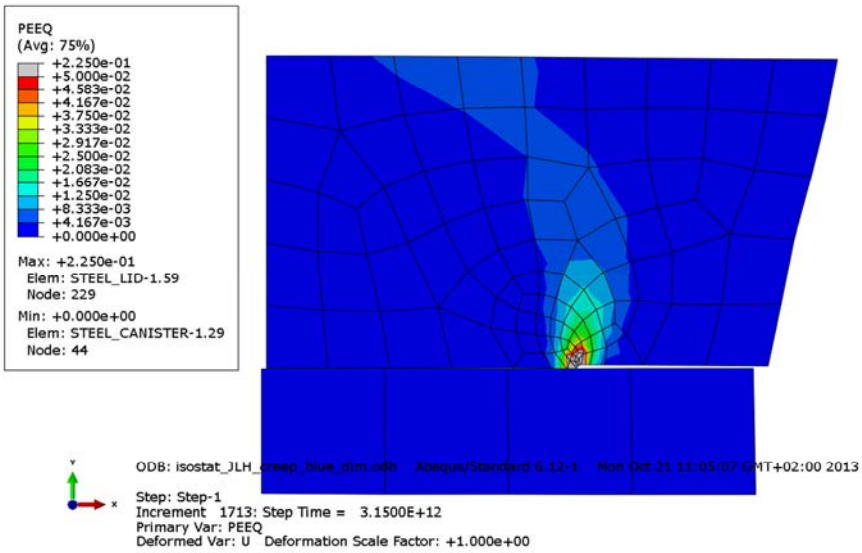

Figure A3-25. *Plot showing the equivalent plastic strain at the steel lid after 100,000 years; see also Fig 4.3 for understanding of the detail.*

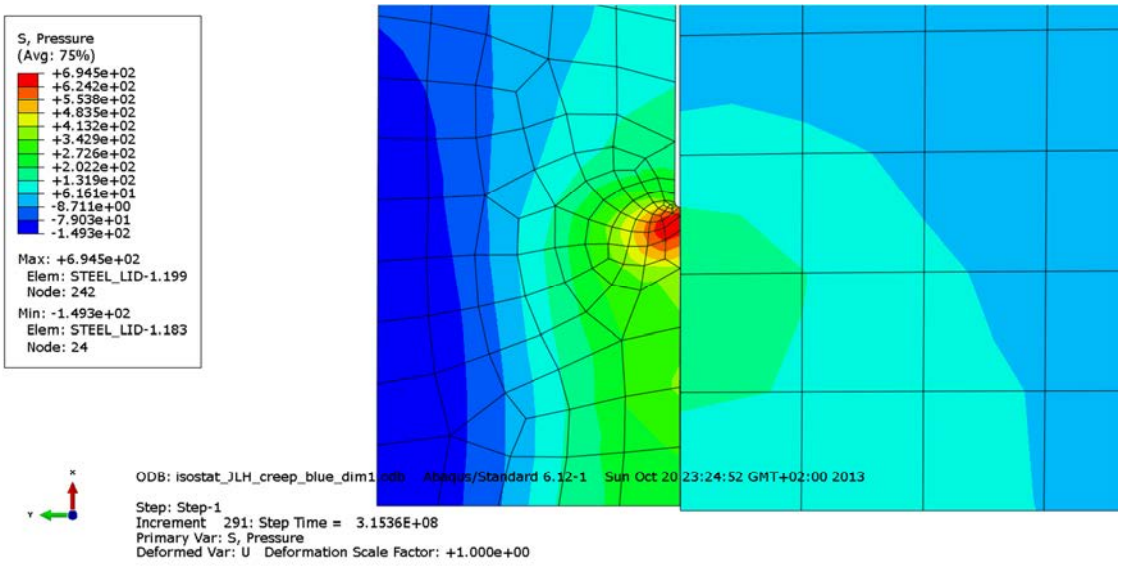

Figure A3-26. *Plot showing the pressure stress at discontinuity of insert after 10 years. Gas pressure is applied.*

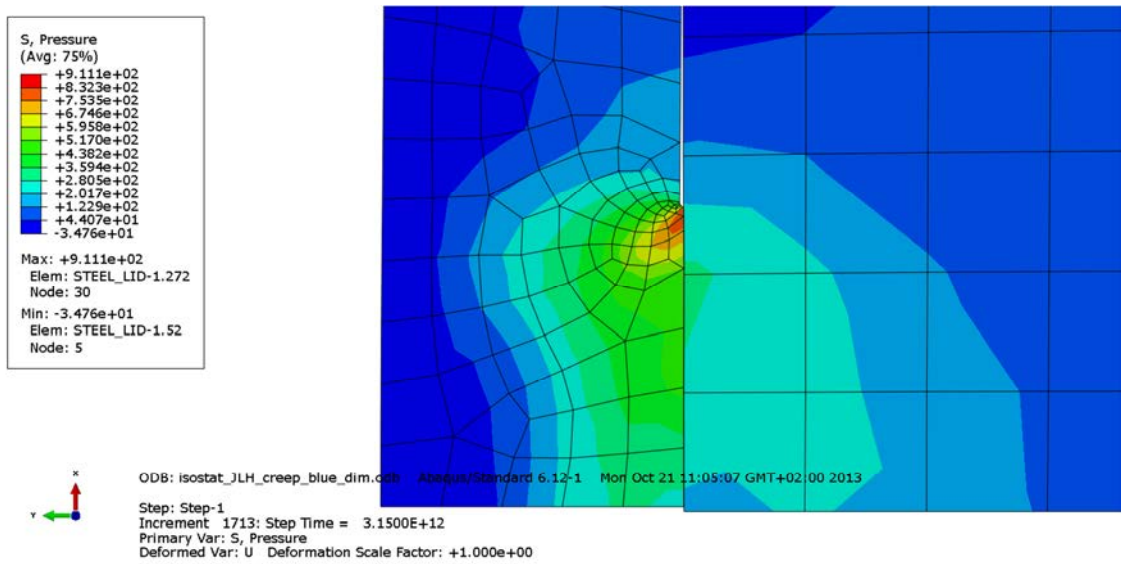

Figure A3-27. *Plot showing the pressure stress at discontinuity of insert after 100,000 years.*

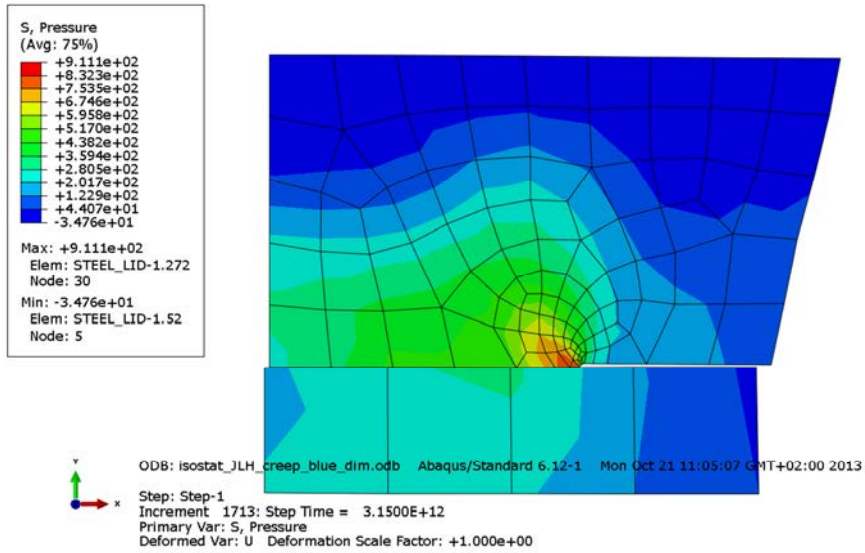

Figure A3-28. *Plot showing the pressure stress at the steel lid after 100,000 years; see also Fig 4.3 for understanding of the detail.*

Appendix 4 – Isostat_JLH_creep_blue_mean

Plots showing temperature and pressure contours and history.

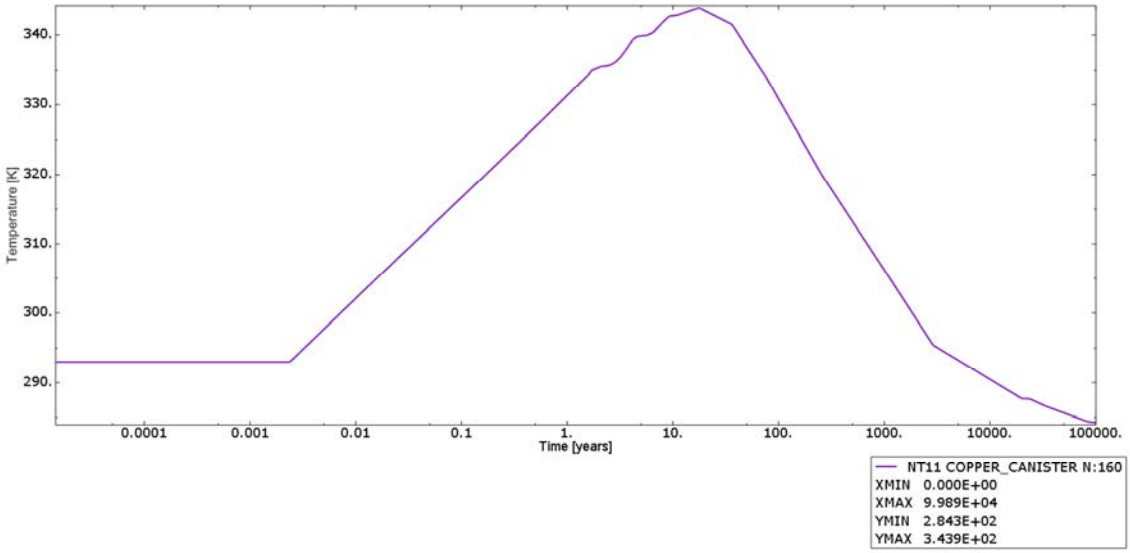

Figure A4-1. *Plot showing the temperature history. Time is in years, temperature is in Kelvin.*

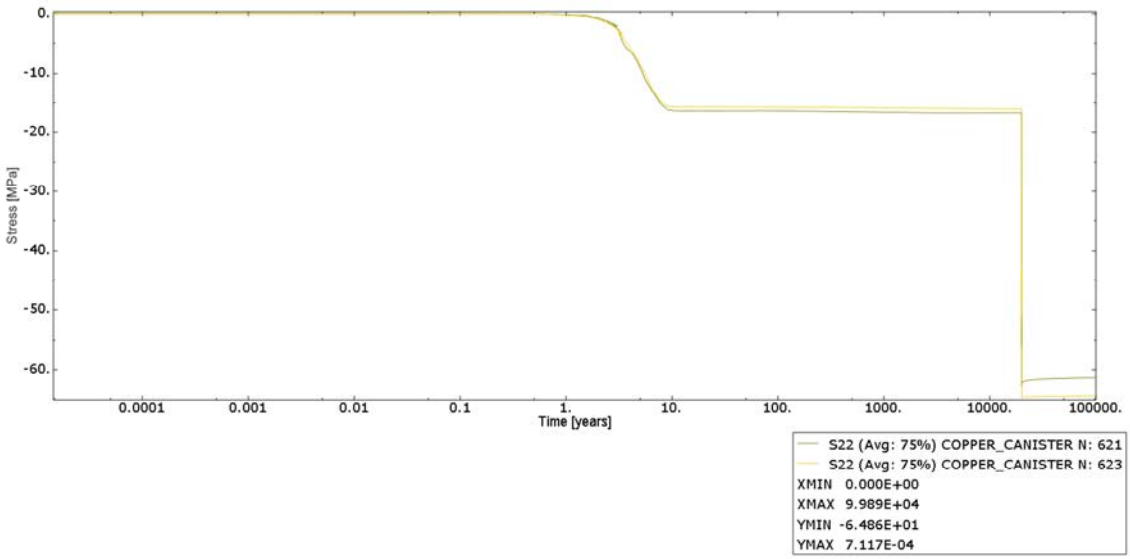

Figure A4-2. *Plot showing the applied pressure at the top lid of the copper shell. Time is in years and stress is in MPa.*

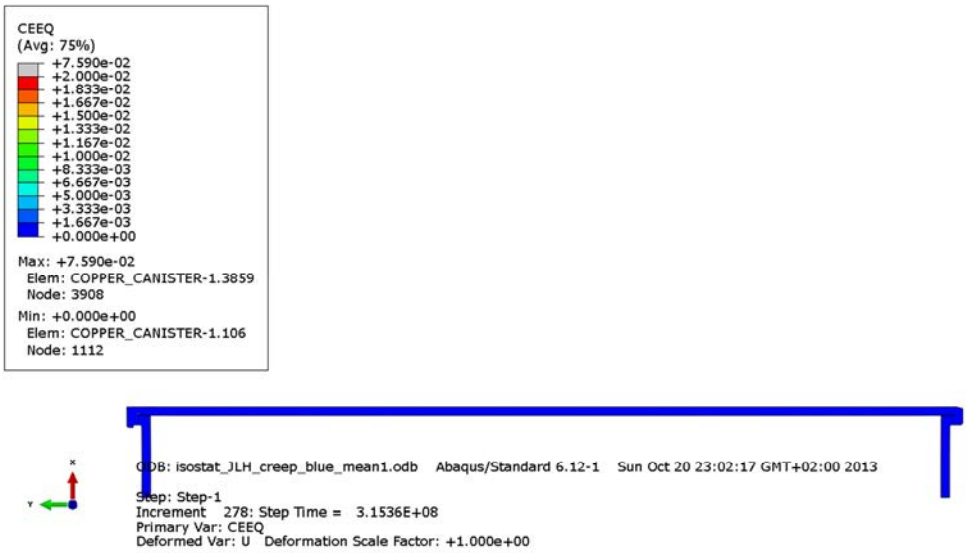

Figure A4-3. *Plot showing the equivalent creep strain after 10 years.Gas pressure is applied.*

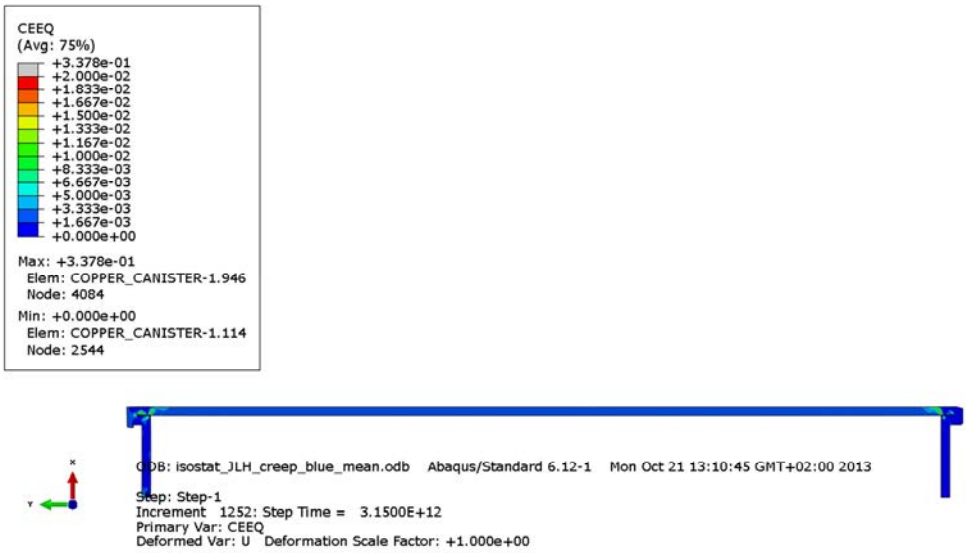

Figure A4-4. *Plot showing the equivalent creep strain after 100,000 years.*

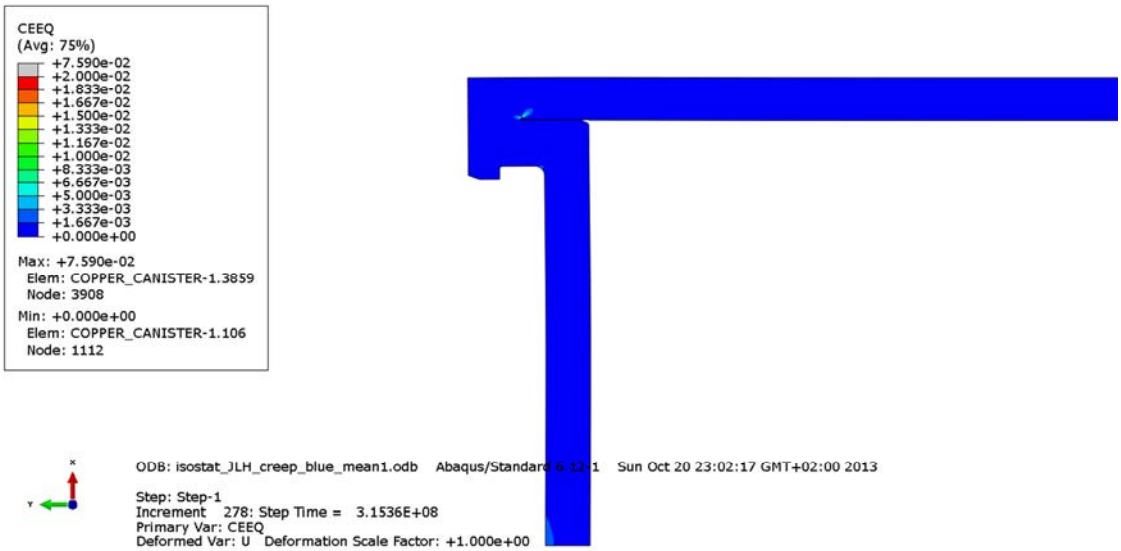

Figure A4-5. *Plot showing the equivalent creep strain at the top weld of the copper shell after 10 years. Gas pressure is applied.*

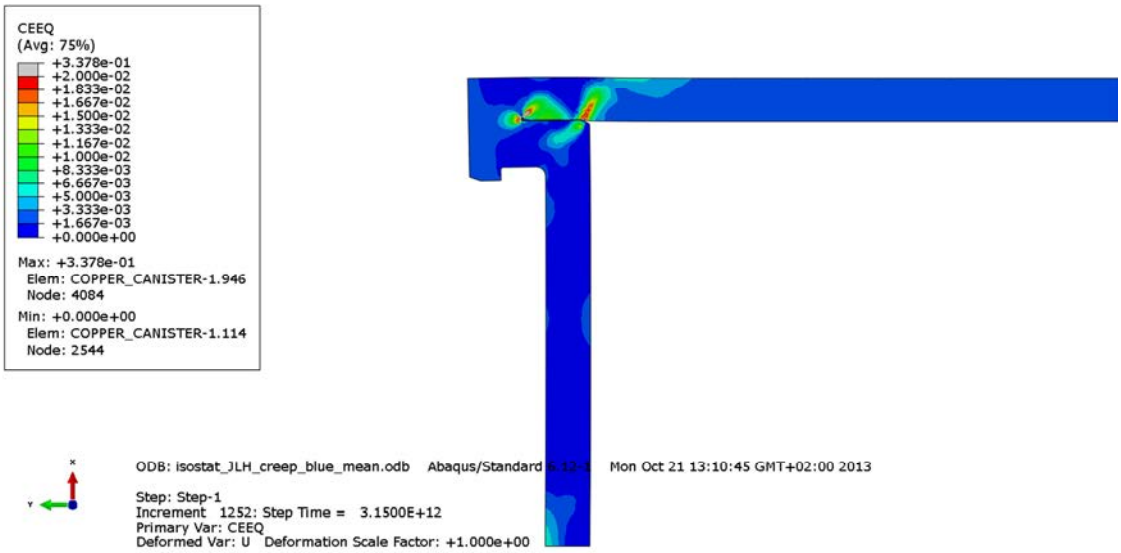

Figure A4-6. *Plot showing the equivalent creep strain at the top weld of the copper shell after 100,000 years.*

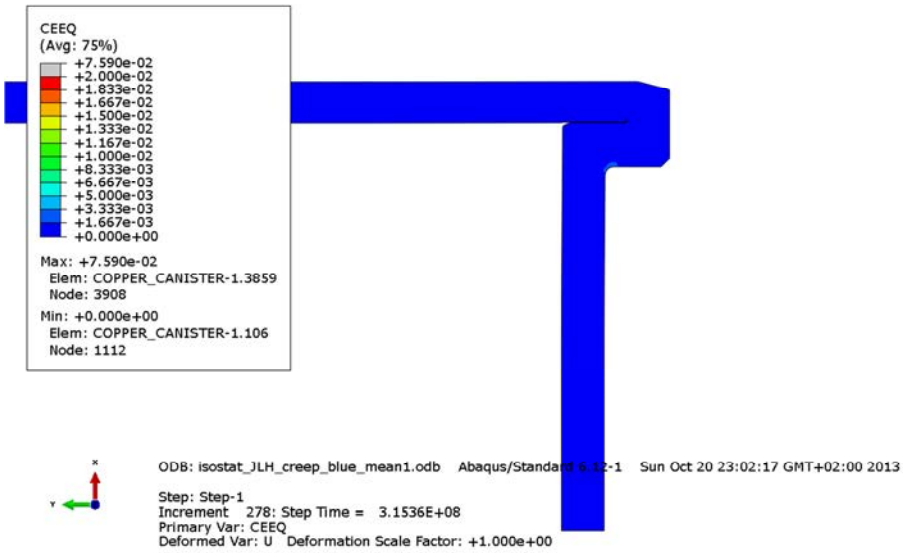

Figure A4-7. Plot showing the equivalent creep strain at the bottom weld of the copper shell after 10 years. Gas pressure is applied.

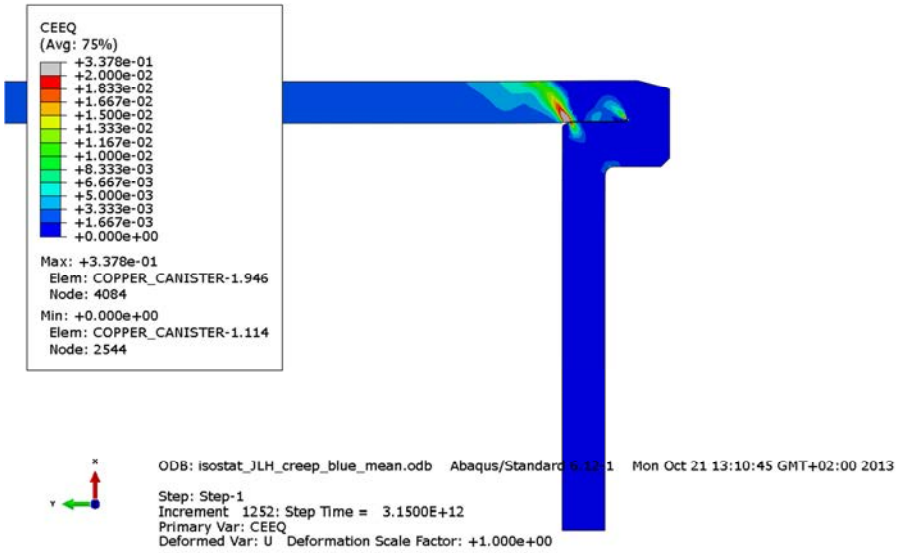

Figure A4-8. *Plot showing the equivalent creep strain at the bottom weld of the copper shell after 100,000 years.*

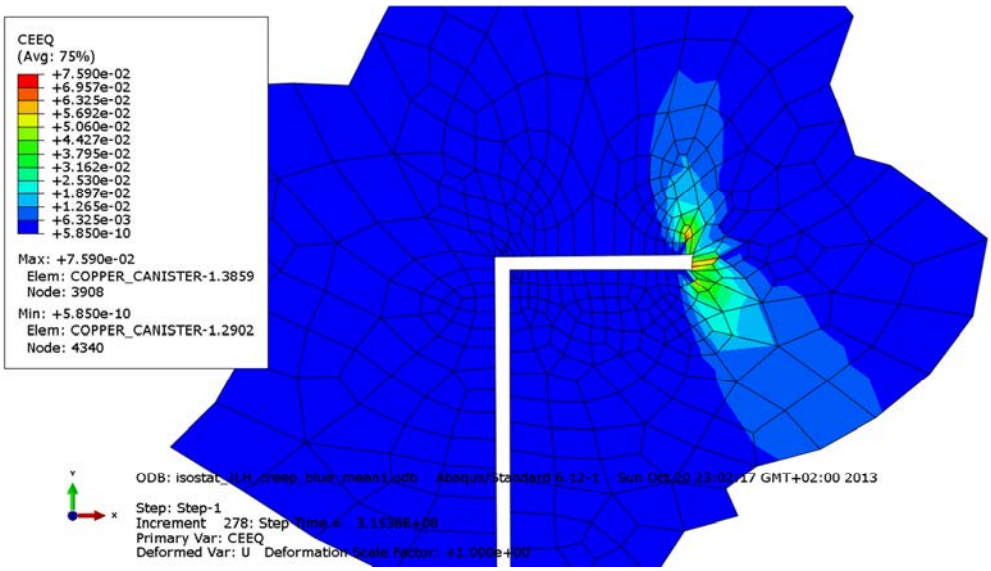

Figure A4-9. Plot showing the equivalent creep strain at the copper shell top weld after 10 years. Gas pressure is applied.

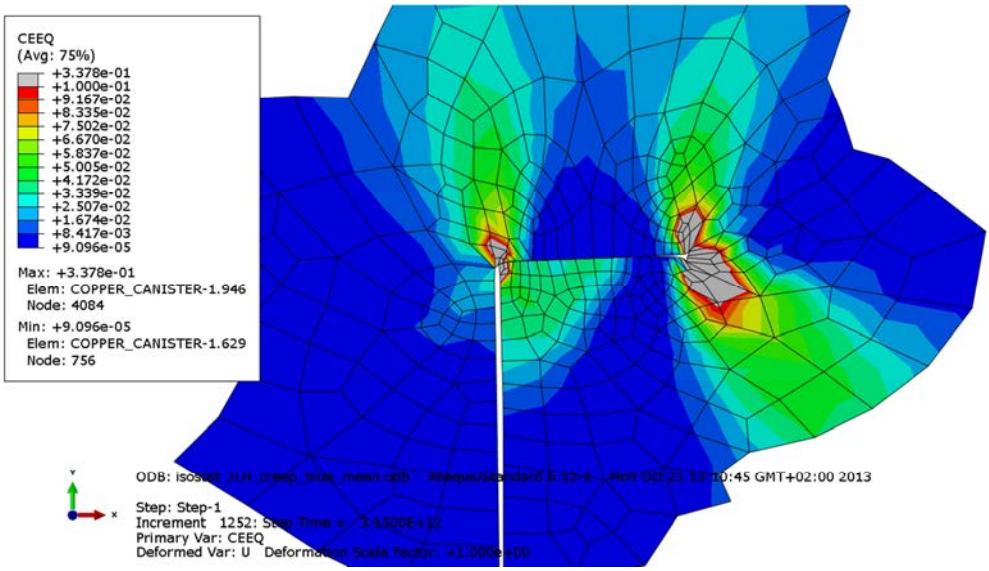

Figure A4-10. *Plot showing the equivalent creep strain at the copper shell top weld after 100,000 years.*

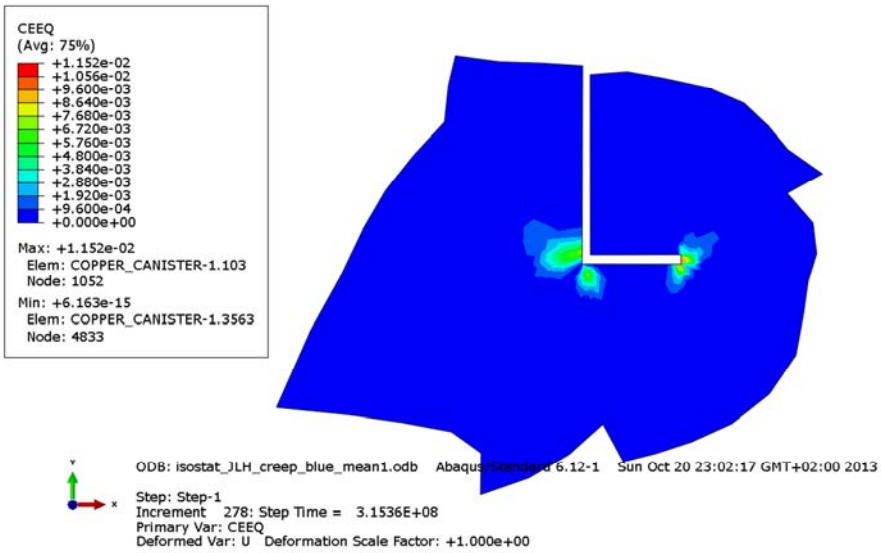

Figure A4-11. *Plot showing the equivalent creep strain at the copper shell bottom weld after 10 years. Gas pressure is applied.*

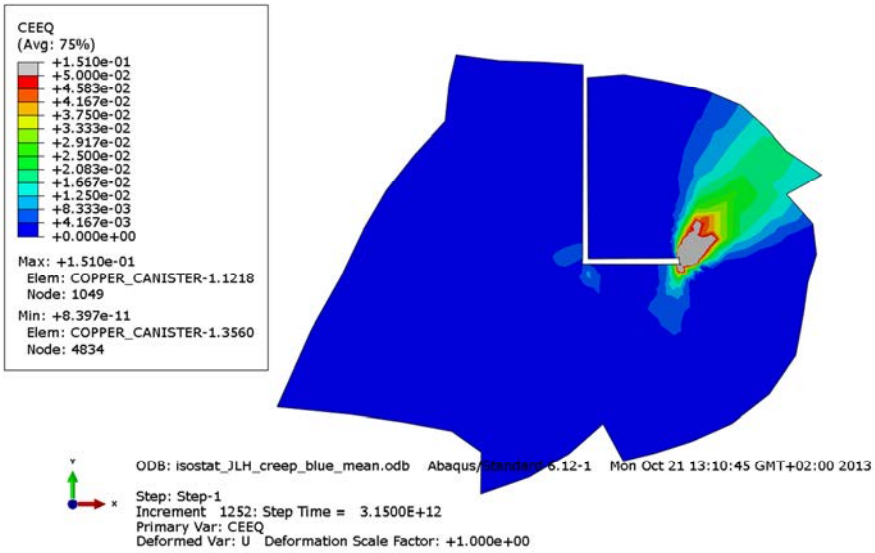

Figure A4-12. *Plot showing the equivalent creep strain at the copper shell bottom weld after 100,000 years.*

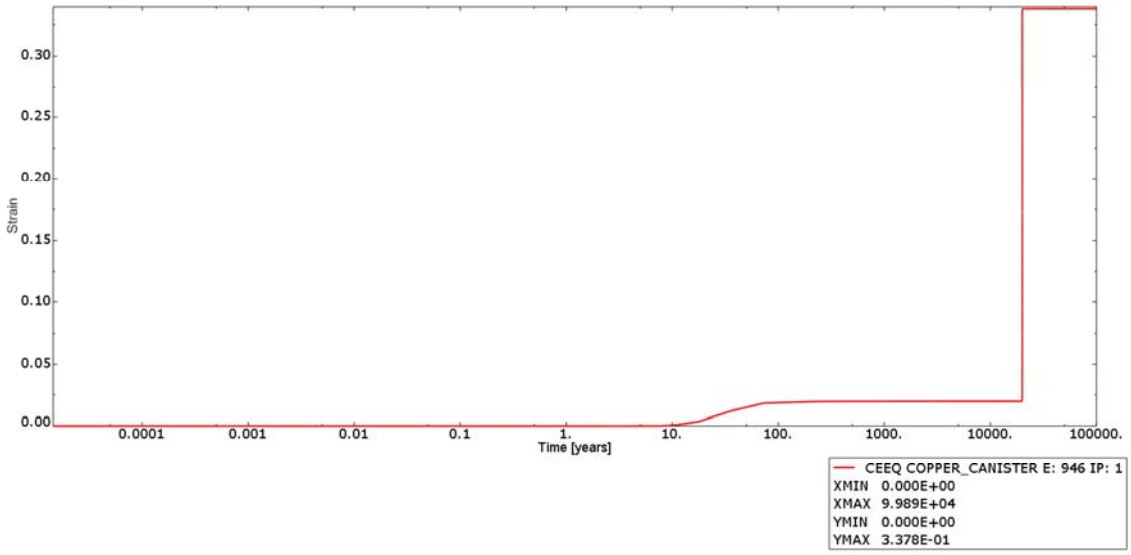

Figure A4-13. *Plot showing the history of equivalent creep strain in the element having the maximum magnitude. Time is in years and strain is dimensionless.*

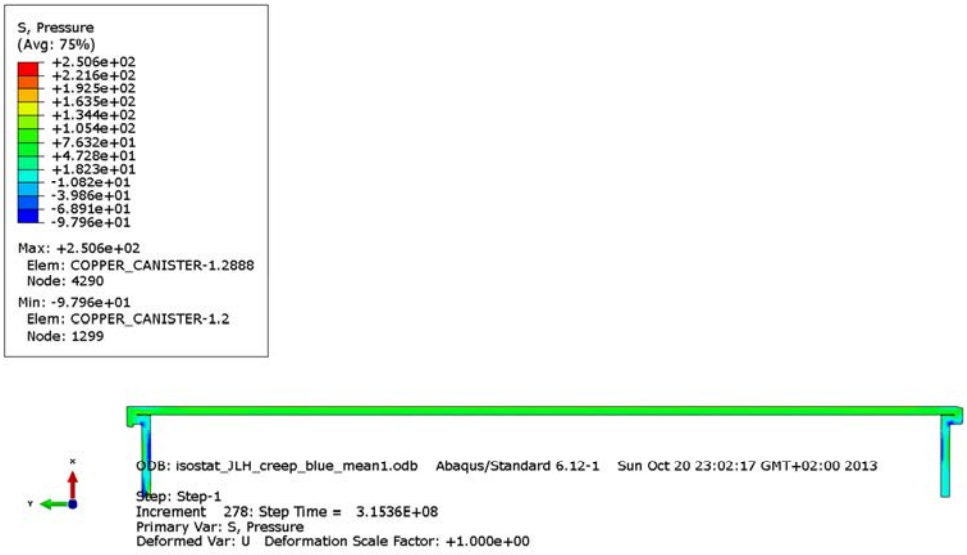

Figure A4-14. *Plot showing the pressure stress in the copper shell after 10 years. Gas pressure is applied.*

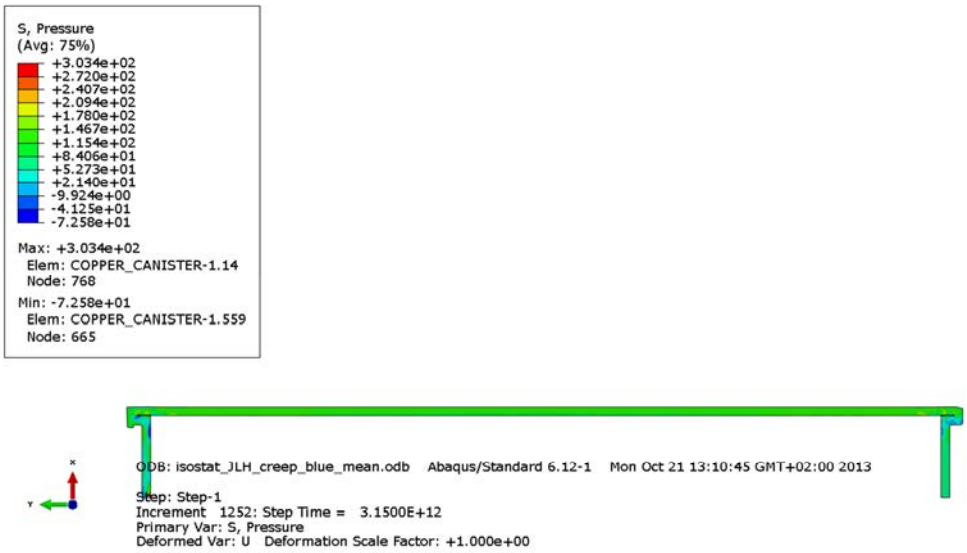

Figure A4-15. *Plot showing the pressure stress in the copper shell after 100,000 years.*

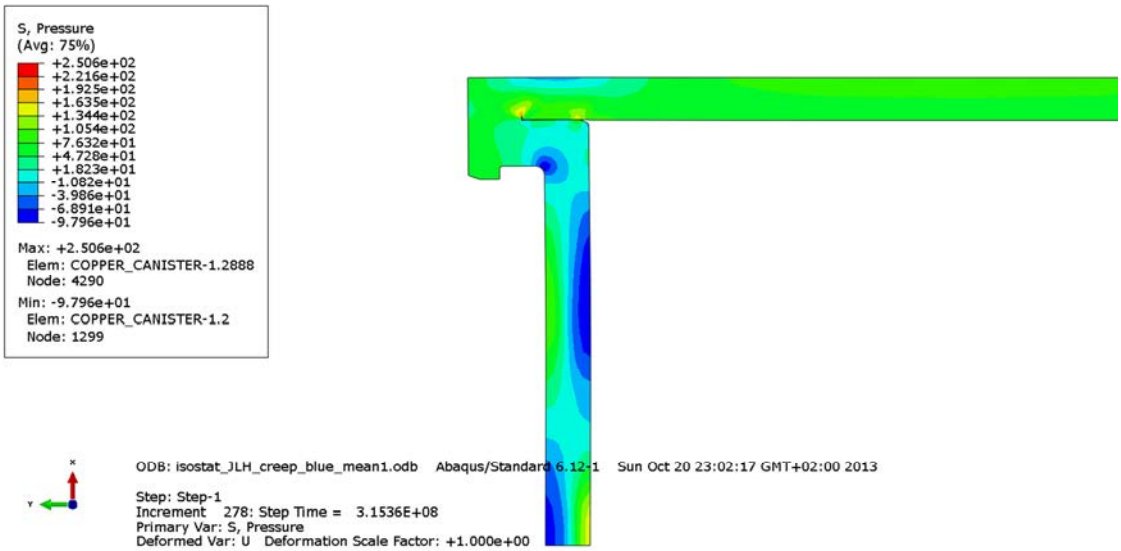

Figure A4-16. *Plot showing the pressure stress at the copper shell top weld after 10 years. Gas pressure is applied.*

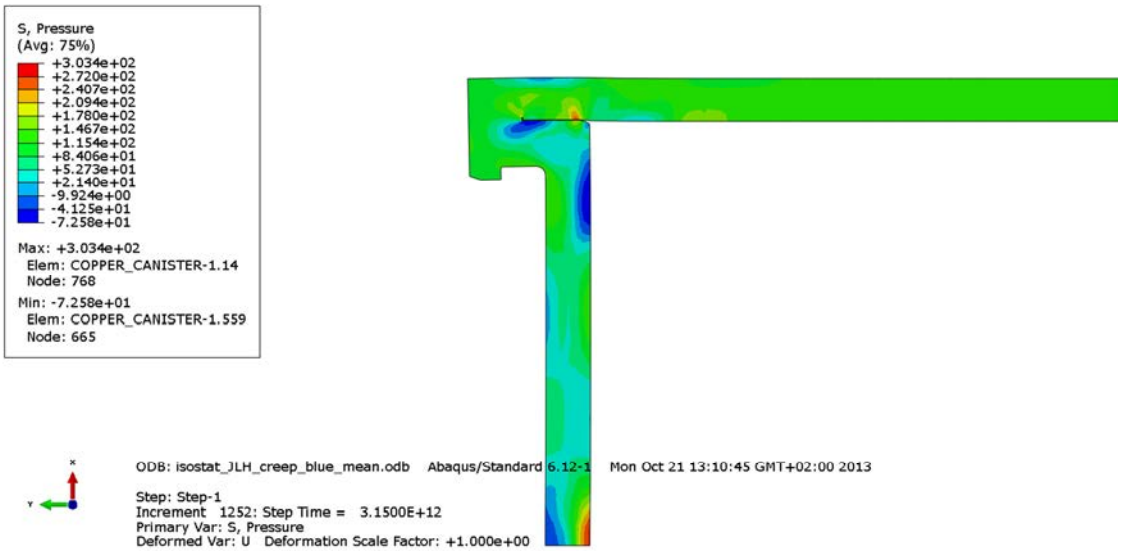

Figure A4-17. *Plot showing the pressure stress at the copper shell top weld after 100,000 years.*

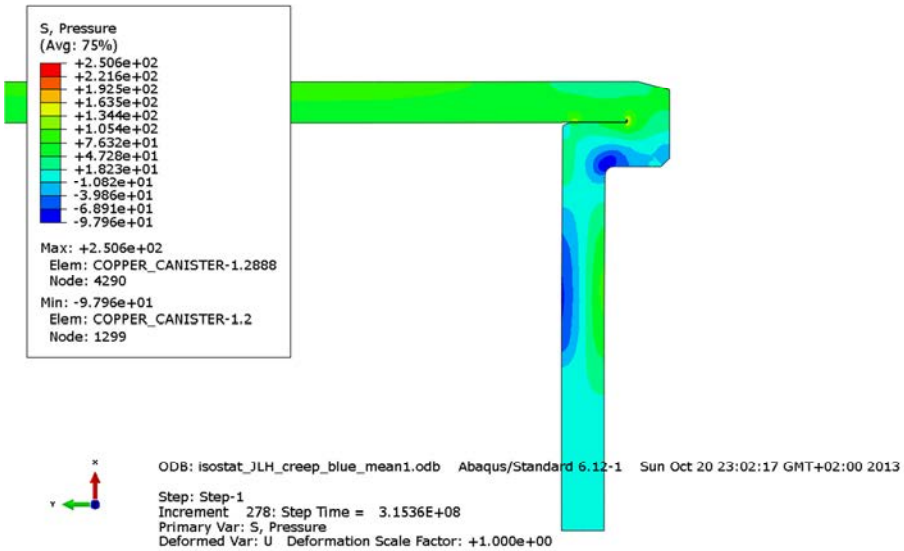

Figure A4-18. *Plot showing the pressure stress at the copper shell bottom weld after 10 years. Gas pressure is applied.*

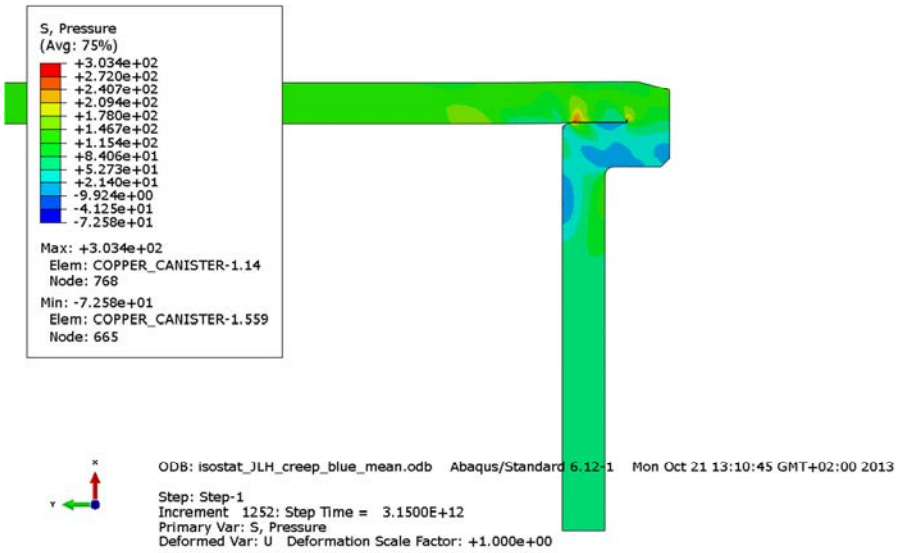

Figure A4-19. *Plot showing the pressure stress at the copper shell bottom weld after 100,000 years.*

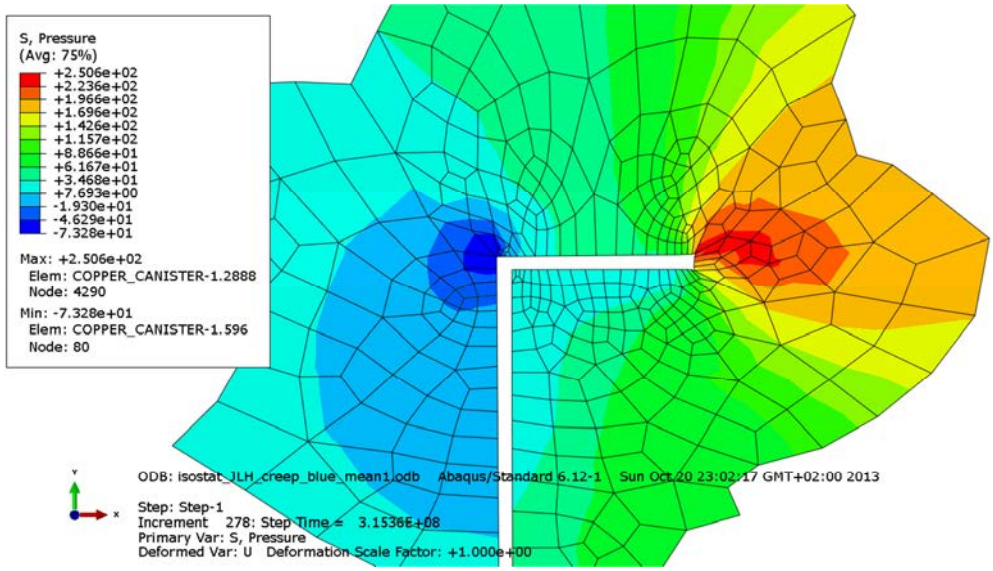

Figure A4-20. *Plot showing the pressure stress at the copper shell top weld after 10 years. Gas pressure is applied.*

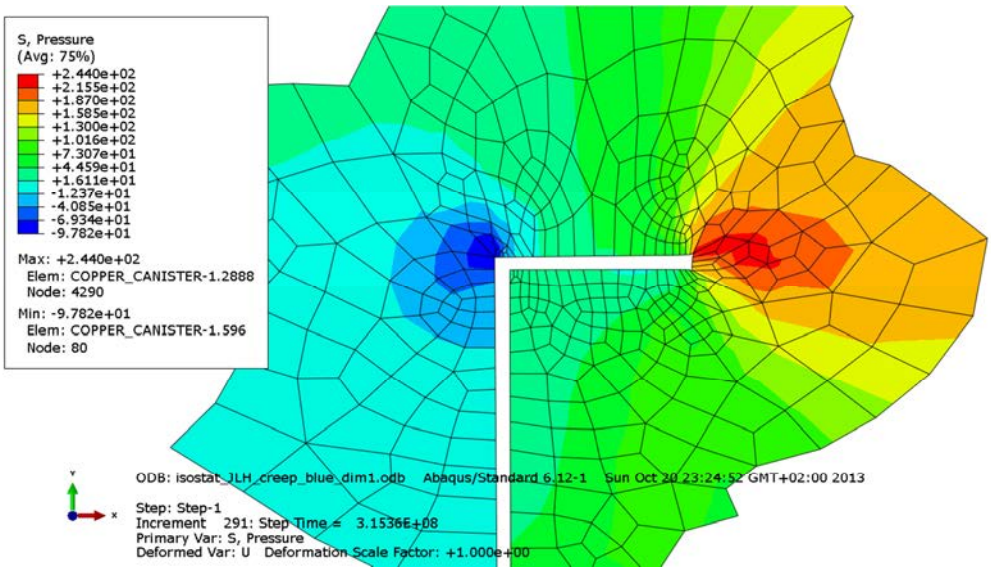

Figure A4-21. *Plot showing the pressure stress at the copper shell top weld after 10,000 years.*

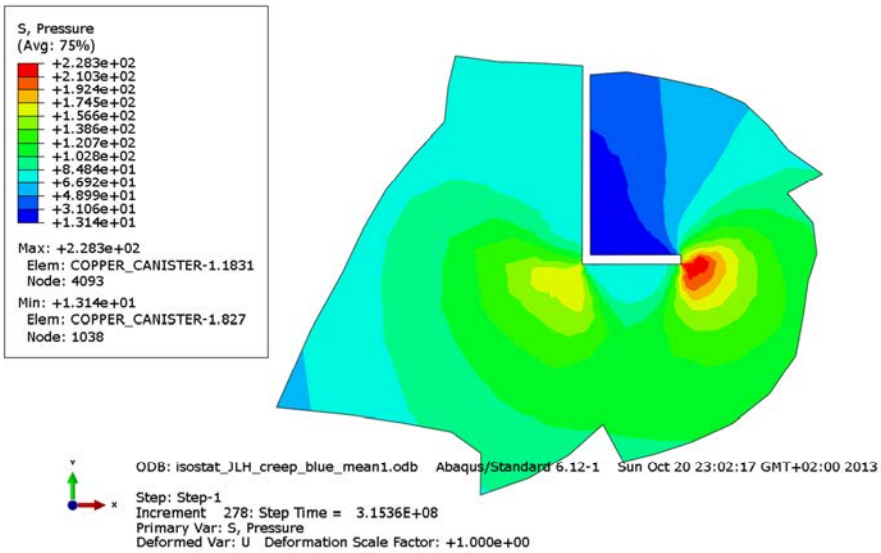

Figure A4-22. *Plot showing the pressure stress at the copper shell bottom weld after 10 years. Gas pressure is applied.*

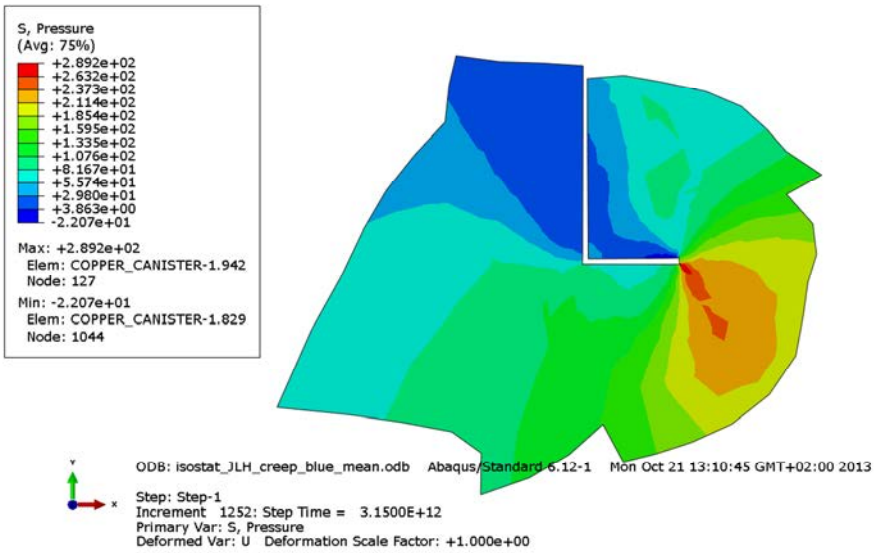

Figure A4-23. *Plot showing pressure stress at the copper shell bottom weld after 100,000 years.*

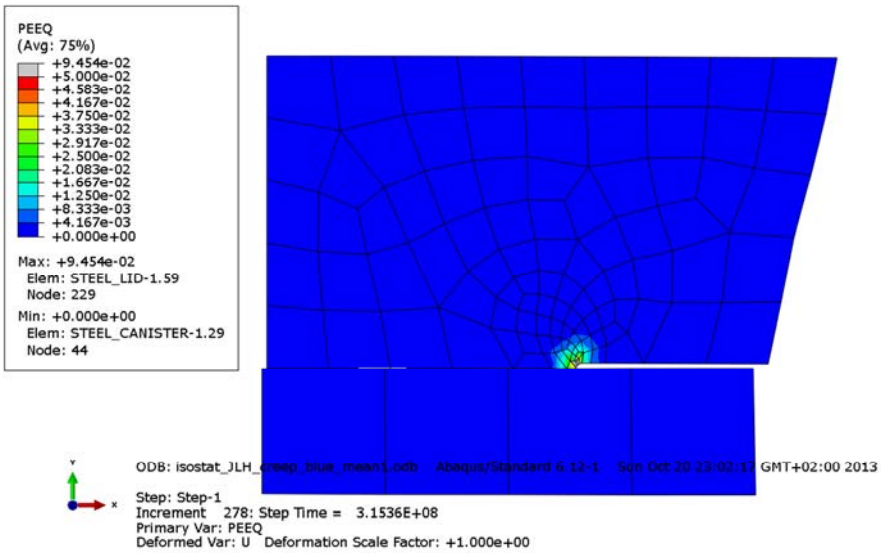

Figure A4-24. *Plot showing the equivalent plastic strain at the steel lid after 10 years; see also Fig 4.3 for understanding of the detail. Gas pressure is applied.*

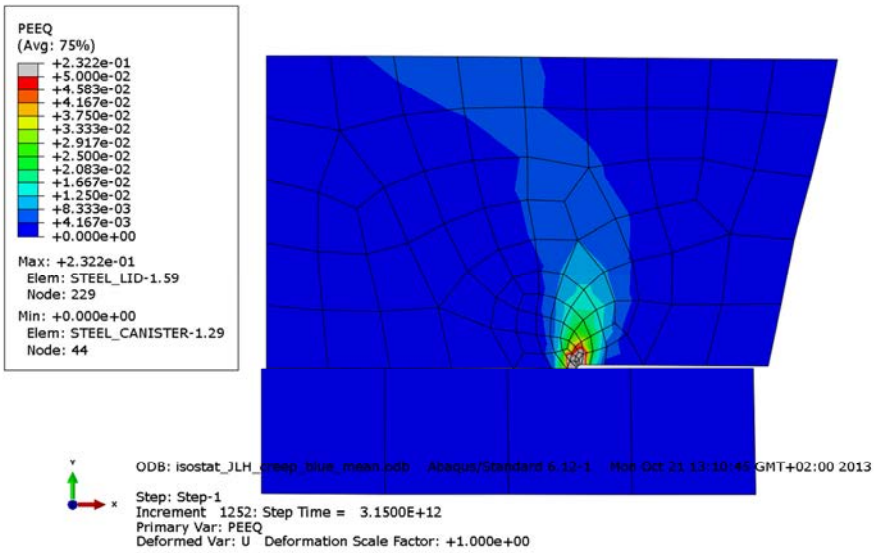

Figure A4-25. *Plot showing the equivalent plastic strain at the steel lid after 100,000 years; see also Fig 4.3 for understanding of the detail.*

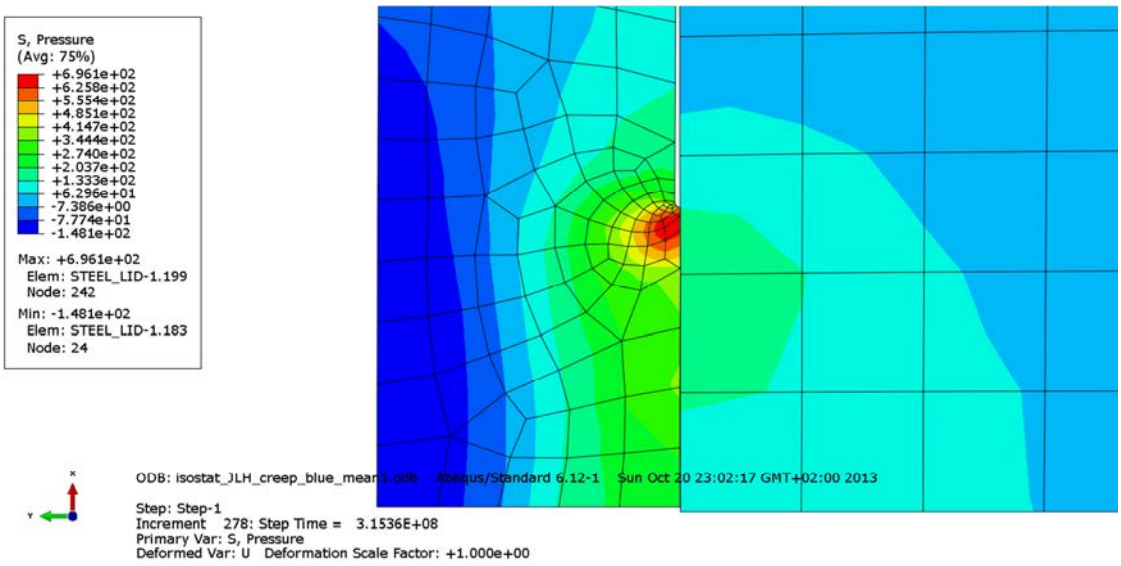

Figure A4-26. *Plot showing the pressure stress at discontinuity of insert after 10 years. Gas pressure is applied.*

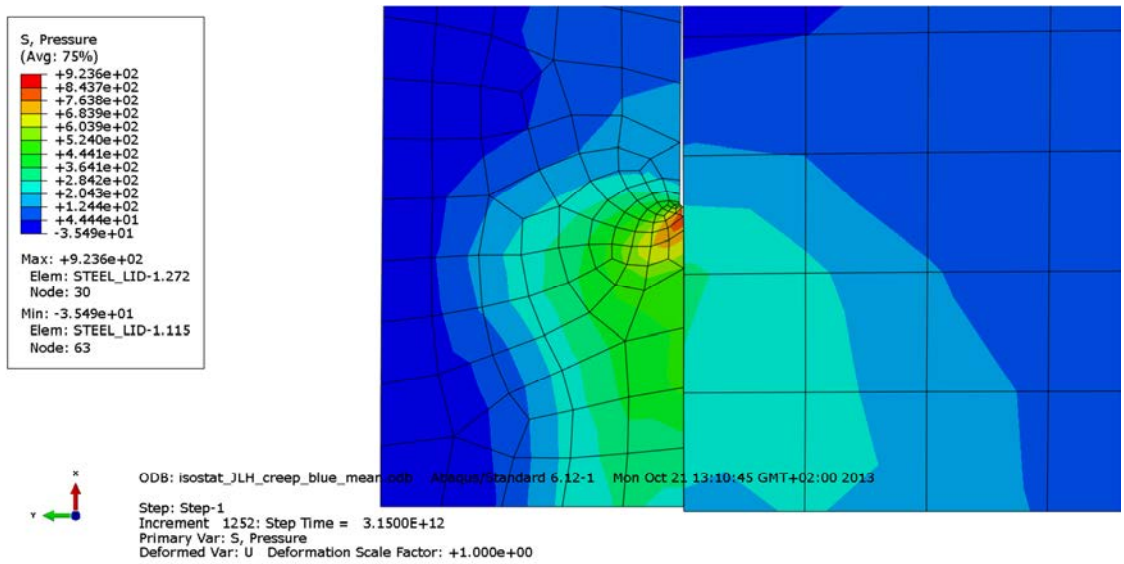

Figure A4-27. *Plot showing the pressure stress at discontinuity of insert after 100,000 years.*

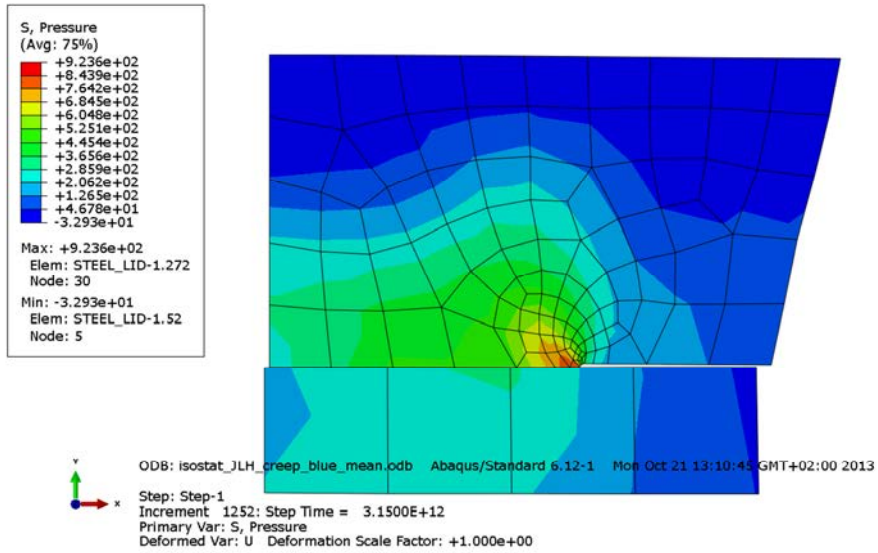

Figure A4-28. *Plot showing the pressure stress at the steel lid after 100,000 years; see also Fig 4.3 for understanding of the detail.*

Appendix 5 – Storage of files

This report is based on the results from a lot of FE-simulations using ABAQUS which is a commercial available code and is thus not stored as part of the work. Below is a short description of files used in the project and directories for storage of these. These files are also stored at SKB.

The files are stored in directories as:

geometry
Inputfiles
plots
Isostat.docx - this report
scripts
subroutines

1 – Plot-files used in the report

Contents in C:\Users\jhd\mappar\skb\Isostat\plots

compare_creep_components_history.png
compare_creep_history.png
half_3d_JLH-bc.png
half_3d_JLH-mesh1.png
half_3d_JLH-mesh_copper.png
half_3d_JLH-mesh_copper_creep_red_dim-ceeq.png
half_3d_JLH-mesh_insert.png
half_3d_JLH-mesh_steel_lid.png
Restart_half_3d_JLH_creep_red_dim7-ceeq_10kyears.png
Restart_half_3d_JLH_creep_red_dim7-ceeq_history.png
Restart_half_3d_JLH_creep_red_dim7-ceeq_max.png
Restart_half_3d_JLH_creep_red_dim7-mises_10kyears.png
Restart_half_3d_JLH_creep_red_dim7-mises_channels_10kyears.png

Plot files used in the report

Appendix 1

isostat_JLH_creep_red_dim-ceeq.png
isostat_JLH_creep_red_dim-ceeq_10kyears.png
isostat_JLH_creep_red_dim-ceeq_contour.png
isostat_JLH_creep_red_dim-ceeq_contour2.png
isostat_JLH_creep_red_dim-ceeq_contour3.png
isostat_JLH_creep_red_dim-ceeq_contour4.png
isostat_JLH_creep_red_dim-ceeq_contour4b.png
isostat_JLH_creep_red_dim-ceeq_contour5.png
isostat_JLH_creep_red_dim-ceeq_contour5b.png
isostat_JLH_creep_red_dim-gap_corner.png
isostat_JLH_creep_red_dim-mesh_1.png
isostat_JLH_creep_red_dim-mesh_2.png
isostat_JLH_creep_red_dim-mesh_3.png
isostat_JLH_creep_red_dim-mesh_4.png
isostat_JLH_creep_red_dim-mesh_5.png
isostat_JLH_creep_red_dim-peeq_2.png
isostat_JLH_creep_red_dim-peeq_contour.png
isostat_JLH_creep_red_dim-peeq_contour2.png
isostat_JLH_creep_red_dim-pressure.png
isostat_JLH_creep_red_dim-pressure_canister1.png
isostat_JLH_creep_red_dim-pressure_copper1.png
isostat_JLH_creep_red_dim-pressure_copper2.png
isostat_JLH_creep_red_dim-pressure_copper3.png
isostat_JLH_creep_red_dim-pressure_copper4.png
isostat_JLH_creep_red_dim-pressure_copper4b.png
isostat_JLH_creep_red_dim-pressure_copper5b.png
isostat_JLH_creep_red_dim-s22.png
isostat_JLH_creep_red_dim-temp.png
isostat_JLH_creep_red_dim-u2.png

Appendix 2

isostat_JLH_creep_red_mean-ceeq.png
isostat_JLH_creep_red_mean-ceeq_10kyears.png
isostat_JLH_creep_red_mean-ceeq_contour.png
isostat_JLH_creep_red_mean-ceeq_contour2.png
isostat_JLH_creep_red_mean-ceeq_contour3.png
isostat_JLH_creep_red_mean-ceeq_contour4.png
isostat_JLH_creep_red_mean-ceeq_contour4b.png
isostat_JLH_creep_red_mean-ceeq_contour5.png
isostat_JLH_creep_red_mean-ceeq_contour5b.png
isostat_JLH_creep_red_mean-peeq_1.png
isostat_JLH_creep_red_mean-peeq_2.png
isostat_JLH_creep_red_mean-peeq_contour.png
isostat_JLH_creep_red_mean-peeq_contour2.png
isostat_JLH_creep_red_mean-pressure_canister1.png
isostat_JLH_creep_red_mean-pressure_copper1.png
isostat_JLH_creep_red_mean-pressure_copper2.png
isostat_JLH_creep_red_mean-pressure_copper3.png
isostat_JLH_creep_red_mean-pressure_copper4.png
isostat_JLH_creep_red_mean-pressure_copper4b.png
isostat_JLH_creep_red_mean-pressure_copper5b.png
isostat_JLH_creep_red_mean-s22.png
isostat_JLH_creep_red_mean-temp.png
isostat_JLH_creep_red_mean-u2.png

Plot files used in the report

Appendix 3

isostat_JLH_creep_blue_dim-ceeq.png
isostat_JLH_creep_blue_dim-ceeq_10kyears.png
isostat_JLH_creep_blue_dim-ceeq_contour.png
isostat_JLH_creep_blue_dim-ceeq_contour2.png
isostat_JLH_creep_blue_dim-ceeq_contour3.png
isostat_JLH_creep_blue_dim-ceeq_contour4.png
isostat_JLH_creep_blue_dim-ceeq_contour4b.png
isostat_JLH_creep_blue_dim-ceeq_contour5.png
isostat_JLH_creep_blue_dim-ceeq_contour5b.png
isostat_JLH_creep_blue_dim-peeq_1.png
isostat_JLH_creep_blue_dim-peeq_2.png
isostat_JLH_creep_blue_dim-peeq_contour.png
isostat_JLH_creep_blue_dim-peeq_contour2.png
isostat_JLH_creep_blue_dim-pressure_canister1.png
isostat_JLH_creep_blue_dim-pressure_copper1.png
isostat_JLH_creep_blue_dim-pressure_copper2.png
isostat_JLH_creep_blue_dim-pressure_copper3.png
isostat_JLH_creep_blue_dim-pressure_copper4.png
isostat_JLH_creep_blue_dim-pressure_copper4b.png
isostat_JLH_creep_blue_dim-pressure_copper5b.png
isostat_JLH_creep_blue_dim-s22.png
isostat_JLH_creep_blue_dim-temp.png
isostat_JLH_creep_blue_dim-u2.png

Appendix 4

isostat_JLH_creep_blue_mean-ceeq.png
isostat_JLH_creep_blue_mean-ceeq_10kyears.png
isostat_JLH_creep_blue_mean-ceeq_contour.png
isostat_JLH_creep_blue_mean-ceeq_contour2.png
isostat_JLH_creep_blue_mean-ceeq_contour3.png
isostat_JLH_creep_blue_mean-ceeq_contour4.png
isostat_JLH_creep_blue_mean-ceeq_contour4b.png
isostat_JLH_creep_blue_mean-ceeq_contour5.png
isostat_JLH_creep_blue_mean-ceeq_contour5b.png
isostat_JLH_creep_blue_mean-peeq_1.png
isostat_JLH_creep_blue_mean-peeq_2.png
isostat_JLH_creep_blue_mean-peeq_contour.png
isostat_JLH_creep_blue_mean-peeq_contour2.png
isostat_JLH_creep_blue_mean-pressure_canister1.png
isostat_JLH_creep_blue_mean-pressure_copper1.png
isostat_JLH_creep_blue_mean-pressure_copper2.png
isostat_JLH_creep_blue_mean-pressure_copper3.png
isostat_JLH_creep_blue_mean-pressure_copper4.png
isostat_JLH_creep_blue_mean-pressure_copper4b.png
isostat_JLH_creep_blue_mean-pressure_copper5b.png
isostat_JLH_creep_blue_mean-s22.png
isostat_JLH_creep_blue_mean-temp.png
isostat_JLH_creep_blue_mean-u2.png

2 – Input files used for the simulations

Each analysis is started by abaqus job=input-file (w/o .inp) user=creep_rs_march2009.

Files with extension “incl” are referenced by some of the input-files (extension “inp”).

Contents in C:\Users\jhd\mappar\skb\Isostat\InputFiles

Isostat_JLH_creep_red_dim.inp	- temperature, dimensioning and dry buffer
Isostat_JLH_creep_red_mean.inp	- temperature, mean and dry buffer
Isostat_JLH_creep_blue_dim.inp	- temperature, dimensioning and wet buffer
Isostat_JLH_creep_blue_mean.inp	- temperature, mean and wet buffer
material_isostat.incl	- material definitions
half_3d_JLH_creep_red_dim7.inp	- 3D-analysis
half_3d_JLH_creep_red_dim7_r1b.inp	-3D-analysis, restart 1
half_3d_JLH_creep_red_dim7_r2b.inp	-3D-analysis, restart 2

4 – Scripts used for post-processing

Used inside ABAQUS/CAE or by abaqus cae startup=script.py after appropriate editing of job-name inside the script-file.

Contents in C:\Users\jhd\mappar\skb\Isostat\scripts

half_3d_JLH.py	- post processing file 3D-analysis
isostat_JLH.py	- post processing file for axi-symmetric analyses
postprocessing_130528.py	- additional plots

5 – Geometry definitions

Contents in C:\Users\jhd\mappar\skb\Isostat\geometry

isostat.cae - ABAQUS/CAE-database
isostat.jnl - journal file
isostat-6_11-1.jnl -journal file for previous version (ABAQUS 6-11).